Journal of Experimental Botany, Vol. 62, No. 8, pp. 2521–2569, 2011
doi:10.1093/jxb/erq434
This paper is available online free of all access charges (see http://jxb.oxfordjournals.org/open_access.html for further details)

Journal of Experimental Botany
www.jxb.oxfordjournals.org

RESEARCH PAPER

A DIGE-based quantitative proteomic analysis of grape berry flesh development and ripening reveals key events in sugar and organic acid metabolism

Maria José Martínez-Esteso[1,‡], Susana Sellés-Marchart[1], Diego Lijavetzky[2,†], Maria Angeles Pedreño[3] and Roque Bru-Martínez[1,*]

[1] Grupo de Proteómica y Genómica Funcional de Plantas, Dept. Agroquímica y Bioquímica, Facultad de Ciencias, Universidad de Alicante, Apartado 99, E-03080 Alicante, Spain
[2] Department Genética Molecular de Plantas, Centro Nacional de Biotecnología, Consejo Superior de Investigaciones Científicas (CSIC), C/Darwin 3, 28049 Madrid, Spain
[3] Grupo de Peroxidasas Vegetales, Department Fisiología Vegetal, Facultad de Biología, Universidad de Murcia, Campus de Espinardo, E-30100 Murcia, Spain

[†] New permanent address: Instituto de Biología Agrícola de Mendoza, Consejo Nacional de Investigaciones Científicas y Tecnológicas. Facultad de Ciencias Agrarias/Universidad Nacional de Cuyo, Almirante Brown 500, M5528AHB Chacras de Coria, Argentina
[‡] This article is part of María José Martínez-Esteso's PhD Thesis.
[*] To whom correspondence should be addressed. E-mail: roque.bru@ua.es

Received 10 September 2010; Revised 12 November 2010; Accepted 1 December 2010

Abstract

Grapevine (*Vitis vinifera* L.) is an economically important fruit crop. Quality-determining grape components, such as sugars, acids, flavours, anthocyanins, tannins, etc., are accumulated during the different grape berry development stages. Thus, correlating the proteomic profiles with the biochemical and physiological changes occurring in grape is of paramount importance to advance the understanding of the berry development and ripening processes. Here, the developmental analysis of *V. vinifera* cv. Muscat Hamburg berries is reported at protein level, from fruit set to full ripening. A top-down proteomic approach based on differential in-gel electrophoresis (DIGE) followed by tandem mass spectrometry led to identification and quantification of 156 and 61 differentially expressed proteins in green and ripening phases, respectively. Two key points in development, with respect to changes in protein level, were detected: end of green development and beginning of ripening. The profiles of carbohydrate metabolism enzymes were consistent with a net conversion of sucrose to malate during green development. Pyrophosphate-dependent phosphofructokinase is likely to play a key role to allow an unrestricted carbon flow. The well-known change of imported sucrose fate at the beginning of ripening from accumulation of organic acid (malate) to hexoses (glucose and fructose) was well correlated with a switch in abundance between sucrose synthase and soluble acid invertase. The role of the identified proteins is discussed in relation to their biological function, grape berry development, and to quality traits. Another DIGE experiment comparing fully ripe berries from two vintages showed very few spots changing, thus indicating that protein changes detected throughout development are specific.

Key words: Development, DIGE, grape, mesocarp, proteomics, quantitative, ripening, *Vitis vinifera*.

Abbreviations: ABA, abscisic acid; ACN, acetonitrile; AsA, L-ascorbic acid; AspAT, Asp aminotransferase; DIGE, difference in-gel electrophoresis; DTT, dithiothreitol; FA, formic acid; FS, fruit set; GA, gibberellin; GME, GDP-mannose-3',5'-epimerase; GS, glutamine synthase; HSP, heat shock protein; IEF, isoelectric focusing; IFRL6, isoflavone reductase-like protein 6; INV, invertase; JA, jasmonic acid; LC, liquid chromatography; L-IdnDH, L-idonate dehydrogenase; LOX, lipoxygenase; MDH, malate dehydrogenase; ME, malic enzyme; MLP, major latex protein; MS, mass spectrometry; Mw, molecular weight; OA, oxalic acid; PEP, phosphoenolpyruvate; PEPC, phosphoenolpyruvate carboxylase; PFP, phosphofructokinase; PK, pyruvate kinase; PPO, polyphenol oxidase; PR, pathogenesis-related; PVPP, polyvinylpryrrolidone; qRT-PCR, quantitative reverse transcription-polymerase chain reaction; ROS, reactive oxygen species; SAM, S-adenosyl methionine; SuSy, sucrose synthase; TA, tartaric acid; TCA, tricarboxylic acid; TFA, trifluoroacetic acid; UBX, ubiquitin regulatory X; UDP-GP, UDP-glucose pyrophosphorylase; USP, universal stress protein; V-PPase, vacuolar H^+-translocating inorganic pyrophosphatase; XET, xyloglucan endotransglycosylase.

Introduction

Grapevine (*Vitis vinifera* L.) is the most important crop fruit in the world. In 2007, according to the FAO statistics, ~7.5 million ha were dedicated to this crop in the world producing over 65 million tons of grapes in the same year (FAO, 2007). Berries are consumed as a fresh fruit, dried fruit, or processed, mainly for must production and wine-making. However, more recently, extracts from leaf, seed, and skin have been used in the nutraceutical and cosmetic industries as well as for research purposes.

The grape berry is a non-climateric fruit that exhibits a double sigmoid pattern of growth. The first growth phase after fruit set is characterized by rapid cell division, which increases the number of cells, and by an expansion of existing cells (Harris *et al.*, 1968). Stage I is followed by a lag phase where little or no growth occurs (Coombe, 1992). The second growth phase coincides with the onset of ripening, called véraison, which is characterized by important biochemical and physiological changes such us softening and colouring of the grape, in the case of coloured cultivars (Boss *et al.*, 1996). As grape berries develop, they change in size and composition from being small, firm, and acidic with little sugar and desirable flavours or aroma to becoming larger, softened, sweet, highly flavoured, less acidic, and highly coloured fruit. The development of these characteristics determines the quality of the final product. During the first growth period chlorophyll is the main pigment present in fruit and cells are rich in organic acids; the most prevalent compounds are tartaric and malic acids, which accumulate mainly in skin and flesh. There is a massive increase in compounds starting at véraison, the major ones being glucose and fructose (Davies and Robinson, 1996), in addition to phenolic and aromatic compounds (Kanellis and Roubelakis-Angelakis, 1993), while malate concentration decreases (Ruffner and Hawker, 1977). The development of flavour in grapes is partly due to the acid–sugar balance (Boss and Davies, 2001), which is particularly important in table grapes. Muscat Hamburg is a classical cultivar of black table grape grown in many parts of Europe, highly appreciated for its pleasant Muscat flavour (Ribéreau-Gayon *et al.*, 1975; Marino *et al.*, 1995). Aromas arise from volatile compounds such as terpenes, norisoprenoids, and thiols stored as sugar or amino acid conjugates (Lund and Bohlmann, 2006), some of which are differentially accumulated between skin and flesh (Wilson *et al.*, 1986). As a result, particular quality traits can be linked to specific tissues; skin composition plays an important role in determining the colour, aroma, and other organoleptic properties of wine; the pulp contains most of the sugars, which are transformed into alcohol during the fermentation process; the seed is the main source of flavan-3-ol monomers and proanthocyanidins, which contribute to important organoleptic properties in wine (Grimplet *et al.*, 2007).

The correct ripening of the grape berry is fundamental for both the commercial value of the fruit and the quality of wine. For this reason, grape berry development has been investigated using different approaches in order to elucidate the changes undergone at molecular level and the factors influencing them. First studies were devoted to a gene-by-gene analysis of berry development and ripening (Davies and Robinson, 1996; Boss *et al.*, 1996; Tattersall *et al.*, 1997; Davies *et al.*, 1999). However, since genomic resources for *V. vinifera* and related species proliferate in the form of large and publicly available expressed sequence tags (ESTs; >347879 in July 2008; http://compbio.dfci.harvard.edu/cgi-bin/tgi/gimain.pl?gudb=grape), large-scale mRNA expression profiling studies of berry development using cDNA or oligonucleotide microarrays have been carried out (Terrier *et al.*, 2005; Waters *et al.*, 2005; Waters *et al.*, 2006; Deluc *et al.*, 2007; Fernandez *et al.*, 2007).

In recent years, proteomics-based technologies have been successfully applied to grapevine for the analysis of stress responses (Vincent *et al.*, 2007, Jellouli *et al.*, 2008) and berry development (Sarry *et al.*, 2004; Vincent *et al.*, 2006; Deytieux *et al.*, 2007; Giribaldi *et al.*, 2007; Zhang *et al.*, 2008). These studies, carried out using single stain two-dimensional gel electrophoresis (2-DE), have improved our understanding of changes of some dozens of proteins in grape berries with a proteomic approach. The application of more robust, advanced, and powerful quantitative proteomic techniques should lead to an increase in the coverage of the differential proteome of grape berries during development and thus an improvement in our knowledge of this process. These techniques include mass-spectrometry (MS)-based quantitative stable isotopic labelling (Gygi *et al.*, 1999; Cagney and Emili, 2002; Ong *et al.*, 2002; Ross *et al.*, 2004; Che and Fricker, 2005; Rao *et al.*, 2005) and 2-DE-based difference in-gel electrophoresis (DIGE) (Unlu *et al.*, 1997). Lücker *et al.* (2009) reported several hundred proteins changing while studying the grape berry ripening initiation period using quantitative MS-based iTRAQ labelling. 2-DE remains one of the most widely used strategies for proteomics and 2-D DIGE accuracy for quantitative proteomics has been confirmed by analysing the same samples using inmunoblotting (Alfonso *et al.*, 2006; Deng *et al.*, 2007), metabolic stable isotope labelling (Kolkman *et al.*, 2005), and liquid chromatography (LC)-based quantitative proteomics (Wu *et al.*, 2006). Significant relative changes of protein expression as small as 1.2-fold may be measured with DIGE for large-volume spots. Because detection is based on fluorescence a dynamic range of about four orders is achieved, which allows for the differential expression analysis of proteins that are present at relatively low copy number (Tonge *et al.*, 2001).

Proteomic studies performed so far on the development of grape berries are limited to the ripening period, from pre-véraison to full ripening. In this study, the issue of protein expression changes is addressed in pericarp/mesocarp tissues in grape berry covering all developmental phases. To this end, berries were sampled from fruit set until full ripening taking four biological replicates to analyse proteome changes using the powerful proteomic quantitative approach of 2-DE-based DIGE. The results obtained

provide a global insight into proteome changes throughout the whole development with robust statistical analysis. Likewise, inter-seasonal differences were searched by comparing fully ripened berries from two different years.

Materials and methods

Plant material

Grape berries (*V. vinifera* L. cv. Muscat Hamburg) were collected in the 2005 and 2006 seasons from an experimental vineyard at the Instituto Murciano de Investigación y Desarrollo Agrario Alimentario located in Torrepacheco (Murcia, Spain). Berries were sampled from four selected vines and were collected at seven different developmental stages from fruit set until full ripening through the two growing seasons. Individual grapes were developmentally staged based on different parameters related to berry growth pattern. Green berries were classified into fruit set (FS stage) and then according to equatorial diameter of fruit into 4, 7, and 15 mm. The beginning of the second growth phase of berry, labelled as 100% véraison (stage V-100), was assessed visually as berries turned pink on 100% of their surface. Ripening berries were classified according to their estimated density by flotation in different NaCl solutions: 100–110 g/l (stage 110 g/l); 130–140 g/l (stage 140 g/l). Grapes sampled from detached bunches were sorted based on size and density. Berries in the same developmental stage sampled from the same vine constituted one biological replicate for that stage; these were immediately frozen in liquid nitrogen and stored at –80 °C. A parallel set of sampled berries was refrigerated after detaching and transported to the laboratory for determination of colour index, juice pH, total acidity, and °Brix, which showed typical profiles for grapevine berries; methods and results are reported elsewhere (Fenoll *et al.*, 2009).

Protein extraction

The three main berry tissues, seed or endocarp, flesh or mesocarp, and skin or exocarp differentiate at different developmental stages, thus their dissection is only possible after certain stages. Prior to total protein extraction seeds were removed from berries from stage 4 mm onwards while exocarp tissue was peeled away from berries from stages V-100 onwards. Thus, green berry proteins were extracted from pericarp and ripening berry proteins from the mesocarp. The berry tissue was ground to a fine powder in a mortar with liquid nitrogen. Throughout the procedure each wash was followed by centrifugation for 20 min at 15 700 *g* at 4 °C, unless otherwise stated.

Ripening stages (V-100, 110g/l, 140 g/l). Twenty grams of ground mesocarp were homogenized in 20 ml of extraction buffer containing 50 mM Na_2HPO_2 pH 7.0, 1 mM EDTA, 0.1 M NaCl, 1% polyvinyl pyrrolidone (PVPP), 1 mM $Na_2O_5S_2$, 10 mM ascorbic acid, and a cocktail of protease inhibitors [4-(2-aminoethyl) benzenesulfonyl fluoride, E-64, bestatin, leupeptin, aprotinin, and sodium EDTA (Sigma-Aldrich)]. All procedures described below were carried out at 4 °C. The homogenate was filtered through eight layers of cotton gauze and the filtrate was centrifuged at 60 000 *g*. The pellet was washed once in a buffer containing 50 mM Na_2HPO_2 pH 7.0, 1 mM EDTA, 0.1 M NaCl, 10 mM ascorbic acid, and recovered by centrifugation at 37 000 *g*. Then the pellet was cleaned as described previously for olive oil leaves (Wang *et al.*, 2003) with modifications. Briefly, the pellet was washed once in ethyl acetate:ethanol 1:2 (v/v), then twice with aqueous 10% tricarboxylic acid (TCA) (w/v) and twice with chilled 80% acetone. After recovery by centrifugation the white pellet was dried at 4 °C and processed for protein extraction as described in Saravanan and Rose (2004) with some modifications. The pellet was homogenized in 500 µl of phenol extraction buffer adjusted to pH 7.5 [0.7 M sucrose, 0.1 M KCl, 0.5 M Tris, 50 mM EDTA, 1% PVPP, 1% dithiothreitol (DTT), and a cocktail of protease inhibitors] and incubated for 30 min with frequent vortexing. An equal volume of Tris-saturated phenol pH 7.5 (Applichem, Darmstadt, Germany) was added and the mixture was incubated for 30 min with vortex every 5 min. Sharp phase separation was achieved by centrifugation at 15 700 *g* for 40 min. The upper phenol phase was recovered and the aqueous phase was submitted to a second phenol extraction. Both phenol phases were pooled and washed twice with an equal volume of phenol washing buffer adjusted to pH 7.0 (0.7 M sucrose, 0.1 M KCl, 0.5 M Tris, 50 mM EDTA, 1% DTT, and a cocktail of protease inhibitors). The recovered phenol was precipitated with 5 vols of 0.1 M ammonium acetate (w/v) in methanol overnight. The precipitate was three times washed in 0.1 M ammonium acetate (w/v) in methanol and twice in 80% acetone (v/v).

Green stages (FS, 4, 7, and 15 mm). The protocol described above for ripening stages was used for green pericarp with some modifications. Three grams of frozen powdered berry tissue were directly washed with ethyl acetate:ethanol (1:2, v/v) for 30 min at –20 °C with periodic vortexing. The pellet recovered by centrifugation was washed twice with chilled 80% acetone, and then transferred to a mortar and dried at 4 °C. The pellet (150 mg) was finely ground with sand (1:3, w/w) and washed with chilled 10% TCA (w/v) in acetone between five and seven times. This was followed by four or five washes with aqueous 10% TCA (v/v), three with chilled 80% acetone (v/v), and drying at 4 °C. Subsequently the white pellet was processed for phenol-based protein extraction as described above.

Labelling of proteins with CyDye

The precipitated and air-dried proteins were solubilized in labelling buffer (7 M urea, 2 M thiourea, 30 mM Tris–HCl, 4% CHAPS pH 9.0). Insoluble material was pelleted by centrifugation (12 000 *g*, room temperature, 5 min) and protein concentration in the supernatant was measured using the RCDC method (Bio-Rad, Madrid, Spain). Two hundred micrograms of protein were adjusted to 1 µg/µl with labelling buffer and further cleaned with the Ettan 2D Clean-up kit (GE Healthcare, Madrid, Spain) according to the manufacturer's recommendations. The recovered precipitated protein was solubilized in 30 µl of labelling buffer, the pH was adjusted to 8.5 using NaOH (100 mM), and the protein content was measured again. For labelling of the proteins, 400 pmol of CyDye in 1 µl was mixed with 18 µl of sample containing 50 µg of protein and incubated on ice for 30 min in the dark. The labelling reaction was terminated by adding 1 µl of 10 mM lysine. Each sample was covalently labelled with a fluorophore, either Cy3 or Cy5. A mixture of equal amounts of protein from every sample in the experiment was labelled with Cy2 and used as internal standard.

2-DE and image scanning

For analytical 2-D DIGE analysis 20 µl each of Cy3-, Cy5-, and Cy2-labelled sample (150 µg of protein) were combined, mixed with 60 µl of sample buffer 1 (7 M urea, 2 M thiourea, 30 mM Tris–HCl, 4% CHAPS, 100 mM DTT), and incubated for 10 min on ice. Then, samples were adjusted to 150 µl of sample buffer 2 (7 M urea, 2 M thiourea, 30 mM Tris–HCl, 4% CHAPS, 50 mM DTT) and submitted to IEF as the first-dimension separation. IPG strips, pH 3–10 NL, 18-cm (GE Healthcare) were swollen overnight in 340 µl of rehydration buffer (7 M urea, 2 M thiourea, 2% CHAPS, 50 mM DTT, 0.5% IPG buffer, 0.005% bromophenol blue), and samples were applied by a cup-loading method (Görg *et al.*, 2006). IEF was performed at 20 °C on an IPGphor Unit (GE Healthcare/Amersham Biosciences) using the following settings: 3 h at 300 V, 6 h gradient from 300 to 1000 V, 3 h

gradient from 1000 to 8000 V, 5 h at 8000 V until an accumulated voltage of 56 kVh was achieved. Strips were equilibrated after focusing in two steps: 30 min in equilibration buffer [50 mM Tris–HCl pH 8.8, 6 M urea, 30% glycerol (v/v), 2% SDS (w/v)] supplemented with 1% DTT followed by 30 min in equilibration buffer supplemented with 1.25% iodoacetamide. SDS-PAGE was carried out as the second-dimension separation in 12.5% acrylamide gels in an Ettan Dalt-six (GE Healthcare/Amersham Biosciences) vertical unit. The separation was run overnight: first step at 80 V, 10 mA/gel, and 1 W/gel for 1 h, second step at 150 V, 12 mA/gel, and 2 W/gel until bromophenol blue line reached to the bottom of gel. Images of the Cy3-, Cy2-, and Cy5-labelled samples were acquired in a Typhoon 9410 scanner (GE Healthcare/Amersham Biosciences) according to the manufacturer's recommendations.

DIGE image analysis

DIGE images were analysed using the Progenesis SameSpots v3.0 software (Non-linear Dynamics, Newcastle, UK). First, images were aligned. Prominent spots were used to manually assign ~60 vectors to digitized images within each gel and then the automatic vector tool was used to add additional vectors (~500 total vectors), which were manually revised and edited for correction if necessary. These vectors were used to warp and align gel images with a reference image of one internal standard across and within each gel. After automatic spot detection, spots were manually revised with edition tools for correct detection. Gel groups were established according to the experimental design and spot-normalized volume was used to select statistically significant (fold-change, ANOVA, false discovery rate) differentiated spots between grape berry developmental stages analysed in the experiment. The setting was fixed in each experiment so that fewer than three spots would be considered as a false positive result. The abundance patterns of the selected spots were analysed and grouped by hierarchical clustering and assessed by principal component analysis implemented in Progenesis SameSpots.

Spot picking and tryptic digestion

Preparative 2-D gels loaded with 1 mg of protein were used for spot picking. After 2-DE the gel was stained with the colloidal Coomassie blue G250 method (Neuhoff *et al.*, 1988), scanned in a transmission-light densitometer (Image Scanner; GE-Healthcare), and aligned with the DIGE reference image with SameSpots to outline the spots of interest selected in the previous analysis. The spots were excised using a manual spot picker (The Gel Company, Tübingen, Germany) with a 1.5 mm diameter picker head.

Trypsin in-gel digestion (Shevchenko *et al.*, 1996) was carried out in a Progest (Genomic Solutions, Huntingdon, UK) automatic in-gel protein digestor according to the manufacturer's recommendations for colloidal Coomassie brilliant blue-stained samples. The gel plugs were extensively washed to remove dye and SDS impurities with 25 mM ammonium bicarbonate, in-gel reduced with 60 mM DTT and *S*-alkylated with excess iodoacetamide followed by digestion with modified porcine trypsin (Promega, Madison, WI, USA) at 37 °C for 6 h. Peptides were extracted in ammonium bicarbonate, then in 70% acetonitrile (ACN) and finally in 1% formic acid (FA). Extracted peptides were dried down in a speed-vac bench-top centrifuge and resuspended in 0.1% FA (typically 10 µl).

MS-based protein identification

For analysis in the MALDI-TOF/TOF MS instrument, the tryptic fragments were desalted using Zip Tips C18 (Agilent Technologies, Madrid, Spain) according to the manufacturer's instructions. Eluted peptides were completely dehydrated in a vacuum centrifuge and resuspended in 0.1% trifluoroacetic acid (TFA). A droplet of 0.8 µl was spotted onto the MALDI target plate. After the droplets were air-dried at room temperature, 0.8 µl of matrix [4.7 mg/ml α-cyano-4-hydroxycinnamic acid (Sigma-Aldrich) resuspended in 4 mM ammonium phosphate/50% ACN/0.1% TFA (v/v)] was added and allowed to air-dry at room temperature. MALDI MS and MS/MS data were acquired with a 4700 Proteomics analyser (Applied Biosystems, Foster City, CA, USA) in positive reflectron mode by 3000 shots in MS/MS mode, selecting the five most intensive precursors (not analysed previously) for MS/MS analysis (3000 shots per precursor). All resulting MS/MS spectra were sent to the MASCOT server (http://www.matrixscience.com) using GPS software (Applied Biosystems) with the following settings: trypsin, up to one missed cleavage, fixed modification carbamidomethyl, asparagine deamidation, and methionine oxidation as variable modifications and a mass tolerance of 100 ppm for the precursor and 0.6 Da for fragment ions. The search was performed against NCBInr restricted to viridiplantae taxonomy. The samples without a positive identification were analysed by LC-MS/MS. The tryptic fragments were analysed by LC-MS/MS using an Agilent 1100 series nano-HPLC system lined on an XCTplus ion trap mass spectrometer (Agilent) equipped with a nano-ESI source. Sample concentration and desalting were performed on a Zorbax 300SB-C18 trap column (0.3×5 mm, 5 µm) at 0.3 µl/min while peptide separation was achieved on a Zorbax 300SB-C18 analytical column (75 µm×15 cm, 3.5 µm) using a 30-min linear gradient of 5–35% ACN containing 0.1% (v/v) FA at a constant flow rate of 0.3 µl/min. MS and MS/MS spectra were acquired in the standard enhanced mode (26 000 *m*/z per second) and the ultrascan mode (8100 *m*/*z* per second), respectively. Mass spectrometer settings for MS/MS analyses included an ionization potential of 1.8 kV and an ICC smart target (number of ions in the trap before scan out) of 400 000 or 150 ms of accumulation. MS/MS analyses were performed using automated switching with a preference for doubly charged ions and a threshold of 10^5 counts and 1.3 V fragmentation amplitude. Each MS/MS spectra dataset (~1200 spectra/run) was processed to determine monoisotopic masses and charge states, to merge MS/MS spectra with the same precursor ($\Delta m/z$<1.4 Da and chromatographic Δt<15 s) and to select high-quality spectra with the Extraction tool of the SpectrumMill Proteomics Workbench (Agilent). The reduced dataset was searched against the NCBInr in the identity mode with the MS/MS Search tool of the SpectrumMill Proteomics Workbench using the following parameters: trypsin, up to two missed cleavages, fixed modification *S*-carbamidomethyl, and a mass tolerance of 2.5 Da for the precursor and 0.7 Da for product ions. Peptide hits were validated first in the peptide mode and then in the protein mode according to the manufacturer's recommended score settings. Validated files were summarized in the protein mode to assemble peptides into proteins.

A protein was considered identified with a minimum of two different peptides and a score above threshold marked for the MASCOT and SpectrumMill search engines, respectively.

Functional analysis

Gene ontology (Götz *et al.*, 2008) analysis of identified proteins was performed using Blast2GO v2.3.6. A file of Fasta sequences of the identified and/or quantified protein set was batch retrieved from the NCBI website. Blast2GO was fed with the Fasta file and run first to incorporate sequence description by performing a BLASTp search against NCBInr (e-value cut-off 1×10^{-50}), second to map GO, EC, and Interpro terms, and then to annotate the sequences (E-value Hit-Filter of 1×10^{-6}, a Hsp-Hit coverage cut-off of 0, an Annotation cut-off of 55, and a GO weight of 5). The sets of proteins identified from green, ripe, and seasonal DIGE experiments analysed by Blast2GO are supplied in Supplementary Files S1, S2, and S3, respectively (available at *JXB* online).

RNA isolation, cDNA synthesis, and real-time quantitative RT-PCR

Total RNA was extracted from frozen mesocarp (15 mm, V-100, and 140 g/l stages) according to Reid *et al.* (2006) and further purified using the RNeasy Mini Kit (Qiagen, Madrid, Spain) according to standard protocols. cDNA synthesis and quantitative RT-PCR (qRT-PCR) procedures were performed as described elsewhere (Diaz-Riquelme *et al.*, 2009). Total RNA (1 mg) was reverse transcribed in a reaction mixture of 20 ml containing 13 PCR buffer II (Applied Biosystems), 5 mM $MgCl_2$, 1 mM deoxynucleoside triphosphates, 20 units of RNase inhibitor, 50 units of murine leukaemia virus reverse transcriptase (Applied Biosystems), 2.5 mM oligo(dT)18, and diethyl pyrocarbonate-treated water. Transcript levels were determined by qRT-PCR using a 7300 Real-Time PCR System (Applied Biosystems) and SYBR Green dye (Applied Biosystems). Grapevine-gene-specific primers were designed using the Oligo Explorer 1.2 software (Gene Link). Primer sequences used in the qRT-PCR analyses for isoflavone reductase like-6 (IFRL6; Gene Bank accession number: ABN000711) are as follows: IFRL6-F, GACCAGTTTGTGTGA-GAGGTA; IFRL6-R, TGCTCAATGGCATAGACAAGG with an expected product size of 107 bp. Data were analysed using the 7300 SDS software 1.3 (Applied Biosystems). Transcript level was calculated using the standard curve method and normalized against the grapevine *EF1* gene (UniGene Vvi.1750) used as reference control (Reid *et al.*, 2006).

Table 1. Experimental design of three DIGE experiments

(A) First stage of development experiment: FS (A), 4 mm (B), 7 mm (C), 15 mm (D); (B) ripening experiment: V-100 (E), 110 g/l (F), 140 g/l (G); and (C) seasonal comparison experiment at 140 g/l stage: 2005 (H) and 2006 (I).Four biological replicates (1–4) were used for each sampling point.

Gel number	Cy3 sample	Cy5 sample
(A) Comparison between green stages		
1	A1	B3
2	A2	C3
3	B1	A3
4	B2	D3
5	C1	B4
6	C2	D4
7	D1	A4
8	D2	C4
(B) Comparison between ripe stages		
1	E1	F2
2	E2	G1
3	F1	E3
4	G2	F4
5	G3	E4
6	F3	G4
(C) Comparison between seasons		
1	I2	H4
2	I1	H3
3	H2	I3
4	H1	I4

Results and discussion

Grape berry development was analysed by a 2-D DIGE technique followed by MS-based protein identification. One DIGE experiment covered four time-points of the first growth period spanning the stages from fruit set to pre-véraison and another DIGE experiment covered three time-points of the second growth period from onset to full ripening, as described in the previous section. Likewise, we performed a third DIGE experiment comparing the late ripening stage of 140 g/l between the 2005 and 2006 seasons to detect potential environmental effects on berry developmental control. The experimental design for individual experiments is described in Table 1 (overlapped DIGE images in Supplementary Fig. S1 at *JXB* online).

Protein abundance patterns

Green development stages of grape berries.: 2-D DIGE gel maps resolved ~921 unique spots across the compared stages. According to data analysis setting (see Materials and methods), 262 spots (28.4% of unique spots) were selected for subsequent protein identification (fold-change ⩾1.5, ANOVA $P<0.014$). Protein identity was successfully achieved for 154 of the selected spots (Table 2). Figure 1A shows the reference gel image for the first DIGE experiment in which the selected differentially expressed spots are outlined.

The unsupervised PCA bi-plot of gels and spots (Fig. 1B) shows a gel grouping (coloured dots), which agrees with the experimental groups. The close plotting of the 4 and 7 mm stage gels indicates that minimal change occurs between these two stages in relation to both FS and 15 mm stages. One of the gels in the 15 mm group (an orange dot) was found to be an outlier, and was not included in the subsequent analysis. The removal of this gel was not detrimental to the statistical quality of the analysis as 97.7% of the selected spots had a power of >0.8 for three biological replicates (Fig. 1C). The 262 selected spots were classified into nine clusters according to their expression patterns based on a hierarchical clustering analysis (Fig. 1D). Five profiles showed an increase (Clusters 1, 2, 3, 6, and 7) and four a decline (Clusters 4, 5, 8, and 9) through development. Altogether, these results show two important global changes at the protein level linked to respective growth stages from FS to 4 mm and from 7 mm to 15 mm according to the sampling performed in this experiment.

Ripening stages of grape berries.: The analysis of V-100, 110 g/l, and 140 g/l stages resulted in 804 unique spots across the gels. According to the data analysis setting (see Materials and methods), 67 spots (8.3% of unique spots) were selected for the subsequent protein identification (fold-change ⩾1.3, ANOVA $P<0.047$). Protein identity was successfully achieved for 61 of the selected spots (Table 3). Figure 2A shows the reference gel image for this second DIGE experiment in which the selected differentially expressed spots are outlined. The unsupervised PCA bi-plot of gels and spots (Fig. 2B) shows a gel grouping that agrees with the experimental groups. The first component separates clearly the V-100 stage gels from the others and the second component separates 110 g/l from 140 g/l stage gels. The statistical quality of the analysis is quite high as >90% of the selected spots had a power of >0.8 for four biological

Table 2. Proteins differentially expressed in DIGE covering first growth period (FS, 4mm, 7mm, 15 mm stages)

Selection and quantification of spots of interest was assisted by Progenesis SameSpots software v3.0. Spots selected were classified into nine different clusters according to their protein abundance profile among analysed stages. Spots were excised from the gel, trypsin in-gel digested, and the eluted peptides were analysed by mass spectrometry (MALDI-MS/MS and/or ESI-MS/MS). Proteins were identified by MS/MS search against NCBInr protein database using MASCOT and SpectrumMill.

	Statistical analysis					Norm. Vol./Norm. Vol. FS[g]					Spot data				Identification parameters[h]		
Spot number (g)	Cluster	Fold	Anova (*P*)	Power	Accession number	FS	4 mm	7 mm	15 mm	Protein description	Experimental		Theoretical		Score[e]/ EmPAI[f]	Peptides number	Mass spectometer instrument
											Mw (Da)[c]	pI[c]	Mw (Da)[d]	pI[d]			
457	2	2.0	7.69E-03	0.83	gil118482419[b]	1	1.121	1.11	1.969	Unknown (*Populus trichocarpa*) vacuolar ATP synthase subunit f	15538	6.23	14439.56	5.79	44.19	2	ESI
281	2	2.3	7.69E-03	0.83	gil147811500[a]	1	–1.079	–1.03	2.557	Nucleoside diphosphate kinase	16212	6.16	16299.47	6.85	220	7	MALDI-SQ
21	3	8.3	4.05E-08	1	gil157338652[a]	1	1.297	1.989	8.292	20S proteasome α-subunit	23515	5.17	24855.83	7.89	252	16	MALDI-SQ
529	3	1.7	6.69E-03	0.791	gil157343521[a]	1	–1.108	1.005	1.514	Aspartic proteinase nepenthesin–1	40530	3.91	53050.26	5.69	48.79	4	ESI
210	3	3.2	1.33E-06	1	gil157342785[a]	1	1.012	1.269	3.215	Thioredoxin-dependent peroxidase	18262	4.66	17252.04	5.15	239	11	MALDI-SQ
369	3	2.3	1.51E-03	0.953	gil147791852[a]	1	1.131	1.45	2.303	33 kDa precursor protein of oxygen-evolving complex	31123	4.27	33212.82	5.87	111	7	MALDI-PMF
239	3	3.0	1.67E-07	1	gil157340819[a]	1	–1.546	–1.314	1.958	Glycine-rich RNA-binding protein	16508	5.53	16319.45	6.32	50.93	3	ESI
484	3	1.9	7.60E-03	0.84	gil147791852[a]	1	1.012	1.309	1.872	33 kDa precursor protein of oxygen-evolving complex	31241	4.47	33212.82	5.87	106	20	MALDI-PMF
446	3	2	2.47E-04	0.99	gil147819925[a]	1	1.256	1.266	1.998	ATP synthase	26674	8.13	27677.88	9.47	80	10	MALDI-SQ
49	3	5.8	2.27E-07	1	gil157331849[a]	1	1.221	1.975	5.789	Quinone oxidoreductase	25667	5.52	25542.50	6.05	30.66	2	ESI
51	3	5.7	2.58E-05	1	gil157343051[a]	1	1.112	1.804	5.673	Multicatalytic endopeptidase proteasome β-subunit	242554	5.06	24981.59	5.46	120	5	MALDI-SQ
42	3	6.2	2.55E-06	1	gil14582465	1	1.265	2.643	6.174	Putative transcription factor (*V. vinifera*)	210440	5.58	16692.90	5.68	39.35	2	ESI
186	3	3.4	1.38E-03	0.945	gil157357206[a]	1	1.098	1.326	3.4	UBX-domain-containing protein	89365	3.66	58405.01	4.71	56.35	3	ESI
427	3	2.1	1.38E-03	0.942	gil147781540[a]	1	1.145	1.246	2.082	Thioredoxin-dependent peroxidase	18270	5.28	17250.22	5.15	26.37	2	ESI
381	3	2.3	1.73E-04	0.997	gil157353015[a]	1	1.225	1.333	2.253	Universal stress protein	18249	5.13	18044.37	5.74	33.28	2	ESI
243*	3	3.0	4.66E-06	1	gil147767013[a]	1	1.015	1.197	2.976	3-Isopropylmalate small subunit	23616	4.93	26962.61	7.04	83.03/–	4	ESI
					gil157336064					Similar to PBC1 (20S proteasome β-subunit C1) peptidase isoform 1 (*V. vinifera*)			21508.85	5.48	37.11/0.14	5	

Table 2. *Continued*

Spot number (g)	Statistical analysis				Accession number	Norm. Vol./Norm. Vol. FS[g]				Protein description	Spot data				Identification parameters[h]		
	Cluster	Fold	Anova (*P*)	Power		FS	4 mm	7 mm	15 mm		Experimental		Theoretical		Score[e]/ EmPAI[f]	Peptides number	Mass spectometer instrument
											Mw (Da)[c]	pI[c]	Mw (Da)[d]	pI[d]			
					gil147804704[a]					Light-harvesting complex II protein lhcb6			27199.20	7.89	35.89/–	2	
368	3	2.3	2.45E-04	0.995	gil147811500[a]	1	–1.226	–1.074	1.88	Nucleoside diphosphate kinase	16094	5.99	16299.47	6.85	225	6	MALDI-SQ
133	3	3.8	4.37E-06	1	gil157342492[a]	1	–1.267	1.272	3.037	Chloroplast chaperonin 21	248904	5.30	26994.49	8.76	42.85	2	ESI
400	3	2.2	2.82E-03	0.936	gil76559896	1	–1.082	1.078	2.023	Isoflavone reductase-like protein 6 (*V. vinifera*)	31193	5.87	33907.84	6.02	154	4	MALDI-SQ
398	3	2.2	3.21E-03	0.884	gil147791852[a]	1	1.003	1.026	2.193	33 kDa precursor protein of oxygen-evolving complex	31095	4.65	33212.82	5.87	176	11	MALDI-SQ
183	3	3.4	4.91E-04	0.992	gil147836228[a]	1	1.166	1.355	3.417	c2-domain-containing protein	32709	3.73	30776.4	4.60	62.22	3	ESI
276*	3	2.8	5.20E-05	1	gil147788048[a] gil37999810	1	1.021	1.412	2.776	Benzoquinone reductase Superoxide dismutase (Mn), mitochondrial precursor (*Prunus persica*)	22432	6.02	21725.97 25439.22	5.83 8.62	63.63/0.16 35.92/0.13	5 3	ESI
378	3	2.3	1.71E-03	0.946	gil147818815[a]	1	–1.122	1.114	2.016	ATP synthase D chain, mitochondrial, putative	19961	4.91	19756.08	5.34	168	12	MALDI-SQ
172	3	3.6	1.64E-04	0.998	gil147853192[a]	1	1.183	1.592	3.556	Salt-tolerant expressed	35131	3.76	34919.14	4.67	34.66	2	ESI
277	3	2.8	3.67E-05	1	gil147787750[a]	1	1.117	1.319	2.769	23 kDa polypeptide of oxygen-evolving complex	23485	4.59	27777.07	8.33	88	9	MALDI-SQ
140	3	3.8	1.01E-05	1	gil147843860[a]	1	1.291	1.774	3.778	Proteasome chain protein	20814	5.86	22476.40	5.85	36.34	2	ESI
127	3	3.9	2.45E-04	0.997	gil147781540[a]	1	1.151	1.153	3.918	Thioredoxin-dependent peroxidase	18242	4.32	17250.22	5.15	23.8	4	ESI
250	3	2.9	1.10E-04	0.999	gil147771556[a]	1	–1.051	–1.002	2.791	Xyloglucan endotransglycosylase	31313	5.93	33180.6	5.98	75.23	4	ESI
75	3	5.1	2.67E-06	1	gil147811500[a]	1	–1.73	–1.079	2.92	Nucleoside diphosphate kinase	16506	5.72	16299.47	6.82	25.86	2	ESI
921	3	14	3.14E-06	0.999	gil1839578	1	1.786	2.046	14.317	Vacuolar invertase 1	67648	3.50	71546.90	4.60	92.80	6	ESI
353	3	2.4	2.38E-03	0.928	gil147811500[a]	1	–1.46	–1.216	1.615	Nucleoside diphosphate kinase	16090	6.44	16299.47	6.85	99	5	MALDI-SQ
335	4	2.4	9.16E-03	0.725	gil157336429[a]	1	–2.417	–1.993	–1.909	Thioredoxin-dependent peroxidase	19838	5.92	21811.36	8.74	34.21	2	ESI
494	4	1.8	4.91E-05	0.999	gil157340819[a]	1	–1.822	–1.79	–1.623	Glycine-rich RNA-binding protein	16544	5.65	16319.45	6.32	17.83	1	ESI
502*	5	1.8	3.74E-05	0.999	gil162694103[b]	1	–1.192	–1.783	–1.789	Predicted protein (*Physcomitrella patens* subsp. *patens*)RuBisCo subunit binding-protein β-subunit	61181	4.98	63792.60	5.44	30.15	2	ESI

Table 2. *Continued*

Spot number (g)	Statistical analysis				Accession number	Norm. Vol./Norm. Vol. FS[g]				Protein description	Spot data				Identification parameters[h]		
	Cluster	Fold	Anova (*P*)	Power		FS	4 mm	7 mm	15 mm		Experimental		Theoretical		Score[e]/ EmPAI[f]	Peptides number	Mass spectometer instrument
											Mw (Da)[c]	pI[c]	Mw (Da)[d]	pI[d]			
					gil30685604[a]					Chaperonin CPN60-2, mitochondrial precursor (*Arabidopsis thaliana*)			61939.47	6.37	26.52	2	
275	5	2.8	1.58E-04	0.997	gil147837950[a]	1	–1.156	–1.631	–2.778	Dehydroquinate dehydratase shikimate:NADP oxidoreductase	57198	6.09	57282.97	6.69	81	13	MALDI-SQ
269	5	2.8	1.47E-04	0.996	gil147799448[a]	1	–1.067	–1.622	–2.82	Dihydroflavonol 4-reductase	36456	5.89	35694.23	6.27	98	12	MALDI-SQ
73	5	5.1	5.62E-04	0.943	gil3288721	1	–1.627	–2.763	–5.075	Chalcone synthase (*V. vinifera*)	44944	5.87	42785.08	5.98	107	13	MALDI-SQ
295	5	2.6	1.17E-04	0.998	gil147856360[a]	1	–1.348	–1.574	–2.629	Transcription factor APFI	29133	5.75	29552.19	5.89	22.71	2	ESI
249	5	2.9	7.32E-05	0.997	gil147843754[a]	1	–1.354	–2.001	–2.935	Cytosolic phosphoglycerate kinase 1	43570	5.90	42395.72	6.29	216	19	MALDI-SQ
47	5	5.8	3.49E-07	1	gil18376655	1	–1.573	–2.807	–5.831	Chalcone synthase (*V. vinifera*)	44622	5.96	42891.16	6.10	234	21	MALDI-SQ
202*	5	3.3	8.58E-07	1	gil59857604	1	–1.2	–1.754	–3.28	Anthocyanidin reductase (*V. vinifera*)[f1]	36808	5.71	36739.92	5.93	98.45/0.67	7	ESI
					gil147843754					Cytosolic phosphoglycerate kinase (*V. vinifera*)			42395.72	6.29	64.98/–	4	
					gil157347533					NAD-dependent isocitrate dehydrogenase α-subunit (*V. vinifera*)			40152.41	6.38	63.2/0.08	3	
					gil157354907[a]					Fructose bisphosphate aldolase			42777.06	7.55	34.81/0.09	2	
					gil157335300[a]					Dihydroflavonol 4-reductase			36314.13	7.02	34.64/0.18	2	
341	6	2.4	9.33E-05	0.999	gil157346726[a]	1	1.564	1.357	2.391	RuBisCo subunit binding-protein α-subunit	63160	3.96	61672.92	5.06	136	21	MALDI-SQ
111	6	4.2	1.19E-03	0.961	gil147838052[a]	1	1.659	2.852	4.181	Cyclase family protein	30938	4.28	29850.09	5.15	90	5	MALDI-SQ
68	6	5.3	1.49E-05	1	gil157335141[a]	1	3.77	4.068	5.3	Heat shock protein 90	94024	4.04	91679.69	4.97	138	12	MALDI-SQ
61	6	5.4	2.53E-03	0.916	gil157346387[a]	1	2.104	2.884	5.428	Single-strand nucleic acid-binding protein	100934	3.93	95431.95	5.51	21.1	1	ESI
461	6	2.0	3.67E-04	0.986	gil147838052[a]	1	1.485	1.84	1.956	Cyclase family protein	30743	4.82	29850.09	5.15	253	10	MALDI-SQ
256	6	2.9	3.75E-06	1	gil153799897	1	2.137	2.372	2.91	β-Tubulin (*Eucalyptus grandis*)	53112	5.79	49627.63	4.74	86	8	MALDI-SQ
313	6	2.5	2.19E-07	1	gil147802483[a]	1	2.225	2.49	2.514	α-Tubulin 1	51439	4.24	49559.30	4.89	245	21	MALDI-SQ
17*	6	9.2	2.61E-07	1	gil157339226[a]	1	5.862	6.506	9.226	Clathrin binding	80818	3.77	60229.33	4.82	41.17/0.11	2	ESI
					gil157345827[a]					Hsp90			90408.79	4.93	31.27/0.11	2	

Table 2. *Continued*

Spot number (g)	Statistical analysis				Accession number	Norm. Vol./Norm. Vol. FS[g]				Protein description	Spot data				Identification parameters[h]		
	Cluster	Fold	Anova (*P*)	Power		FS	4 mm	7 mm	15 mm		Experimental		Theoretical		Score[e]/ EmPAI[f]	Peptides number	Mass spectometer instrument
											Mw (Da)[c]	pI[c]	Mw (Da)[d]	pI[d]			
199	6	3.3	1.24E-04	0.998	gil147838052[a]	1	1.712	2.184	3.295	Cyclase family protein	30861	4.55	17219.16	6.52	244	9	MALDI-SQ
159	6	3.7	2.31E-05	1	gil147770307[a]	1	3.467	3.598	3.652	Hsp90	79465	4.23	79962.21	5.01	236	26	MALDI-SQ
197	6	3.3	2.38E-03	0.923	gil147838052[a]	1	1.56	2.459	3.306	Cyclase family protein	30956	4.45	17219.16	6.52	198	7	MALDI-SQ
305	7	2.6	1.13E-02	0.67	gil81074298	1	2.585	1.799	1.799	Hsp90-2-like (*Solanum tuberosum*)	81896	3.89	80365.94	5.08	84.36	4	ESI
500	7	1.8	5.70E-03	0.795	gil147844532[a]	1	1.8	1.625	1.492	Heat shock protein	83582	4.41	88624.82	5.38	106	17	MALDI-SQ
69	8	5.3	1.48E-05	1	gil157838576	1	–1.334	–1.566	–5.284	Anthocyanidin synthase (*V. vinifera*)	43173	5.68	40137.77	5.63	197	15	MALDI-SQ
27	8	7.7	1.16E-04	0.995	gil157359341[a]	1	1.89	–1.089	–4.1	Methionine synthase	80361	6.14	84937.63	6.09	143.49	12	ESI
113	8	4.2	2.79E-04	0.994	gil19070130	1	–1.164	–1.194	–4.164	Catalase (*V. vinifera*)	53126	6.64	56944.39	6.71	167	21	MALDI-SQ
23	8	7.9	1.35E-06	1	gil157353024[a]	1	–1.375	–1.593	–7.861	ATP citrate lyase	64619	6.53	65948.05	6.91	111	24	MALDI-SQ
70	8	5.1	1.44E-06	1	gil15242863	1	–1.146	–1.558	–5.131	Pyruvate kinase, putative(*A. thaliana*)	56883	6.72	54982.45	6.24	86	14	MALDI-SQ
					gil157353413[a]					Pyruvate kinase			53137.01	8.50	82	12	
9	8	11.6	1.44E-05	1	gil157342473[a]	1	1.097	–1.128	–10.544	Sucrose synthase	90080	5.91	92384.63	5.98	128	21	MALDI-SQ
126	8	3.9	3.71E-06	1	gil157341208[a]	1	–1.393	–1.82	–3.936	Chalcone synthase	44238	6.06	42890.13	6.10	117	15	MALDI-SQ
18	8	9.2	2.25E-04	0.996	gil225454009[a]	1	1.189	–1.173	–7.744	Transketolase-like protein	82292	5.85	80614.95	6.62	175.98	12	ESI
128	8	3.9	1.14E-04	0.998	gil157342079[a]	1	–1.222	–1.457	–3.907	*S*-Adenosyl-L-homocysteine hydrolase	59553	5.69	48588.70	6.15	76	12	MALDI-SQ
19	8	8.9	1.87E-05	1	gil157337907[a]	1	1.082	–1.105	–8.194	Aconitate citrate hydrolyase	94801	5.79	109986.71	6.66	43.80	3	ESI
16	8	9.3	3.15E-06	1	gil974782	1	–1.055	–1.27	–9.309	Cobalamine-independent methionine synthase (*Solenostemon scutellarioides*)	87674	6.06	86716.86	6.17	152	16	MALDI-SQ
					gil147821107[a]					Methionine synthase			81585.59	6.19	151	16	
14	8	9.7	1.81E-04	0.998	gil147835837[a]	1	1.336	–1.196	–7.292	Transketolase 1	82594	5.90	80612.99	6.62	94	18	MALDI-SQ
6	8	12.5	3.88E-07	1	gil157348808[a]	1	–1.024	–1.207	–12.496	Elongation factor 2	87816	5.78	56141.58	6.08	117	14	MALDI-SQ
77	8	5.0	9.79E-05	0.998	gil157340247[a]	1	1.757	1.278	–2.866	Hsp70	93782	4.58	43963.28	8.22	81	10	MALDI-SQ
141	8	3.8	1.58E-04	0.997	gil19070130	1	–1.174	–1.171	–3.775	Catalase (*V. vinifera*)	53250	6.52	56944.39	6.71	216	22	MALDI-SQ
143	8	3.8	3.61E-06	1	gil157337620[a]	1	–1.09	–1.144	–3.77	LOX	94961	5.66	101619.34	6.13	276.80	15	ESI
63	8	5.4	2.77E-05	1	gil157352072[a]	1	–1.096	–1.536	–5.397	GDP-mannose-3,5-epimerase	42183	5.87	42516.00	5.94	76	7	MALDI-SQ
79	8	5.0	9.65E-05	0.999	gil157338441[a]	1	–1.172	–1.215	–4.984	Rhamnose biosynthetic enzyme expressed	73186	6.27	75698.29	6.65	80	16	MALDI-SQ
4	8	13.1	5.13E-07	1	gil225468576[a]	1	1.054	–1.644	–12.457	Cytoplasmic aconitate hydratase	96222	5.90	98124.69	6.04	38.61	3	ESI
153	8	3.7	1.68E-04	0.994	gil157353934[a]	1	–1.179	–1.267	–3.686	UDP-glucose pyrophosphorylase	52266	6.35	51218.25	6.64	94	9	MALDI-SQ
154	8	3.7	3.44E-06	1	gil157337620[a]	1	–1.178	–1.312	–3.681	LOX	94594	5.42	101619.34	6.13	126	25	MALDI-SQ
2*	8	14.6	8.66E-07	1	gil157348808[a]	1	1.17	–1.271	–12.461	Elongation factor 2[f1]	95863	5.86	56141.58	6.08	60.49/0.11	3	ESI

Table 2. *Continued*

Spot number (g)	Statistical analysis				Accession number	Norm. Vol./Norm. Vol. FS[g]				Protein description	Spot data				Identification parameters[h]		
	Cluster	Fold	Anova (*P*)	Power		FS	4 mm	7 mm	15 mm		Experimental		Theoretical		Score[e]/ EmPAI[f]	Peptides number	Mass spectometer instrument
											Mw (Da)[c]	pI[c]	Mw (Da)[d]	pI[d]			
					gil157329909[a]					Cytoplasmic aconitate hydratase			97018.13	6.04	29.52/–	2	
5	8	12.8	9.62E-06	1	gil157348808[a]	1	1.737	–1.33	–7.37	Elongation factor 2	88454	5.89	56141.58	6.08	88	15	MALDI-SQ
162	8	3.6	2.50E-04	0.994	gil157337427[a]	1	–1.268	–1.513	–3.636	Ascorbate peroxidase	27325	5.73	27135.91	5.86	126	15	MALDI-SQ
					gil73647738					Ascorbate peroxidase (*Vitis pseudoreticulata*)			27598.04	5.58	98	13	
163	8	3.6	4.39E-04	0.978	gil157342743[a]	1	–1.264	–1.561	–3.63	NADP-malic enzyme	64310	5.89	54803.59	8.27	106	17	MALDI-SQ
					gil1708924					NADP-dependent malic enzyme (*V. vinifera*)			65185.77	6.09	104	18	
170	8	3.6	5.34E-04	0.98	gil157467219	1	–1.348	–1.271	–3.572	Ran3 GTP-binding protein (*Iberis amara*)	24176	6.27	18484.54	9.44	81	9	MALDI-SQ
171	8	3.6	6.52E-04	0.95	gil157838576	1	–1.459	–1.613	–3.571	Anthocyanidin synthase (*V. vinifera*)	43362	5.60	40137.77	5.63	211	11	MALDI-SQ
185	8	3.4	8.92E-05	0.999	gil10764573	1	–1.051	–1.137	–3.405	Ribulose-1.5-bisphosphate carboxylase/oxygenase large subunit (*Weinmannia bangii*)	53280	5.88	50037.76	5.95	41.24	2	ESI
96	8	4.6	7.68E-04	0.982	gil157353934[a]	1	–1.083	–1.288	–4.553	UDP-glucose pyrophosphorylase	52533	6.15	51218.25	6.64	96	11	MALDI-SQ
30	8		4.76E-05	1	gil147835837[a]	1	1.963	–1.057	–3.605	Transketolase 1	82748	5.94	80612.99	6.62	53	5	ESI
105	8	4.3	1.61E-05	1	gil146432257	1	–1.096	–1.247	–4.326	GDP-mannose-3,5-epimerase (*V. vinifera*)	42790	5.81	42535.04	5.99	166	15	MALDI-SQ
225	8	3.1	2.13E-05	1	gil157327869[a]	1	–1.166	–1.334	–3.128	Glyceraldehyde-3 phosphate dehydrogenase	35009	7.22	34618.85	6.62	301	16	MALDI-SQ
201	8	3.3	3.07E-04	0.996	gil147794688[a]	1	–1.06	–1.199	–3.288	GDP-mannose-3,5-epimerase	43130	5.73	42534.19	5.94	304	19	MALDI-SQ
214	8	3.2	4.25E-04	0.989	gil157344281[a]	1	–1.03	1.009	–3.17	Triosephosphate isomerase	26221	5.96	27111.10	6.35	167	9	MALDI-SQ
330	8	2.4	4.31E-09	1	gil1707955	1	–1.157	–1.357	–2.448	Glutamine synthetase cytosolic isozyme 1 (*V. vinifera*)	37325	5.59	39174.68	5.79	225	15	MALDI-SQ
					gil1707959					Glutamine synthetase cytosolic isozyme 2 (*V. vinifera*)			39297.70	5.69	182	10	
321	8	2.5	9.34E-05	0.999	gil157352072[a]	1	1.096	–1.272	–2.275	GDP-mannose-3,5-epimerase	46176	5.87	42516.00	5.94	118	13	MALDI-SQ
					gil147794688[a]					GDP-mannose-3,5-epimerase			42534.19	5.94	109	12	

Table 2. *Continued*

Spot number (g)	Statistical analysis				Accession number	Norm. Vol./Norm. Vol. FS[g]				Protein description	Spot data				Identification parameters[h]		
	Cluster	Fold	Anova (*P*)	Power		FS	4 mm	7 mm	15 mm		Experimental		Theoretical		Score[e]/ EmPAI[f]	Peptides number	Mass spectometer instrument
											Mw (Da)[c]	pI[c]	Mw (Da)[d]	pI[d]			
473	8	1.9	2.24E-04	0.994	gil157346280[a]	1	−1.028	−1.066	−1.909	Enolase	59066	5.61	18266.62	8.79	76	6	MALDI_SQ
459	8	2.0	2.13E-04	0.997	gil147784318[a]	1	−1.169	−1.224	−1.964	WD-40 repeat protein	35114	6.88	36020.26	7.62	169	12	MALDI-SQ
432	8	2.1	2.38E-04	0.994	gil30685604	1	1.104	−1.465	−1.864	Chaperonin 60-2, mitochondrial precursor (*A. thaliana*)	61144	5.12	61939.47	6.37	29.69	2	ESI
242	8	3.0	1.77E-03	0.923	gil147823108[a]	1	−1.125	−1.019	−2.984	Phosphoglycerate dehydrogenase	63443	5.80	64957.36	8.86	84	10	MALDI-SQ
416	8	2.1	4.59E-05	1	gil114411	1	1.084	−1.056	−1.957	ATP synthase subunit α, mitochondrial (*Phaseolus vulgaris*)	52295	5.74	55310.03	6.52	82	9	MALDI-SQ
					gil5305369					ATP synthase α-chain (*Vigna radiata*)			55274.12	6.23	81	9	
411	8	2.1	3.46E-03	0.877	gil157355637[a]	1	−1.128	−1.13	−2.141	at5g23940 mro11_2	54402	5.56	54102.45	5.46	37.04	2	ESI
379	8	2.3	4.98E-03	0.856	gil157337916[a]	1	1.071	−1.078	−2.11	Unknown protein	79033	6.30	78553.86	8.72	75	27	MALDI-SQ
366	8	2.3	1.21E-05	1	gil157337620[a]	1	−1.145	−1.155	−2.312	LOX	94591	5.38	101619.34	6.13	88	19	M ALDI-SQ
351	8	2.4	8.34E-05	0.999	gil147783188[a]	1	−1.06	−1.076	−2.362	*S*-adenosyl-L-homocysteine hydrolase	52326	5.80	53146.98	5.94	275	24	MALDI-SQ
251	8	2.9	3.05E-05	1	gil157327869[a]	1	−1.145	−1.142	−2.931	Glyceraldehyde-3-phosphate dehydrogenase	35092	6.97	34618.85	6.62	166	14	MALDI-SQ
263	8	2.9	2.02E-04	0.997	gil147797489[a]	1	−1.053	−1.374	−2.856	Multicatalytic endopeptidase complex α-subunit-like	27012	5.79	27307.91	5.91	140	12	MALDI-SQ
					gil12229897					Proteasome subunit αtype-6 (20S proteasome α-subunit A) (20S proteasome subunit α-1) (*Glycine max*)			27374.88	5.83	102	9	
264	8	2.8	4.63E-05	1	gil157346279[a]	1	−1.093	−1.21	−2.842	Enolase	51976	5.68	29832.13	5.16	214	14	MALDI-SQ
					gil157346280[a]					Enolase			18266.62	8.79	87	6	
280	8	2.8	2.05E-07	1	gil157353414[a]	1	−1.219	−1.524	−2.766	Bisphosphoglycerate-independent phosphoglycerate mutase	64722	5.52	60156.48	5.40	301	22	MALDI-SQ
					gil3914394					Bisphosphoglycerate-independent phosphoglycerate mutase (*Mesembryanthemum crystallinum*)			61145.01	5.39	88	9	
285	8	2.7	4.39E-04	0.992	gil157344266[a]	1	1.339	1.068	−2.032	Hsp70	71311	4.42	71126.08	5.17	165	43	MALDI-SQ
539*	8	1.6	5.29E-04	0.98	gil225468372[a]	1	1.058	−1.119	−1.541	Hsp70	68704	4.84	55479.89	5.11	25.76/0.05	2	ESI

Table 2. *Continued*

Spot number (g)	Statistical analysis				Accession number	Norm. Vol./Norm. Vol. FS[g]				Protein description	Spot data				Identification parameters[h]		
	Cluster	Fold	Anova (*P*)	Power		FS	4 mm	7 mm	15 mm		Experimental		Theoretical		Score[e]/ EmPAI[f]	Peptides number	Mass spectometer instrument
											Mw (Da)[c]	pI[c]	Mw (Da)[d]	pI[d]			
					gil15219234					Vacuolar ATP synthase subunit A (*A. thaliana*)			68768.83	5.11	24.32/0.05	2	
274	8	2.8	5.03E-05	1	gil147823108[a]	1	1.138	–1.06	–2.442	Phosphoglycerate dehydrogenase	63135	5.74	64957.36	8.86	129	16	MALDI-SQ
347	8	2.4	4.81E-04	0.982	gil147767264[a]	1	–1.148	–1.316	–2.377	Ketol-acid reductoisomerase	66549	5.60	63446.46	6.40	87	11	MALDI-SQ
307	8	2.6	1.92E-04	0.998	gil147805763[a]	1	–1.041	–1.315	–2.565	Proteasome subunit α type 3	26873	5.84	27173.77	6.11	73.69	6	ESI
328	8	2.5	1.61E-05	1	gil157327869[a]	1	–1.201	–1.235	–2.458	Glyceraldehyde-3-phosphate dehydrogenase	35065	6.80	34618.85	6.62	281	16	MALDI-SQ
					gil125662890					Glyceraldehyde-3-phosphate dehydogenase (*Beta vulgaris*)			36649.87	6.77	183	10	
290	8	2.7	8.49E-05	0.998	gil122893272[a]	1	–1.266	–1.414	–2.682	Flavanone 3-hydroxylase (*V. vinifera*)	42851	4.83	40787.75	5.37	94	18	MALDI-SQ
332	8	2.4	4.19E-04	0.974	gil18376653	1	1.237	–1.163	–1.962	Chalcone synthase (*V. vinifera*)	41721	6.19	42569.83	6.18	146	17	MALDI-SQ
					gil231798					Chalcone synthase 6 (*G. max*)			42504.76	5.75	86	14	
329	8	3.4	6.64E-04	0.98	gil225456471[a]	1	1.037	1.118	–2.191	ATP-dependent Clp protease, ATP-binding subunit	92190	5.37	102283.68	6.32	26.14	2	ESI
300	8	2.6	1.64E-05	1	gil147799989[a]	1	–1.009	–1.365	–2.604	20S proteasome subunit pac1	27108	5.92	27244.69	6.60	84	7	MALDI-SQ
					gil2511584[b]					Multicatalytic endopeptidase (*A. thaliana*)20S proteasome subunit pac1			27485.89	6.60	79	6	
41	8	6.2	1.16E-04	0.999	gil157355854[a]	1	1.127	–1.06	–5.483	Transketolase 1	74473	5.81	67137.09	5.95	85	18	MALDI-SQ
100	8	4.5	7.51E-06	1	gil6911553	1	1.216	–1.156	–3.665	Hsp70 (*Cucumis sativus*)	708904	4.50	70784.09	5.29	140	38	MALDI-SQ
					gil157344266[a]					Hsp70			71126.08	5.17	135	40	
97	8	4.5	7.46E-04	0.982	gil91984000	1	–1.045	–1.063	–4.544	Ribulose-bisphosphate carboxylase large subunit (*V. vinifera*)	52380	5.94	52485.54	6.33	98	25	MALDI-SQ
34	8	6.9	2.34E-04	0.996	gil91984000	1	–1.092	–1.33	–6.934	Ribulose-bisphosphate carboxylase large subunit (*V. vinifera*)	51686	6.01	52485.54	6.33	124	26	MALDI-SQ
85	8	4.8	7.21E-05	0.999	gil157337620[a]	1	1.092	1.041	–4.37	LOX	94795	5.74	101619.34	6.13	235.9	15	ESI
60	8	5.5	4.85E-06	1	gil147772088[a]	1	–1.263	–1.554	–5.451	*S*-adenosylmethionine synthetase	45910	5.63	43096.98	5.65	97	16	MALDI-SQ
55	8	5.6	2.27E-05	1	gil157359341[a]	1	1.809	1.041	–3.084	Methionine synthase	87837	6.11	84937.63	6.09	99	18	MALDI-SQ
					gil974782					Cobalamine-independent methionine synthase (*S. scutellarioides*)			86716.86	6.17	93	18	
59	8	5.5	1.72E-04	0.998	gil157352447[a]	1	–1.265	–1.7	–5.468	Serine hydroxymethyltransferase	51609	6.77	26599.86	9.10	135	7	MALDI-SQ

Table 2. *Continued*

Spot number (g)	Statistical analysis				Accession number	Norm. Vol./Norm. Vol. FS[g]				Protein description	Spot data				Identification parameters[h]		
	Cluster	Fold	Anova (*P*)	Power		FS	4 mm	7 mm	15 mm		Experimental		Theoretical		Score[e]/ EmPAI[f]	Peptides number	Mass spectometer instrument
											Mw (Da)[c]	pI[c]	Mw (Da)[d]	pI[d]			
					gil15236375					Serine hydroxymethyltransferase 4 (*A. thaliana*)			51685.18	6.80	104	11	
46	8	5.8	3.51E-04	0.992	gil7413662	1	1.22	–1.329	–4.792	Ribulose 1,5-bisphosphate carboxylase/oxygenase (*Bersama lucens*)	51723	6.11	51834.01	6.24	145	13	MALDI-SQ
189	8	3.4	2.84E-05	1	gil157337620[a]	1	–1.158	–1.652	–3.384	LOX	94782	5.62	101619.34	6.13	39.51	3	ESI
53	8	5.6	2.76E-05	1	gil157467219	1	–1.12	–1.178	–5.591	Ran3 GTP-binding protein (*I. amara*)	22698	6.25	18484.54	9.44	140	12	MALDI-SQ
					gil157339644[a]					Small ras-like GTP-binding protein			29171.59	6.45	123	13	
1	8	16.2	4.05E-06	1	gil157348808[a]	1	1.006	–1.419	–16.056	Elongation factor 2	94982	5.84	56141.58	6.08	174	19	MALDI-SQ
					gil115456914[b]					Os04g0118400 [*O. sativa* (*japonica* cultivar-group)]elongation factor 2			93912.56	5.85	97	19	
134*	9	3.8	4.05E-04	0.986	gil157342794[a]	1	–1.487	–1.454	–3.839	Aspartate aminotransferase	38317	6.72	45087.19	6.84	63.48/0.15	3	ESI
					gil147767778[a]					L-idonate dehydrogenase[f1]			39661.63	6.40	54.51/0.37	3	
					gil147781269[f1]					Fructose-bisphosphate aldolase			38606.02	8.03	35.59/–	2	
					gil462141					Glyceraldehyde-3-phosphate dehydrogenase (*A. nummularia*)			39072.99	6.41	23.09/–	2	
338	9	2.4	4.74E-05	1	gil147821099	1	–1.199	–1.367	–2.411	Protein disulfide isomerase(*V. vinifera*)	37528	5.51	39244.06	5.57	78	8	MALDI-SQ
152	9	3.7	1.28E-05	1	gil114411	1	–1.178	–1.24	–3.688	ATP synthase subunit α, mitocondrial (*P. vulgaris*)	55138	5.86	55310.03	6.52	123	22	MALDI-SQ
					gil114404					ATP synthase subunit α, mitocondrial (*Helianthus annuus*)			55451.91	6.02	120	21	
248	9	2.9	3.02E-06	1	gil157337620[a]	1	–1.165	–1.311	–2.935	LOX	94600	5.52	101619.34	6.13	181	29	MALDI-SQ
62	9	5.4	2.31E-06	1	gil59857604	1	–1.427	–1.882	–5.416	Anthocyanidin reductase (*V. vinifera*)	34999	5.81	36739.92	5.93	102	9	MALDI-SQ
410	9	2.1	9.65E-06	1	gil157353414[a]	1	–1.025	–1.293	–2.148	Bisphosphoglycerate-independent phosphoglycerate mutase	64315	5.60	60156.48	5.40	112	11	MALDI-SQ
98	9	4.5	4.77E-06	1	gil157337620[a]	1	–1.245	–1.49	–4.51	LOX	94604	5.57	101619.34	6.13	199.32	11	ESI
241	9	3.0	4.75E-05	0.999	gil147784036[a]	1	–1.274	–1.442	–2.986	T-complex protein 1 θ-chain	58884	5.95	61186.78	6.03	85	15	MALDI-SQ
112	9	4.2	2.36E-03	0.86	gil157350588[a]	1	–1.451	–1.501	–4.181	Cytosolic malate dehydrogenase	34643	5.96	35482.27	6.18	254	20	MALDI-SQ
413	9	2.1	4.92E-04	0.986	gil147853970[a]	1	–1.13	–1.164	–2.135	mal d. PR-10 protein	17051	4.44	14876.67	5.72	94	4	MALDI-SQ

Table 2. *Continued*

Spot number (g)	Statistical analysis				Accession number	Norm. Vol./Norm. Vol. FS[g]				Protein description	Spot data				Identification parameters[h]		
	Cluster	Fold	Anova (*P*)	Power		FS	4 mm	7 mm	15 mm		Experimental		Theoretical		Score[e]/ EmPAI[f]	Peptides number	Mass spectometer instrument
											Mw (Da)[c]	pI[c]	Mw (Da)[d]	pI[d]			
441	9	2.0	9.95E-06	1	gil157337766[a]	1	−1.193	−1.508	−2.017	cpn60b (chaperonin 60 β) ATP-binding protein binding unfolded protein binding	67648	4.83	64298.01	5.80	31.53	2	ESI
					gil12239607					Putative 60 kDa chaperonin β-subunit (*Catharanthusroseus*)			13961.70	8.83	29.64	2	
442	9	2.0	2.94E-05	0.999	gil157327869[a]	1	−1.176	−1.127	−2.012	Glyceraldehyde-3-phosphate dehydrogenase	35378	6.49	34618.85	6.62	339	15	MALDI-SQ
					gil125662890					Glyceraldehyde-3-phosphate dehydrogenase (*B. vulgaris*)			36649.87	6.77	253	8	
464	9	1.9	1.20E-04	0.994	gil157346978[a]	1	−1.242	−1.087	−1.934	*S*-adenosylmethionine synthetase	51300	5.29	42903.74	5.50	252	20	MALDI-SQ
					gil3024122[a]					Hypothetical protein OsJ_001504 [*Oryza sativa* (*japonica* cultivar-group)]*S*-adenosylmethionine synthetase 2			42873.61	5.68	204	14	
88	9	4.7	1.40E-03	0.901	gil157342743[a]	1	1.128	1.182	−4.006	NADP-malic enzyme	66810	6.04	54803.59	8.27	107	16	MALDI-SQ
					gil1708924					NADP-dependent malic enzyme (*V. vinifera*)			65185.77	6.09	106	17	
45	9	5.9	2.51E-04	0.984	gil974782	1	1.096	1.056	−5.387	Cobalamine-independent methionine synthase (*S.scutellarioides*)	87668	6.00	86716.86	6.17	107	17	MALDI-SQ
					gil157359341[a]					Methionine synthase			84937.63	6.09	106	16	
489	9	1.8	7.04E-05	0.998	gil157350923[a]	1	−1.361	−1.467	−1.841	Voltage-dependent anion channel	30466	6.89	29408.15	7.01	48.44	3	ESI
37	9	6.7	1.02E-04	0.998	gil147821107[a]	1	1.203	1.292	−5.218	Methionine synthase	80307	5.94	81585.59	6.19	101	14	MALDI-SQ
32	9	7.0	1.85E-04	0.994	gil157359341[a]	1	1.155	1.339	−5.255	Methionine synthase	80168	5.91	84937.63	6.09	91.88	5	ESI
28	9	7.6	6.49E-05	0.999	gil157342473[a]	1	1.003	−1.044	−7.547	Sucrose synthase	89912	5.88	92384.63	5.98	162	23	MALDI-SQ
121*	9	4.0	2.97E-04	0.989	gil157342794	1	−1.274	−1.458	−4.003	Aspartate aminotransferase[f1]	44546	7.02	45087.19	6.84	60.68/0.15	3	ESI
					gil147781269[a]					Fructose-bisphosphate aldolase			38606.02	8.03	56.34/–	3	
					gil157328511					Aminomethyltransferase			44277.79	8.73	29.74/0.09	2	
504	9	1.8	2.37E-05	1	gil13518421	1	−1.097	−1.048	−1.784	ATP synthase CF1 β-subunit (*Lotus japonicus*)	51950	5.41	53779.19	5.37	30.73	2	ESI
331	9	2.4	2.93E-04	0.971	gil122893272	1	−1.365	−1.588	−2.434	Flavanone 3-hydroxylase (*V. vinifera*)	42859	5.03	40787.75	5.37	137	16	MALDI-SQ
528	9	1.7	2.32E-05	1	gil55056878	1	−1	1.013	−1.657	ATP synthase β-subunit (*Serenoa repens*)	52273	5.49	50308.25	5.18	81	16	MALDI-SQ
326	9	2.5	3.77E-04	0.966	gil78192241	1	−1.13	−1.28	−2.464	Chalcone synthase 1 (*G.max*)	44023	6.05	41943.62	6.45	149	11	MALDI-SQ
					gil18376653					Chalcone synthase (*V. vinifera*)			42597.15	6.18	147	10	

Table 2. *Continued*

Spot number (g)	Statistical analysis				Accession number	Norm. Vol./Norm. Vol. FS[g]				Protein description	Spot data				Identification parameters[h]		
	Cluster	Fold	Anova (*P*)	Power		FS	4 mm	7 mm	15 mm		Experimental		Theoretical		Score[e]/ EmPAI[f]	Peptides number	Mass spectometer instrument
											Mw (Da)[c]	pI[c]	Mw (Da)[d]	pI[d]			
301	9	2.6	6.46E-04	0.967	gil157346978[a]	1	−1.023	1.019	−2.555	*S*-adenosylmethionine synthetase	45185	5.43	42903.74	5.50	269	15	MALDI-SQ
					gil3024122					*S*-adenosylmethionine synthetase (*O. sativajaponica* group)			42873.61	5.68	261	14	
10	9	11	6.05E-05	0.998	gil157359341[a]	1	−1.064	−1.296	−10.897	Methionine synthase	87671	6.03	84937.63	6.09	175	17	MALDI-SQ
360	9	2.3	1.95E-04	0.997	gil2765295	1	−1.021	−1.01	−2.347	Ribulose-1,5-bisphosphate carboxylase (*Physena* sp. Schatz 2350)	53019	5.86	48764.65	6.42	90	10	MALDI-SQ
151	9	3.7	1.83E-05	1	gil157329588[a]	1	−1.268	−1.539	−3.722	Pyrophosphate-dependent phosphofructokinase β-subunit	61496	6.03	61316.87	6.17	92	8	MALDI-SQ
158	9	3.7	6.58E-04	0.959	gil7798706	1	−1.425	−1.202	−3.653	Malate dehydrogenase (*V. vinifera*)	38556	6.16	36851.43	8.79	182	13	MALDI-SQ
					gil157354768[a]					Mitochondrial NAD-dependent malate dehydrogenase			36779.37	8.79	182	13	
82	9	4.9	4.29E-05	1	gil157329588[a]	1	−1.192	−1.797	−4.868	Pyrophosphate-dependent phosphofructokinase β-subunit	62024	6.11	61316.87	6.17	113	14	MALDI-SQ
230	9	3.1	5.00E-06	1	gil157336206[a]	1	−1.285	−1.475	−3.081	Dihydrolipoamide dehydrogenase precursor	57027	6.03	52886.53	6.72	103	15	MALDI-SQ

[a] Sequences of *V. vinifera* identified from NCBInr. Description in database is annotated as unnamed protein product/hypothetical protein. Description is given in table based on BLASTp performed by Blast2GO v2.3.6 software against NCBInr.
[b] Sequences identified in species other than *V. vinifera* and species indicated in brackets. BLASTp results indicated in last position.
[c] Experimental Mw (Da)/pI calculated using Progenesis PG240.
[d] Theoretical Mw (Da)/pI calculated using Compute pI/Mw tool from ExPASy.
[e] Score of identification from SpectrumMill software for ESI-MS/MS analysis and MASCOT for MALDI-MS/MS analysis.
[f] EmPAI index calculated in MASCOT. [f1] Sequence with the highest EmPAI factor from set of proteins identified in the same spot.
[g] File output from SameSpots software with detailed information about quantification of all spots detected is provided in Supplementary File S6.
[h] Detailed information of identification for ESI-MS/MS and MALDI-MS/MS is provided in Supplementary Files S4 and S5, respectively.

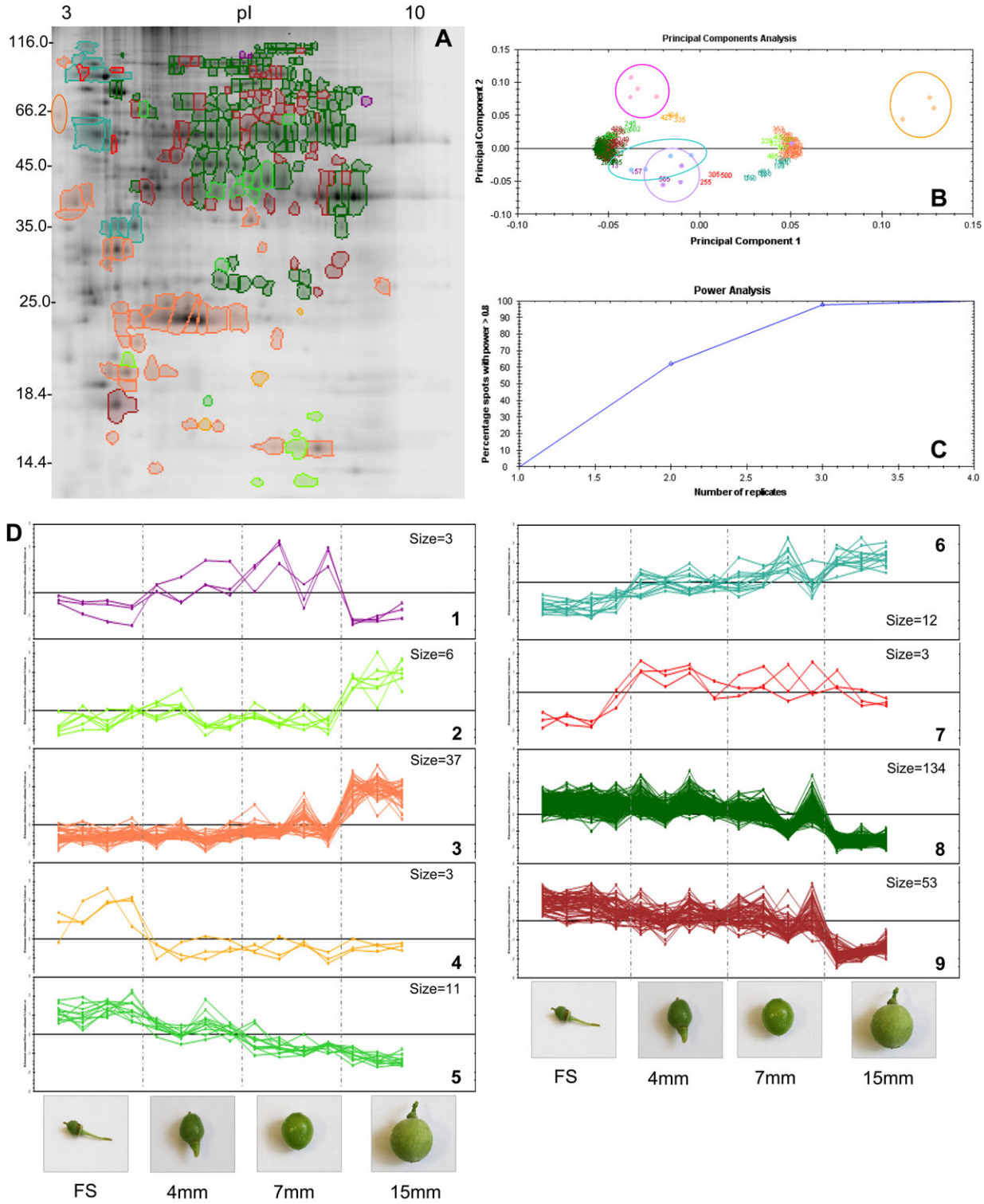

Fig. 1. 2-D DIGE analysis of first development green stages of grape berries. (A) 2-D reference map showing selected regulated protein spots and colour boundaries pertaining to the related cluster. (B) PCA plot of the two first principal components. Both together explained 87.32% of the selected spot's variability. Coloured dots and numbers are the representation of gels and spots, respectively. (C) Power analysis plot indicating the number of replicates needed to achieve a power of >80%, which represents threshold to accept significant expression change. (D) Expression profiles separated into expression pattern clusters (1–9) indicating the number of spots for each cluster. Each line represents the standardized abundance of a spot across all gels and belongs to one of the clusters generated by hierarchical cluster analysis implemented in Progenesis SameSpots. Cluster 1 included three spots whose abundance slightly increased from FS to 4 mm and switched off from 7 to 15 mm. In Cluster 6 the spot volume increases gradually from FS to 15 mm. Clusters 2, 3, and 7 contain spots that accumulate characteristically at some point of the growth phase: accumulation is sharp from 7 to 15 mm in Cluster 2; slight from 4 to 7 mm and sharp from 7 to 15 mm in Cluster 3; sharp from FS to 4 mm in Cluster 7. In contrast, Clusters 4, 8,

replicates (Fig. 2C). The 67 selected spots were classified into five clusters according to their expression patterns based on a hierarchical clustering analysis (Fig. 2D), three of them decreasing (Clusters 1, 2, and 5) and two increasing (Clusters 3 and 4) through ripening. Altogether, these results indicate that major changes during ripening occur between the V-100 and 110 g/l stages, which agrees with data reported from both transcriptomic (Terrier *et al.*, 2005) and proteomic (Giribaldi *et al.*, 2007) experiments.

The number of spots resolved in the experiments, 920 and 804 for gels of green and ripe experiments, respectively, increases the grape berry pericarp and mesocarp proteome coverage reported to date (Sarry *et al.*, 2004; Giribaldi *et al.*, 2007). If both DIGE experiments are compared, it can be clearly seen that the largest changes occur during green berry development in which 262 spots with changes up to 16-fold were found compared with 67 spots with changes up to 2.2-fold found from berry colour change to ripening. In the first experiment, 29.5% of spots of interest present a fold-change of >5.0 and 93.8% spots >2.0-fold. In the second experiment, 32.8% spots of interest present a fold-change of >1.7 and 73% >1.5. These results correlate largely with genomic (da Silva *et al.*, 2005) analysis of grape berry development. This is the first report to study at protein level the green phase of grape berries before triggering of véraison and detecting the largest shifts on proteome in pre-véraison stages of grape berries.

Seasonal changes in fully ripe grape berries.: 2-D DIGE pattern analysis of the 140 g/l stage between the 2005 and 2006 vintages resulted in 615 unique spots across the gels. According to data analysis setting (see Materials and methods), 12 spots (2% of unique spots) were selected for subsequent protein identification (fold-change of $\geqslant$1.4, ANOVA P<0.0045). Protein identity was successfully achieved for five of the selected spots. Figure 3A shows the reference gel image for this second DIGE experiment in which the selected differentially expressed spots are outlined. The unsupervised PCA bi-plot of gels and spots (Fig. 3B) shows a gel grouping that agrees with the experimental groups. The statistical quality of the analysis is quite high as for four biological replicates 100% of the selected spots had a power of >0.8 (Fig. 3C). The 12 differentially expressed spots were classified into two clusters according to their expression patterns based on a hierarchical clustering analysis (Fig. 3D). Cluster 1 contains two proteins that decreased in abundance in the 2006 season, while the remaining proteins displayed the opposite trend and were grouped into Cluster 2. Inter-seasonal biological differences represent just 2% of the proteins detected in our experiment, showing a minimal interference of environmental factors on developmental processes at the protein level. Moreover, changes observed between vintages appeared with a maximum ratio of 2.3 for phosphoenolpyruvate (PEP) carboxylase (PEPC) (Spot 1s) between those spots with statistical significance (Table 4). In the 2006 season, the maturity index reached was lower than in 2005 due to higher acidity (Fenoll *et al.* 2009). Although changes in proteins are subtle, seasonal changes might be related to normal climatological differences between years.

Protein identification and annotation

Of the 328 protein spots tested, 217 gave positive identification results, after either MALDI-TOF/TOF or ESI-MS/MS analysis followed by search on the NCBInr database. Since translated open reading frames from the grapevine genome projects (Jaillon *et al.*, 2007; Velasco *et al.* 2007) have been deployed in public databases, the searches often match an undescribed amino acid sequence. The Blast2GO application (Götz *et al.*, 2008) was then used to automatically assign protein description and take up annotations from homologous sequences of public databases, which were then manually reviewed and enriched if possible.

The complete list of identifications together with their expected and calculated molecular weight (Mw) and pI, scoring, relative abundance across growth stages, and cluster classification is reported in Tables 2 and 3 for the respective DIGE experiments. In the same format, Table 4 shows the list of identifications for the seasonal DIGE comparison.

Although the resolution of the samples in 3–10 NL, 12.5% acrylamide 18×26 cm 2-D gels is quite good (Figs 2A, 3A), co-migration of polypeptides occurred as a limitation inherent in the 2-DE technique. Thus two or more proteins were unambiguously identified in a number of spots occurring more frequently in those analysed by nLC-nESI-MS/MS when compared with MALDI-TOF/TOF. This limitation introduces uncertainty in the assignment of quantitative data to proteins in spots with multiple protein identification but, on the other hand, single protein identifications in MALDI-TOF/TOF analysed spots may just be the result of less exhaustive data acquisition and/or lower sensitivity of the technique. Overall, in 5.2% and 37% of the spots with positive identifications in the first and

and 9 contain spots whose abundance drops characteristically at some point of the growth phase: the decrease is sharp from FS to 4 mm in Cluster 4; slight from FS to 7 mm and sharp from 7 to 15 mm in Cluster 8; and sharp from 7 to 15 mm in Cluster 9. Cluster 5 grouped spots whose abundance decreases gradually from FS to 15 mm. Clusters 8 and 9 grouped 187 spots (71.6% of spots of interest) that have a kinetic profile decreasing in abundance reaching a minimum at the 15 mm stage. Dots: pink (FS), blue (4 mm), purple (7 mm), orange (15 mm). Numbers, clusters, and spot boundaries: purple (Cluster 1 spots), light green (Cluster 2 spots), orange (Cluster 3 spots), yellow (Cluster 4 spots), green (Cluster 5 spots), blue (Cluster 6 spots), red (Cluster 7 spots), dark green (Cluster 8 spots), brown (Cluster 9 spots).

Table 3. Proteins differentially expressed in DIGE covering ripening (V-100, 110 g/l, 140 g/l)

Selection and quantification of spots of interest was assisted by Progenesis SameSpots software v3.0. Spots selected were classified into five different clusters according to their protein abundance profile among analysed stages. Spots were excised from the gel, trypsin in-gel digested, and the eluted peptides were analysed by mass spectrometry (MALDI-MS/MS and/or ESI-MS/MS). Proteins were identified by MS/MS search against NCBInr protein database using MASCOT and SpectrumMill.

	Statistical spot analysis					Norm. Vol./Norm. Vol.V				Spot data[g]				Identification parameters[h]		
Spot number (r)	Cluster	Fold	ANOVA (*P*)	Power	Accession number	V-100	110g/l	140 g/l	Protein description	Experimental		Theoretical		Peptides number	Score[e]/ EmPAI[f]	Mass spectrometer instrument
										Mw[c] (Da)	pI[c]	Mw[d] (Da)	pI[d]			
180	1	1.3	4.20E-04	0.999	gil147787750[a]	1	1.001	–1.249	23 kDa polypeptide of oxygen-evolving complex	21761.6	5.58	27794.3	8.32	3	36.98	ES
30	1	1.7	1.01E-02	0.859	gil225426403[a]	1	1.141	–1.462	Glutathione peroxidase	210345.4	5.44	18659.50	6.73	2	36.95	ESI
5	2	1.9	8.32E-04	0.995	gil1552553	1	–1.632	–1.943	17kDaHSP(*Medicago sativa*)	185601.4	5.57	17996.15	7.74	4	93	MALDI-SQ
					gil99033697				Chaperone (*Agave tequilana*)			17738.04	5.97	4	93	
67	2	1.5	9.84E-03	0.862	gil157337427[a]	1	–1.502	–1.394	Ascorbate peroxidase	247331.2	5.60	27153.1	5.86	4	89.34	ESI
9	2	1.9	6.94E-03	0.901	gil157356616[a]	1	–1.855	–1.171	Phospholipid hydroperoxide Glutathione peroxidase	204725.1	5.84	18671.3	6.73	13	35.12	ESI
14*	2	1.8	3.39E-04	0.999	gil147787082[a]	1	–1.77	–1.785	Cyclophilin[f1]	191631.2	8.95	17938.5	8.93	4	74/1.34	ESI
					gil147835636[a]				60S ribosomal protein L12			17792.7	9.02	4	73.47/0.41	ESI
49	2	1.6	1.34E-03	0.988	gil15227552	1	–1.564	–1.549	17.6 kDa class I small HSP(*A. thaliana*)	19447.9	5.55	17551.96	6.33	2	33.04	ESI
					gil157344152				Unnamed protein product Hsp20 (*Medicago truncatula*)			17040.75	5.80	2	30.39	
4*	3	2.0	2.72E-06	1	gil147809484[a]	1	2.016	1.896	Dienelactone hydrolase family protein[f1]	252641.9	4.35	26284.0	5.04	5	109.47/0.81	ESI
					gil157347902[a]				Dienelactone hydrolase family protein[f1]			25503.2	5.15	6	100.93/0.81	
					gil157356344[a]				Hypothetical protein			27731.95	5.74	3	58.63/0.04	
					gil157354789[a]				Uridylate kinase UMP kinase			29204.6	7.10	3	54.4/0.3	
6*	3	1.9	1.01E-04	1	gil7798706	1	1.665	1.928	Malate dehydrogenase (*V. vinifera*)[f1]	341168.1	5.53	36874.8	8.79	7	144.18/0.29	ESI
					gil157352053[a]				Auxin-induced protein expressed			37935.60	5.66	6	91.55/0.18	
					gil157339324[a]				Nitrilase member 2			33447.06	5.78	4	72.21/0.08	
					gil157349479[a]				Legumin-like protein			38508.97	5.56	4	68.44/0.13	
					gil115457794[b]				Os04g0339400[(*O. sativa* (*japonica* cultivar-group)] auxin-induced protein pcnt115			38273.7	5.66	2	37.99/–	
54	3	1.6	2.35E-04	1	gil147797489[a]	1	1.276	1.55	Multicatalytic endopeptidase complex α-subunit-like	241583.3	5.67	27307.91	5.91	10	87	MALDI-SQ
13*	3	1.8	1.03E-07	1	gil147790725[a]	1	1.526	1.801	Aldo-keto reductase family protein	338539.0	5.80	37054.4	5.70	10	185.12/0.81	ESI
					gil7798706				Mitochondrial NAD-dependent malate dehydrogenase (*V. vinifera*)			36874.8	8.79	7	127.08/0.82	

Table 3. *Continued*

Spot number (r)	Statistical spot analysis				Accession number	Norm. Vol./Norm. Vol.V			Protein description	Spot data[g]				Identification parameters[h]		
	Cluster	Fold	ANOVA (*P*)	Power		V-100	110g/l	140 g/l		Experimental		Theoretical		Peptides number	Score[e]/ EmPAI[f]	Mass spectrometer instrument
										Mw[c] (Da)	pI[c]	Mw[d] (Da)	pI[d]			
					gil157349479[a]				Legumin-like protein			38508.97	5.56	5	95.16/0.18	
					gil462141				Glyceraldehyde-3-phosphate dehydrogenase (*Atriplexnummularia*)			39072.99	6.41	2	37.16/0.09	
					gil118486112				Unknown protein (*P. trichocarpa*) protein, plastidic aldolase			42494.4	8.64	2	31.21/–	
23	3	1.7	9.15E-05	1	gil157337528[a]	1	1.706	1.59	Ripening-related protein Grip22	265185.3	4.33	22798.7	4.92	2	30.74	ESI
118*	3	1.4	2.00E-04	1	gil7798706	1	1.256	1.381	Mitochondrial NAD-dependent malate dehydrogenase (*V. vinifera*)[f1]	328356.1	5.93	36874.8	8.79	5	103.51/0.6	ESI
					gil157353103[a]				Quinone oxidoreductase			35188.00	6.00	3	55.24/–	
					gil157338864[a]				Protein, plastidic aldolase			42867.04	8.85	3	61.85/0.28	
120	3	1.4	8.84E-04	0.994	gil157355881[a]	1	1.154	1.373	Enolase	817626.3	5.71	47570.7	5.99	2	33.69	ESI
29	3	1.7	5.32E-05	1	gil110748606	1	1.674	1.629	Cystatin (*Amaranthus hypochondriacus*)	243799.7	5.88	27719.03	5.67	7	86	MALDI-SQ
					gil52851072				Cysteine protease inhibitor (*Populus tremula*)			15589.13	6.51	5	82	
21*	3	1.7	3.84E-03	0.948	gil33329392	1	1.721	1.704	Class IV chitinase (*V. vinifera*)	257469.5	4.11	27510.58	5.38	2	38.71/0.12	ESI
					gil157348253[a]				Isopentenyl pyrophosphate isomerase[f1]			26922.8	4.99	3	51.21/0.45	
					gil157337528[a]				Ripening-related protein grip22			22783.59	4.92	3	42.17/0.14	
					gil157347902[a]				Dienelactone hydrolase family protein			25503.2	5.15	2	29.58/–	
					gil547680				Hsp70 [*Plasmodium cynomolgi* (strain BEROK)]			74603.1	5.51	2	29.02/–	
31	3	1.7	4.19E-02	0.623	gil2306813	1	1.533	1.666	Class IV endochitinase (*V. vinifera*)	258805.5	3.89	27537.5	5.38	2	35.3	ESI
100	3	1.4	3.86E-06	1	gil157354111[a]	1	1.315	1.419	Glyceraldehyde-3-phosphate dehydrogenase	356302.2	6.63	37113.6	7.72	2	32.38	ESI
99	3	1.4	1.07E-04	1	gil147781269[a]	1	1.294	1.42	Glyceraldehyde-3-phosphate dehydrogenase	339905.9	6.40	38606.02	8.03	7	135.4	ESI
					gil157327869[a]				Glyceraldehyde-3-phosphate dehydrogenase			34640.8	6.62	4	81.88	
					gil125972661				Glyceraldehyde-3-phosphate dehydrogenase (*Clostridium thermocellum*)			36116.35	6.11	2	43.19	
19	3	1.8	2.94E-02	0.692	gil157348466[a]	1	1.723	1.761	β-1–3 glucanase	286128.8	5.83	36653.79	8.45	3	60.38	ESI
43	3	1.6	7.44E-04	0.996	gil76262748	1	1.582	1.42	Chitinase-B (*Sorghum halepense*)	243122.0	6.51	16691.08	9.14	5	80	MALDI-SQ

Table 3. *Continued*

Spot number (r)	Statistical spot analysis				Accession number	Norm. Vol./Norm. Vol.V			Protein description	Spot data[g]				Identification parameters[h]		
	Cluster	Fold	ANOVA (*P*)	Power		V-100	110g/l	140 g/l		Experimental		Theoretical		Peptides number	Score[e]/ EmPAI[f]	Mass spectrometer instrument
										Mw[c] (Da)	pI[c]	Mw[d] (Da)	pI[d]			
					gil48093320				Chitinase (*Zea mays* subsp. *parviglumis*)			28853.45	8.30	6	74	
44	3	1.6	5.08E-04	0.998	gil157344048[a]	1	1.398	1.577	60S acidic ribosomal protein p0	330618.1	6.01	34253.97	5.22	3	58.97	ESI
					gil157351143				60Sacidic ribosomal protein p0 (*Euphorbia esula*)			34260.01	5.23	2	42.53	
98*	3	1.4	3.81E-04	0.999	gil147781269[a]	1	1.255	1.421	Fructose-bisphosphate aldolase	347892.1	6.26	38630.5	8.03	7	123.75/0.08	ESI
					gil157354111[a]				Glyceraldehyde-3-phosphate dehydrogenase[f1]			37113.6	7.72	7	108.43/0.99	
					gil147766093[a]				DTDP-glucose 4–6-dehydratase			38789.6	6.47	4	61.97/0.09	
					gil157345376[a]				GDSL-motif lipase hydrolase family protein			42159.9	6.35	3	60.87/–	
					gil120669				Glyceraldehyde-3-phosphate dehydrogenase (*Magnolia liliiflora*)			36982.6	7.09	4	58.41/–	
					gil125972661				Glyceraldehyde-3-phosphate dehydrogenase [*C. thermocellum* (ATCC 27405)]			36139.4	6.11	2	37.80/–	
18*	3	1.8	9.39E-05	1	gil33329392	1	1.761	1.688	Class IV chitinase (*V. vinifera*)[f1]	266125.3	4.06	27510.58	5.38	4	61.59/0.25	ESI
					gil157337528[a]				Ripening-related protein Grip22			22783.59	4.92	2	26.86	
88	3	1.4	2.74E-04	1	gil147797489[a]	1	1.377	1.437	Multicatalytic endopeptidase complex α-subunit-like	241236.1	5.79	27307.91	5.91	5	84.16	ESI
75	3	1.5	2.41E-02	0.728	gil7406716	1	1.36	1.466	Putative thaumatin-like protein (*V. vinifera*)	220869.2	3.89	24051.1	4.94	5	87.35	ESI
72*	3	1.5	1.02E-02	0.858	gil157340295[a]	1	1.333	1.476	Aspartate aminotransferase[f1]	362966.6	5.77	36906.96	6.35	10	185.04/0.79	ESI
					gil147778328[a]				Reversibly glycosylated polypeptide			41671.2	5.30	9	133.93/0.36	
					gil147843754[a]				Cytosolic phosphoglycerate kinase 1			42395.72	6.29	7	120.25/0.16	
					gil157335296[a]				(1–4)-β-mannan endohydrolase			48935.28	9.19	3	49.13/0.07	
					gil157338864[a]				Protein, plastidic aldolase			42867.04	8.85	3	45.70/–	
					gil157350587[a]				Malate dehydrogenase			35496.28	6.18	2	35.47/0.09	
					gil157327869[a]				Glyceraldehyde-3-phosphate dehydrogenase			34618.85	6.62	2	33.79/–	

Table 3. *Continued*

Spot number (r)	Statistical spot analysis				Accession number	Norm. Vol./Norm. Vol.V			Protein description	Spot data[g]				Identification parameters[h]		
	Cluster	Fold	ANOVA (*P*)	Power		V-100	110g/l	140 g/l		Experimental		Theoretical		Peptides number	Score[e]/ EmPAI[f]	Mass spectrometer instrument
										Mw[c] (Da)	pI[c]	Mw[d] (Da)	pI[d]			
					gil21388544				Putative mitochondrial NAD-dependent malate dehydrogenase (*S. tuberosum*)			36195.1	8.87	2	25.86/–	
68	3	1.5	5.52E-03	0.921	gil147821107[a]	1	1.383	1.498	Methionine synthase	793612.1	5.92	81643.1	6.19	10	191.97	ESI
60	3	1.5	1.65E-04	1	gil157359341[a]	1	1.392	1.527	Methionine synthase	798903.6	5.95	84937.63	6.09	11	198.53	ESI
123	4	1.4	2.18E-04	1	gil76559896	1	1.332	1.357	Isoflavone reductase-like protein 6 (*V. vinifera*)	311113.5	5.88	33942.0	6.55	8	142.25	ESI
24*	4	1.7	2.83E-05	1	gil157349479[a]	1	1.569	1.706	Legumin-like protein	335762.0	5.67	38508.97	5.56	4	83.68/0.13	ESI
					gil7798706				Mitochondrial NAD-dependent malate dehydrogenase (*V. vinifera*)			36874.8	8.79	4	78.21/0.09	
					gil147790725[a]				Aldo-keto reductase family protein			37054.4	5.70	3	54.96/0.18	
					gil118486112				Unknown protein (*P. trichocarpa*) protein, plastidic aldolase			42494.4	8.64	3	49.34/–	
64	4	1.5	5.37E-03	0.924	gil157355881[a]	1	1.38	1.52	Enolase	489164.6	5.90	47570.7	5.99	9	152.71	ESI
					gil162458207				Enolase1 (*Z. mays*)			48063.8	5.20	3	37.08	
114	4	1.4	7.50E-04	0.996	gil157354841[a]	1	1.273	1.39	Proteasome-like protein α-subunit-like	250245.1	6.63	27178.17	6.62	10	93	MALDI-SQ
					gil12229936				Proteasome subunit α type-7 (20S proteasome α-subunit D) (20S proteasome subunit α-4) (*Cicer arietinum*)			27080.14	6.86	9	85	
117	4	1.4	9.25E-03	0.87	gil12229904	1	1.248	1.383	Proteasome subunit α type-4 (20S proteasome α-subunit C) (20S proteasome subunit α-3)(*Petunia×hybrida*)	244404.6	5.91	27232.0	5.60	4	79.37	ESI
90	4	1.4	2.03E-02	0.757	gil225455555[a]	1	1.275	1.435	Enolase	492595.1	5.79	48110.3	6.16	4	75.54	ESI
83*	4	1.5	1.05E-03	0.992	gil157341175[a]	1	1.199	1.456	V-ATPase subunit C[t1]	392034.3	5.79	40176.7	6.73	11	188.5/0.81	ESI
					gil147784261[a]				Translational elongation factor EF-TuM			48900.37	6.54	4	77.9/0.14	
					gil157353900[a]				Alcohol dehydrogenase			41253.83	5.97	5	77.17/0.26	
					gil157345376[a]				GDSL-motif lipase hydrolase family protein			42159.9	6.35	2	44.02/0.08	
					gil94312255				Elongation factor Tu (*Ralstonia metallidurans* CH34)			43088.6	5.42	2	38.6/–	
92*	4	1.4	1.08E-02	0.851	gil157335296[a]	1	1.171	1.431	(1–4)-β-mannan endohydrolase	350113.6	5.66	48935.28	9.19	5	101.50/0.22	ESI
					gil157352185[a]				Apospory-associated protein c			35352.91	5.75	5	99.71/–	

Table 3. *Continued*

Spot number (r)	Statistical spot analysis				Accession number	Norm. Vol./Norm. Vol.V			Protein description	Spot data[g]				Identification parameters[h]		
	Cluster	Fold	ANOVA (*P*)	Power		V-100	110g/l	140 g/l		Experimental		Theoretical		Peptides number	Score[e]/ EmPAI[f]	Mass spectrometer instrument
										Mw[c] (Da)	pI[c]	Mw[d] (Da)	pI[d]			
					gi157350588[a]				Cytosolic malate dehydrogenase			35482.27	6.18	4	68.18/0.09	
					gi157343704[a]				Aldose 1-epimerase-like protein[f1]			36998.35	5.91	3	56.66/0.43	
					gi147843754[a]				Cytosolic phosphoglycerate kinase 1			42395.72	6.29	3	52.68/0.08	
					gi1169534				Enolase(*Ricinus communis*)			47912.7	5.56	2	42.72/0.07	
					gi157340295[a]				Aspartate aminotransferase			43603.40	6.13	2	34.39/–	
17	5	1.8	3.83E-04	0.999	gi40714365	1	–1.404	–1.766	Maturase K (*Tristicha trifaria*)	703638.1	8.37	61427.49	9.70	7	70	MALDI-PMF
70*	5	1.5	1.01E-04	1	gi157344048[a]	1	–1.439	–1.484	60S acidic ribosomal protein p0	323329.1	4.98	34253.97	5.22	2	44.48/0.1	ESI
					gi157336525[a]				Selenocysteine methyltransferase			35925.16	5.42	2	42.81/–	
73*	5	1.5	4.94E-04	0.998	gi147787750[a]	1	–1.448	–1.474	23 kDa polypeptide of oxygen-evolving complex[f1]	228067.3	5.03	27777.07	8.33	6	116.94/0.96	ESI
					gi147864536[a]				L-asparaginase L-asparagine amidohydrolase			32504.1	5.01	6	112.36/0.59	
					gi157343051[a]				Multicatalytic endopeptidase proteasome β-subunit			24981.59	5.46	2	37.93/–	
					gi157348112[a]				Soluble inorganic pyrophosphatase			26455.6	5.48	2	36.66/–	
82*	5	1.5	1.05E-04	1	gi115461951[b]	1	–1.29	–1.456	Os05g0135700 [*O. sativa* (*japonica* cultivar-group)]*S*-adenosylmethionine synthetase[f1]	434614.4	5.48	43220.2	5.74	5	91.55/0.55	ESI
					gi157346978[a]				*S*-adenosylmethionine synthetase			42903.74	5.50	4	81.58/0.25	
					gi147794688[a]				GDP-mannose-3,5-epimerase			42563.7	5.94	4	74.17/0.16	
					gi115469764				Os06g0701100 [*O. sativa* (*japonica* cultivar-group)] Eukaryotic initiation factor 4a			47088.2	5.37	4	48.59/0.07	
					gi147772088[a]				*S*-adenosylmethionine synthetase			43126.1	5.65	2	40.06/0.34	
56*	5	1.5	3.78E-03	0.949	gi157352072[a]	1	–1.541	–1.49	GDP-mannose-3,5-epimerase[f1]	419861.5	5.66	42516.00	5.94	11	203.94/0.68	ESI
					gi157348748[a]				Eukaryotic translation initiation factor 3			51094.07	5.84	5	83.5/–	
					gi147818879[a]				Ornithine aminotransferase			52191.6	6.29	3	47.50/–	
					gi157349001[a]				Protein disulfide isomerase			45925.0	5.24	2	40.77/–	

Table 3. *Continued*

Spot number (r)	Statistical spot analysis				Accession number	Norm. Vol./Norm. Vol.V			Protein description	Spot data[g]				Identification parameters[h]		
	Cluster	Fold	ANOVA (*P*)	Power		V-100	110g/l	140 g/l		Experimental		Theoretical		Peptides number	Score[e]/ EmPAI[f]	Mass spectrometer instrument
										Mw[c] (Da)	pI[c]	Mw[d] (Da)	pI[d]			
					gil533474				2-Phospho-D-glycerate hydrolase(*M. crystallinum*)			48308.43	5.62	2	39.75/0.07	
62*	5	1.5	8.11E-03	0.885	gil157352072[a]	1	−1.523	−1.325	GDP-mannose-3,5-epimerase[f1]	426077.6	5.73	42516.00	5.94	10	192.38/0.81	ESI
					gil157348748[a]				Eukaryotic translation initiation factor 3			51094.07	5.84	4	71.48/–	
					gil157328672[a]				Cysteine desulfurase			49815.41	6.66	2	38.01/–	
52	5	1.6	2.39E-04	1	gil157352512[a]	1	−1.286	−1.557	Abscisic stress ripening protein	218471.3	5.49	16138.46	5.75	8	120	MALDI-SQ
					gil86156026				Abscisic stress ripening protein (*V. pseudoreticulata*)			16678.88	5.68	8	118	
51*	5	1.6	3.63E-03	0.951	gil115461951[b]	1	−1.317	−1.561	Os05g0135700 [*O. sativa* (*japonica* cultivar-group)]*S*-adenosylmethionine synthetase	431151.9	5.56	43220.2	5.74	4	74.35/0.08	ESI
					gil116786814[a]				Unknown (*Picea sitchensis*) GDP-mannose 3,5-epimerase[f1]			42578.7	6.11	4	71.42/0.16	
					gil147772088[a]				*S*-adenosylmethionine synthetase			43126.1	5.65	3	56.33/–	
93	5	1.4	3.57E-03	0.952	gil81074298	1	−1.431	−1.316	Hsp90 (*S. tuberosum*)	763735.6	4.33	80417.0	5.08	3	48.37	ESI
47	5	1.6	5.17E-04	0.998	gil147787750[a]	1	−1.303	−1.572	23 kDa polypeptide of oxygen-evolving complex	229794.1	5.49	27777.07	8.33	5	78.01	ESI
37*	5	1.6	4.13E-05	1	gil147838052[a]	1	−1.473	−1.617	Cyclase family protein[f1]	304938.2	4.86	29869.4	5.15	4	86.56/0.69	ESI
					gil157346032[a]				Proteasome inhibitor-related			31554.55	5.55	2	38.46/0.22	
35*	5	1.6	5.49E-04	0.998	gil157347388[a]	1	−1.423	−1.622	Chlorophyll a/b binding protein	235186.5	5.38	29511.17	7.84	3	47.84/0.11	ESI
					gil157343051[a]				Multicatalytic endopeptidase proteasome β-subunit			24981.59	5.46	2	44.45/–	
					gil147787750[a]				23 kDa polypeptide of oxygen-evolving complex			27777.07	8.33	2	36.28/0.12	
					gil157360245[a]				Glutathione *S*-transferase[f1]			25569.14	6.06	2	27.83/0.23	
101	5	1.4	1.05E-03	0.992	gil15234354	1	−1.418	−1.401	*S*-adenosylmethionine synthetase 2 (*A. thaliana*)	447852.5	5.64	43255.3	5.67	4	72.21	ESI
					gil157336233[a]				*S*-adenosylmethionine synthetase			43086.77	5.65	3	58.61	
105*	5	1.4	9.11E-06	1	gil114421	1	−1.383	−1.407	ATP synthase subunit β, mitocondrial precursor (*Nicotiana plumbaginifolia*)[f1]	501457.9	4.20	59856.5	5.95	10	199.39/0.45	ESI
					gil147766743[a]				Protein binding protein transporter structural molecule			34935.0	5.21	6	102.15/0.31	

Table 3. *Continued*

Spot number (r)	Statistical spot analysis				Accession number	Norm. Vol./Norm. Vol.V			Protein description	Spot data[g]				Identification parameters[h]		
	Cluster	Fold	ANOVA (*P*)	Power		V-100	110g/l	140 g/l		Experimental		Theoretical		Peptides number	Score[e]/ EmPAI[f]	Mass spectrometer instrument
										Mw[c] (Da)	pI[c]	Mw[d] (Da)	pI[d]			
					gil147792855[a]				Alanine aminotransferase			74874.3	8.09	6	101.99/0.13	
					gil18394812				Tubulin β-5 chain (*A. thaliana*)			50342.8	4.66	5	87.73/0.21	
					gil157329479[a]				Glutaredoxin s17			44049.5	5.09	3	50.86/–	
					gil157342710[a]				Mitochondrial-processing peptidase subunit α			54438.01	5.71	3	64.04/0.06	
					gil46909263				ATP synthase β-subunit (*Saccoglossus kowalevskii*)[f1]			46088.8	4.93	2	40.71/0.39	
					gil157360713[a]				HSP-associated protein-like			42976.5	4.88	2	26.81/–	
107	5	1.4	1.86E-03	0.98	gil147864536[a]	1	–1.363	–1.403	L-Asparaginase L-asparagine amidohydrolase	228081.2	5.18	32477.87	5.01	6	84	MALDI-SQ
86	5	1.4	1.02E-03	0.993	gil147856076[a]	1	–1.443	–1.369	Aldo-keto reductase family protein	324383.6	4.78	34939.54	5.95	5	78.72	ESI
27*	5	1.7	6.85E-03	0.902	gil147787082[a]	1	–1.687	–1.652	Cyclophilin	194905.8	7.32	17926.90	8.93	3	50.64/1.34	ESI
					gil157345480				DNA-binding protein-related (*A. thaliana*)[f1]			15281.92	7.84	2	42.74/2.33	
66	5	1.5	2.26E-04	1	gil809113	1	–1.432	–1.512	33 kDa precursor protein of oxygen-evolving complex (*S. tuberosum*)	275006.3	4.69	35235.92	5.86	7	75	MALDI-PMF
10	5	1.8	4.34E-05	1	gil147838052[a]	1	–1.715	–1.827	Cyclase family protein	305555.3	4.62	29869.4	5.15	4	77.18	ESI
22*	5	1.7	1.76E-02	0.781	gil147865627[a]	1	–1.72	–1.673	Major latex-like protein	18952.1	3.95	17093.53	5.12	2	32.74	ESI
					gil157328903[a]				Polyphenol oxidase			67318.92	6.06	3	47.22	
58*	5	1.5	1.74E-03	0.982	gil3269288	1	–1.304	–1.529	Benzoquinone reductase-like protein (*A. thaliana*)[f1]	219630.9	5.35	22312.8	6.30	2	37.59/0.32	ESI
					gil157331849				Quinone oxidoreductase (*V. vinifera*)[f1]			25559.1	6.05	2	36.9/0.32	
					gil14582465				Abscisic stress ripening protein unnamed protein product (*V. vinifera*).			16703.1	5.68	2	36.38/–	
124	5	1.4	8.01E-03	0.886	gil157328903[a]	1	–1.357	–1.333	Polyphenol oxidase	189012.1	4.21	67318.92	6.06	2	39.2	ESI
175*	5		9.50E-03	0.867	gil157345071[a]	1	–1.204	–1.256	Potential mitochondrial protein fmp13[f1]	861070.8	4.16	44099.0	5.05	8	138.11/0.25	ESI
					gil157339226[a]				Epsin N-terminal homology domain-containing protein			60266.4	4.82	7	119.52/–	
					gil157358962				Peroxisomal targeting signal 1 receptor (*Nicotiana tabacum*)			46851.3	5.28	3	54.37/–	
					gil123656				Chloroplast envelope membrane 70 kDa heat shock-related protein (*Spinacia oleraceae*)			71731.7	5.34	3	33.87/–	
					gil445126				HspHSP81-1(*A. thaliana*)			81192.6	4.95	2	32.32/–	

Table 3. *Continued*

Spot number (r)	Statistical spot analysis				Accession number	Norm. Vol./Norm. Vol.V			Protein description	Spot data[g]				Identification parameters[h]			
	Cluster	Fold	ANOVA (P)	Power		V-100	110g/l	140 g/l		Experimental		Theoretical		Peptides number	Score[e]/ EmPAI[f]	Mass spectrometer instrument
										Mw[c] (Da)	pI[c]	Mw[d] (Da)	pI[d]			
					gil57336053[a]				Protein disulfide isomerase			55636.33	5.93	2	29.75/–	
2	5	2.2	6.54E-04	0.997	gil147791852[a]	1	–1.511	–2.191	33 kDa precursor protein of oxygen-evolving complex	273944.6	4.47	33212.82	5.87	14	349	MALDI-SQ
					gil11134054				33 kDa precursor protein of oxygen-evolving complex (*N. tabacum*)			35206.02	5.89	12	263	

[a] Sequences of *V. vinifera*identified from NCBInr. Description in database is annotated as unnamed protein product/hypothetical protein. Description is given in table based on BLASTp performed by Blast2GO v2.3.6 software against NCBInr.
[b] Sequences identified in species other than *V. vinifera* and species indicated in brackets. BLASTp results indicated in last position.
[c] Experimental Mw (Da)/pI calculated using Progenesis PG240.
[d] Theoretical Mw (Da)/pI calculated using Compute pI/Mw tool from ExPASy.
[e] Score of identification from SpectrumMill software for ESI-MS/MS analysis and MASCOT for MALDI-MS/MS analysis.
[f] EmPAI index calculated in MASCOT. [f1] Sequence with the highest EmPAI factor from set of proteins identified in the same spot.
[g] File output from SameSpots software with detailed information about quantification of all spots detected is provided in Supplementary File S7.
[h] Detailed information of identification for ESI-MS/MS and MALDI- MS/MS is provided in Supplementary Files S4 and S5, respectively.

second DIGE experiments, respectively, more than one protein was found. Multiple protein identification in spots is not often discussed in literature; Vincent *et al.* (2007) found that 4% of excised spots (8 of 199), present multiple protein identifications in grapevine shots and Méchin *et al.* (2004) reported that almost 10% of excised spots (60 of 632) contained cross-contamination in maize seeds. Gygi *et al.* (2000) detected the presence of six different proteins in the same spot ranging from 47.9 to 67.7 kDa and from 5.09 to 5.54 for pI. In order to give an estimate of the abundance of each identified protein within the same spot, the emPAI index (Rappsilber *et al.*, 2002; Ishihama *et al.*, 2005; Yang *et al.*, 2007) as provided in MASCOT searches has been included in Tables 2 and 3.

Proteome changes during development

Figure 4 provides a global picture of the proteome changes between the sampled time-points of grape berry formation. Using the cut-off values of fold-change mentioned above, Fig. 4A shows the total and the positively identified number of spots up- and down-regulated and Fig. 4B the average and the highest fold-change. Median and mean values were very similar, therefore the average is represented by mean data only. The largest changes in both number of spots (234) and fold-change (up to 12-fold) occur during the final stage of green berry development from 7 to 15 mm and where down-regulation was clearly dominant. From FS to 4 mm and from 4 to 7 mm, a similar number of spots changed (33 and 34, respectively) but some changes were clearly larger in the first period (up to 6-fold). Up-regulation was dominant from FS to 4 mm, while down-regulation affects more spots from 4 to 7 mm. During berry mesocarp ripening, most spots changing (50 compared with 67 spots) were found in the stage from V-100 to 110 g/l, with a maximal fold-change of 2. These results suggest that the most important changes at protein level take place at onset of ripening as previous data from genomic (da Silva *et al.*, 2005), oligo/microarray transcriptomic (Terrier *et al.*, 2005; Waters *et al.*, 2005) and proteomic (Giribaldi *et al.*, 2007) studies have also indicated.

Functional distribution of identified proteins

Figure 5 shows a comparative distribution of functional classes between green development (from FS to 15 mm) and ripening (from V-100 to 140 g/l) of the identified and differentially expressed proteins. Some functional groups represent similar proportions of the regulated and identified proteome in both berry formation periods. These include energy metabolism, carbohydrate metabolism, amino acid metabolism, protein fate, stress response, and protein synthesis. The finding of a high frequency of regulated proteins involved in carbohydrate metabolism and energy agrees with previous proteomic results (Sarry *et al.*, 2004; Giribaldi *et al.*, 2007) and genomic studies (Pilati *et al.*, 2007; Deluc *et al.*, 2007). On the other hand, a higher frequency of regulated proteins was found involved in amino acid metabolism than that observed in the proteome

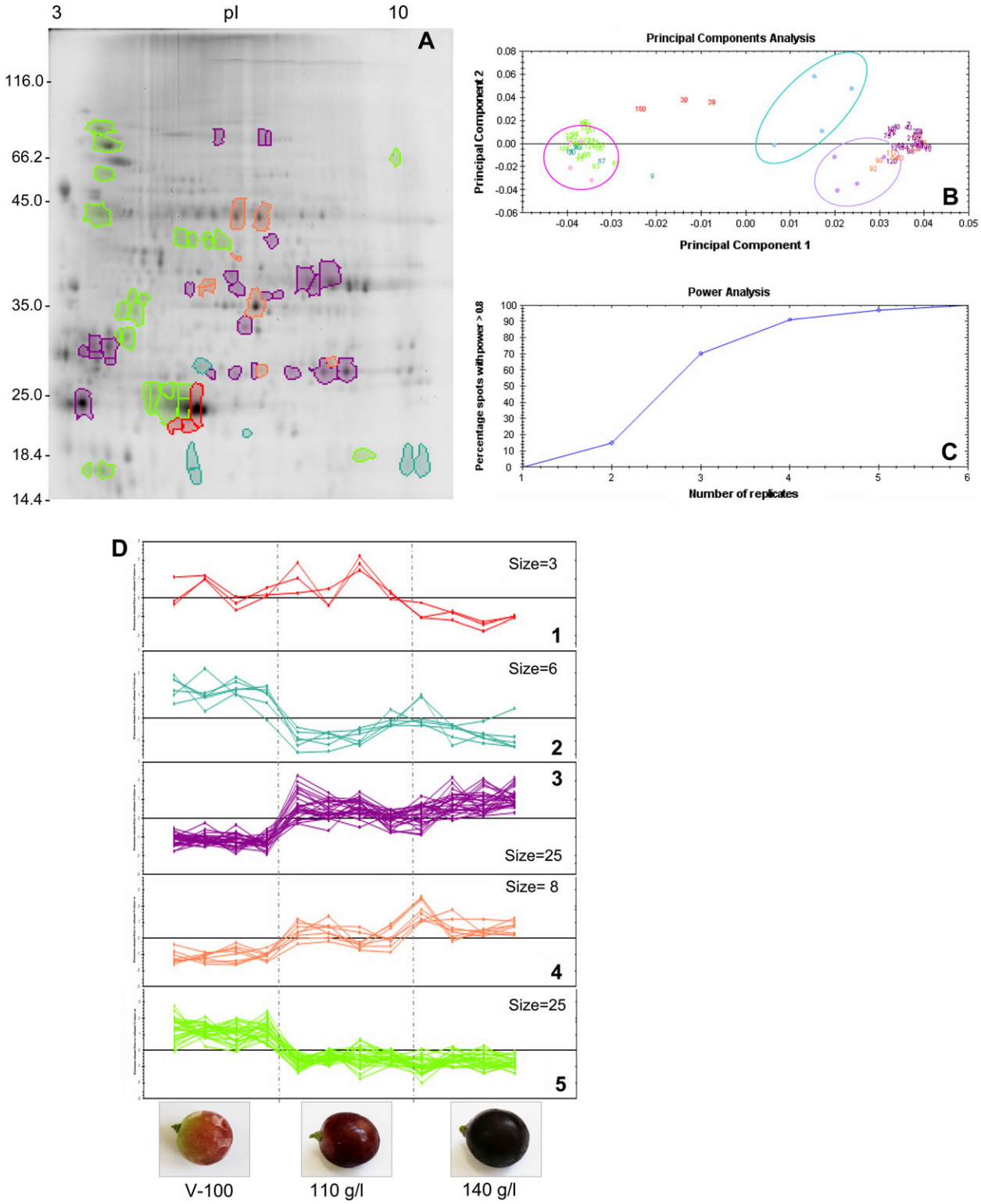

Fig. 2. 2-D DIGE analysis of ripening of grape berries. (A) 2-D reference map showing selected regulated protein spots and colour boundaries pertaining to the related cluster. (B) PCA plot of the first two principal components. Both together explained 81.25% of the selected spot's variability. Coloured dots and numbers are the representation of gels and spots, respectively. (C) Power analysis plot indicating the number of replicates needed to achieve a power of >80%, which represents the threshold to accept significant expression change. (D) Expression profiles separated into expression pattern clusters (1–5) indicating the number of spots for each cluster. Each line represents the standardized abundance of a spot across all gels and belongs to one of the clusters generated by hierarchical cluster analysis implemented in Progenesis SameSpots. Clusters 1, 2, and 5 contain proteins that decrease in abundance during ripening. In Cluster 1, the abundance decreases from 110 g/l to 140 g/l, while in Clusters 2 and 5 there is a sharp decrease from V-100 to 110 g/l. In addition, in Cluster 2 a slight increase in abundance from 110 g/l to 140 g/l occurs. Cluster 3 and 4 contain the proteins that

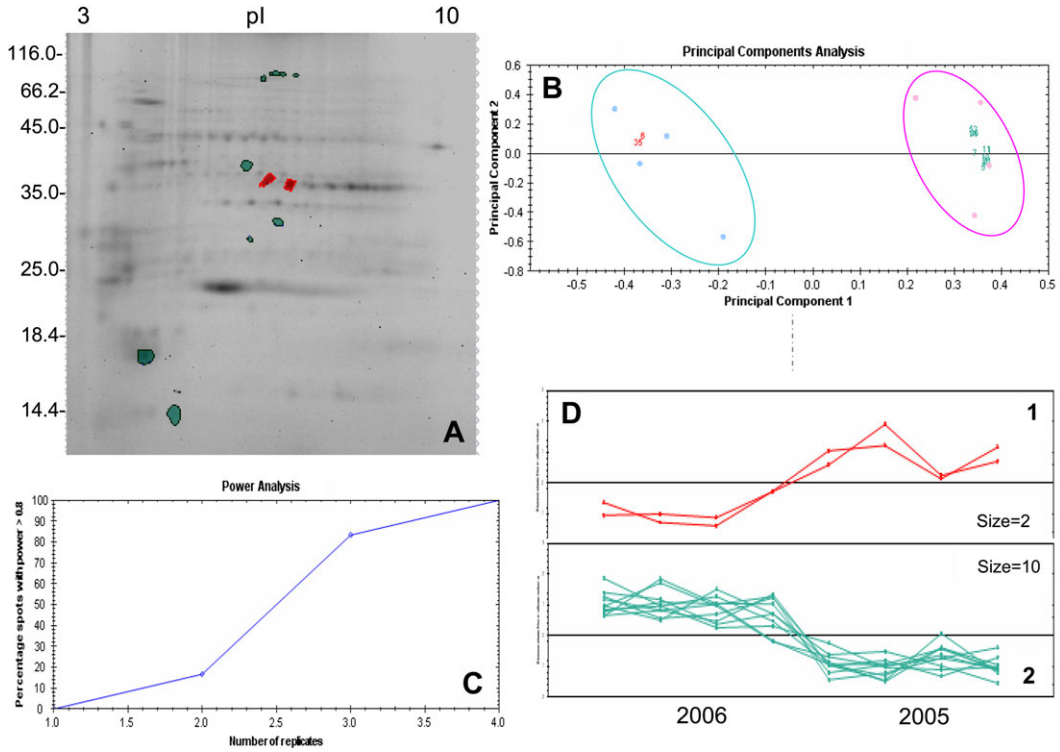

Fig. 3. 2-D DIGE analysis of seasonal changes of ripe grape berries. (A) 2-D reference map showing selected regulated protein spots and colour boundaries pertaining to the related cluster. (B) PCA plot of the two first principal components. Both together explain 80.12% of the selected spot's variability. Coloured dots and numbers are the representation of the gels and the spots respectively. (C) Power analysis plot indicating number of replicates needed to achieve a power of >80%, which represents the threshold to accept significant expression change. (D). Expression profiles separated into expression pattern clusters (1–2) indicating number of spots for each cluster. Each line represents the standardized abundance of a spot across all gels and belongs to one of the clusters generated by hierarchical cluster analysis implemented in Progenesis SameSpots. Dots: pink (2006), blue (2005). Numbers, clusters, and spot boundaries: red (Cluster 1 spots), blue (Cluster 2 spots).

of whole berries (Giribaldi *et al.*, 2007) or isolated mesocarp (Sarry *et al.*, 2004).

Conversely, there are some functional groups whose differential expression occurs more extensively in one of the berry formation periods. On the one hand, secondary metabolism, hormone biosynthesis and regulation, nucleotide metabolism, DNA replication and repair, and signal transduction appear more differentially expressed in the green period than in the ripening period. A high proportion of proteins involved in secondary metabolism were found strongly differentially expressed during the first growth period. Previous proteomic studies started berry development profiling at advanced green berry stages, thus missing that relevant information. As discussed below in detail, the profiles of proteins and transcripts (Deluc *et al.*, 2007) of secondary metabolism correlate extensively in this period. On the other hand, defence response, vesicular trafficking, nitrogen metabolism, nutrient reservoir, and transcription are more differentially expressed in the ripening period. The clear rise in proteins involved in defence from green pericarp to ripe mesocarp is consistent with the increasing expression of defence proteins from véraison (see below), involved in the protection of sugar-accumulating fruit from pathogen attack.

Proteins expressed differentially between the 2005 and 2006 vintages were mainly related to carbohydrate and organic acid metabolism (Spots 1s, 20s, 35s; Table 4). One of these, PEPC, a key enzyme for malate metabolism, increased 2.26-fold on average towards the 2006 season. However, PEPC was not found differentially expressed during development and ripening in our experiments. Fenoll *et al.* (2009) reported a higher acidity of juice (pH 6.2±0.1 compared with 5.2±0.1) without significant changes in total soluble solids (19.7±0.1 °Brix compared with 19.4±0.1) and thus, a lower maturity index (3.17±0.04 compared with 3.74±0.06) in the 2006 than in the 2005 vintage for the same Muscat Hamburg samples. As PEPC participates in the production of oxalacetic acid from PEP to drive the glycolysis pathway into malate synthesis, differences in PEPC levels between vintages may be relevant for the final

accumulate during ripening. The accumulation is rather gradual in Cluster 4 and sharp from V-100 to 110 g/l in Cluster 3. Dots: pink (V-100), blue (110 g/l), purple (140 g/l). Numbers, clusters, and spot boundaries: red (Cluster 1 spots), blue (Cluster 2 spots), purple (Cluster 3 spots), orange (Cluster 4 spots), light green (Cluster 5 spots).

Table 4. Proteins differentially expressed in DIGE of seasonal analysis at 140 g/l stage inthe 2005 and 2006 seasons

Selection and quantification of spots of interest was assisted by Progenesis SameSpots software v3.0. Spots selected were classified into two different clusters according to their protein abundance profile among analysed stages. Spots were excised from the gel, trypsin in-gel digested, and the eluted peptides were analysed by mass spectrometry (MALDI-MS/MS and/or ESI-MS/MS). Proteins were identified by MS/MS search against the NCBInr protein database using MASCOT and SpectrumMill.

	Statistical spot analysis					Norm. Vol./Norm. Vol. 2005[e]			Spot data				Identification parameters[f]		
Spot number (s)	Cluster	Fold	ANOVA (*P*)	Power	Accession number	2005	2006	Protein description	Experimental		Theoretical		Score[d]	Mass spectrometer instrument	Peptides number
									Mw[b] (Da)	pI[b]	Mw[c] (Da)	pI[c]			
35	1	1.4	0.00357	0.968	gil157350587[a]	1	–1.410	Malate dehydrogenase. cytosolic	37180.07	6.85	35496.28	6.18	8	137.95	ESI
20	2	1.6	0.00142	0.995	gil157337907[a]	1	1.581	Cytoplasmic aconitate hydratase	100289.54	6.40	109986.71	6.66	4	53.96	ESI
14	2	1.6	0.00408	0.96	gil7406710	1	1.619	Putative ripening-related protein, grip61 (*V. vinifera*)	17525.39	4.59	17065.50	5.12	6	73	MALDI-SQ
3	2	2.1	0.00396	0.962	gil17402583	1	2.09	Xyloglucan endo-transglycosylase (*Vitis labrusca*× *V. vinifera*)	28698.99	6.63	32733.91	5.55	6	89	MALDI-SQ
1	2	2.3	1.31E-05	1	gil147770696[a]	1	2.255	Phosphoenolpyruvate carboxylase	103671.68	6.72	110252.82	6	12	94	MALDI-SQ

[a] *V. vinifera* sequence identified from NCBInr. Description in database as unnamed protein product/hypothetical protein. Description is given in table based on BLASTp performed by Blast2GO v2.3.6 software against NCBInr.
[b] Experimental Mw (Da)/pI calculated using Progenesis PG240.
[c] Theoretical Mw (Da)/pI calculated using Compute pI/Mw tool from ExPASy
[d] Score of identification from SpectrumMill software for ESI-MS/MS analysis and MASCOT for MALDI-MS/MS analysis.
[e] File output from SameSpots software with detailed information about quantification of all spots detected is provided in Supplementary File S8.
[f] Detailed information of identification for ESI-MS/MS and MALDI- MS/MS is provided in Supplementary File S4 and S5, respectively.

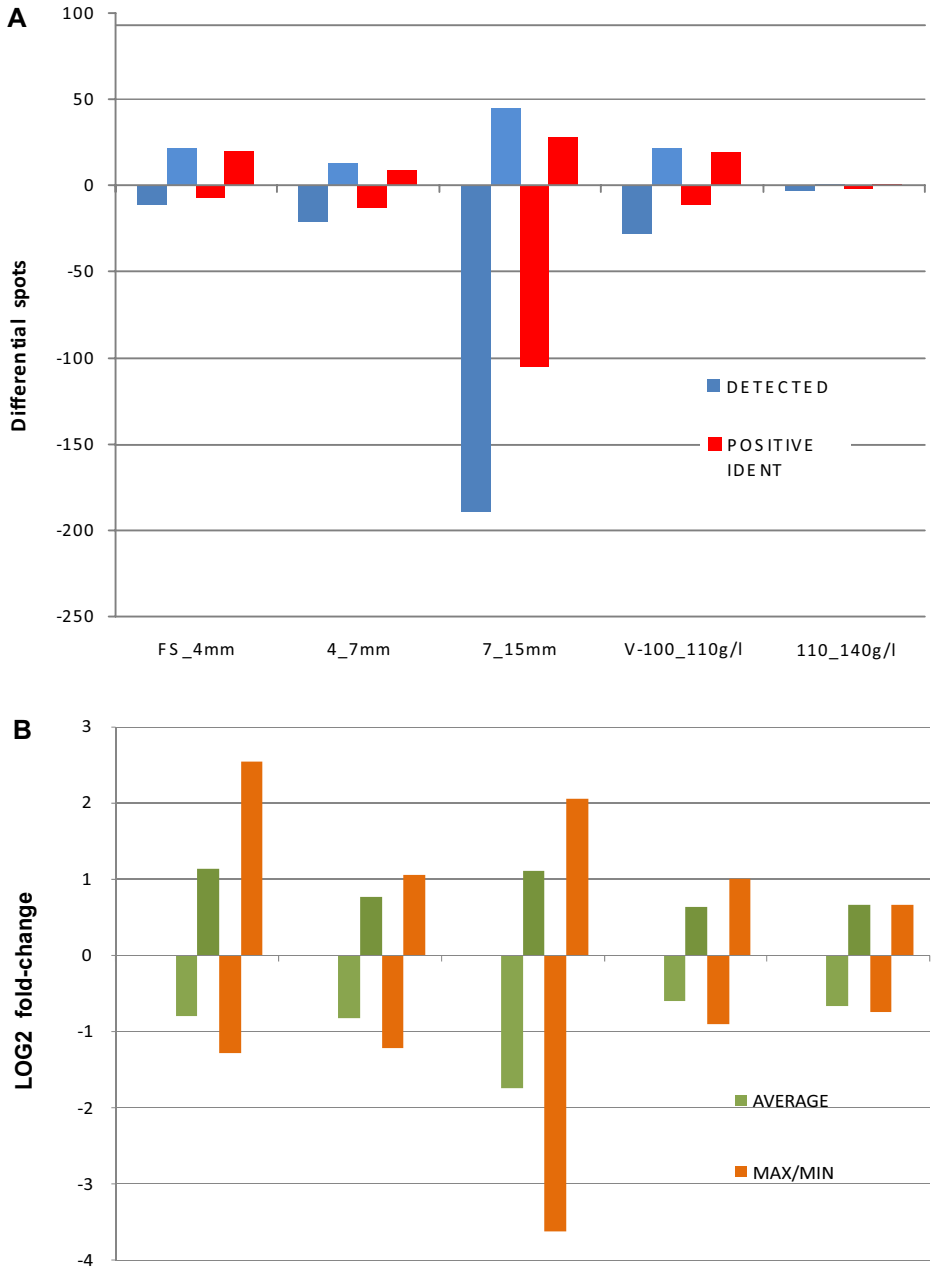

Fig. 4. Overall changes in protein level across berry development. Each value represents (A) the number of spots differentially expressed between two developmental stages, for all proteins detected (blue columns) and all proteins identified (red bars), and (B) the fold-change of regulated protein spots, represented as mean (green) and max/min (orange) changes.

sugar-to-acid balance and thus in the quality parameters of the grape berry. During development, slight changes have been reported at protein level in PEPC, which is translationally and post-translationally regulated and presents decreasing activity throughout ripening (Hawker, 1969; Famiani *et al.*, 2000, Sweetman *et al.*, 2009). Furthermore, in C3 plants such as wheat, PEPC has been suggested to carry out an important role in the adaptation of plants to environmental changes (González *et al.*, 2003), thus supporting the seasonal variations of its levels. Additionally, two proteins were up-regulated in the 2006 season; a XET enzyme (Spot 3s) participating in cell wall remodelling; and grip61 (Spot 14s) ripening-specific protein whose expression is restricted to berries in grape (Davies and Robinson, 2000). The relatively few changes in protein levels obtained in a long time frame experiment through two growing seasons suggest a minimal effect of external conditions on plant development. Thus, proteome changes observed in previous DIGE experiments are more likely to be developmental and ripening specific.

Sugar and organic acid metabolism (Figs 6A, 7A).: The sugar and organic acid metabolism in developing and ripening grape berries have been well characterized at accumulated metabolite level for several decades (Swanson and Elshinshiny, 1958; Hale, 1962; Ruffner and Kliewer,

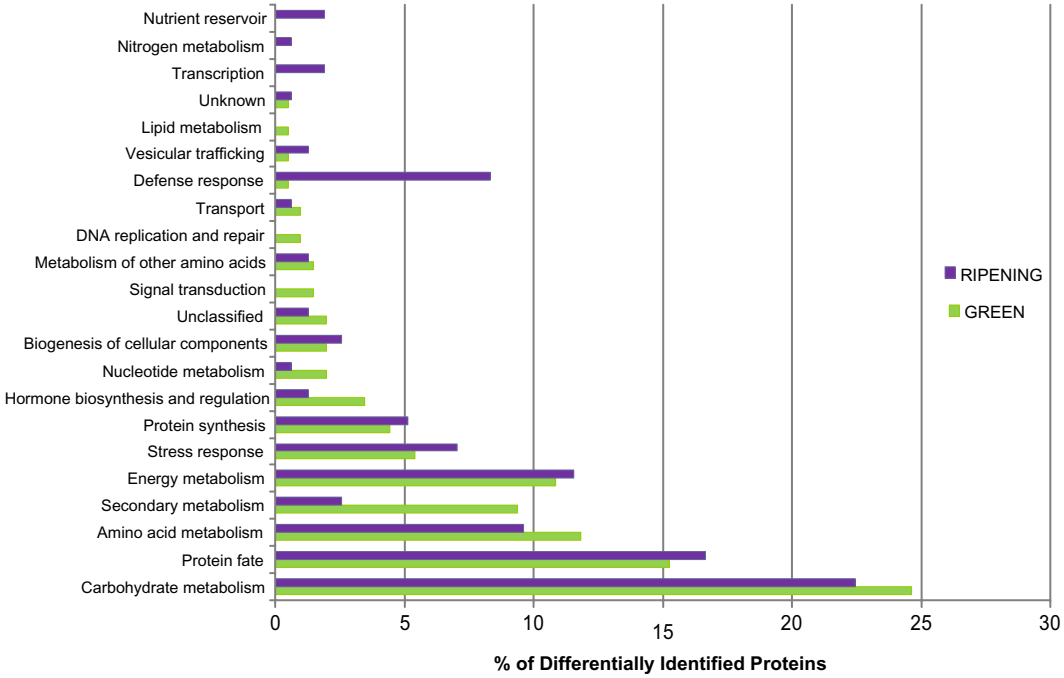

Fig. 5. Functional classification of proteins. Distribution of proteins identified between the first growth period (FS, 4 mm, 7 mm, 15 mm) in green bars and ripening (V-100, 110 g/l, 140 g/l) in purple bars. Percentages are based upon the number of proteins identified in each set.

1975; Ruffner and Hawker, 1977; Ruffner, 1982). Malate is the main organic acid stored in vacuoles of grape berry cells, which accumulates from fruit set until véraison. The major carbon source for malate synthesis is the imported carbohydrates although the carbon fixed through photosynthesis which occurs in the fruit at this phase of development may also contribute to malate synthesis (Sweetman *et al.*, 2009 for review). Just before véraison there is a switch from net accumulation to degradation of malate: accumulation of malate from sugar conversion stops, thus imported sugars are accumulated, while stored malate begins to be used for different pathways of the primary and secondary metabolism and malate is consumed.These processes have been subsequently investigated at the biochemical, molecular, and most recently global transcript and protein levels (Conde *et al.*, 2007 and Sweetman *et al.*, 2009 for reviews). However, many gaps remain.

Here, numerous changes in expression of proteins were found involved in sucrose metabolism, glucolysis/gluconeogenesis, malate and tartrate metabolism, and the tricarboxylic acid cycle. Most of the spots in the green stages (Fig. 6A), belong to Clusters 8 and 9 thus having similar pattern through the first growth period. Eight different glycolytic enzymes have been detected in a total of 14 spots showing a slight decrease in abundance through the early stages of development and a sharp decrease at the end of this growth period, which supports evidence for inhibition of glycolysis at véraison (Ruffner and Hawker, 1977). Two proteins, pyrophosphate-dependent phosphofructokinase (PFP) (Spots 82g, 151g) and pyruvate kinase (PK) (Spot 70g), are key points in glycolysis pathway control. PFP, unlike phosphofructokinase-1 (PFK-1), catalyses reversibly the conversion of fructose 6-phosphate to fructose 1,6-bisphosphate in plants, and is not negatively regulated by PEP or ATP. A possible advantage of PFP over PFK-1 as catalyst of this step in the grape berry is that the glycolytic flow may proceed independently of the accumulation of final products (PEP) or the energy status of the cell (ATP) and, as the reaction is nearly in equilibrium, the flow direction would be conditioned only by substrate availability. The profile of PFP and the rest of the glycolytic enzymes during green development supports that the flux is opened allowing for the continuous net conversion of imported sugars into precursors of malic acid until the lag phase, when the enzymes are down-regulated. Famiani and coworkers (2000) found that PFP has decreased expression through development as well as other enzymes involved in carbohydrate metabolism (GAPDH and aldolase), showing decreasing glycolytic activity that is known to be inhibited from véraison (Ruffner and Hawker, 1977). Previous studies report that glycolysis is down-regulated after véraison in pulp, seeds, and skin (Famiani *et al.*, 2000; Negri *et al.*, 2008). The results shown here indicate that the deactivation of the glycolytic pathway in pericarp of berries begins prior to colour change at véraison. As highlighted in Fig. 8, where a 3-D image of abundance of selected proteins is shown, the profile of sucrose synthase (SuSy) (Spots 9g, 28g) and UDP-glucose pyrophosphorylase (UDP-GP) (Spots 96g, 153g), which are responsible for the conversion of imported sucrose into glycolysis substrates, runs parallel to key glycolytic enzymes (PFP). SuSy and UDP-GP undergo a dramatic down-regulation at the end of this growth period of up to –10.5-fold and –4.5-fold, respectively. The profile of SuSy

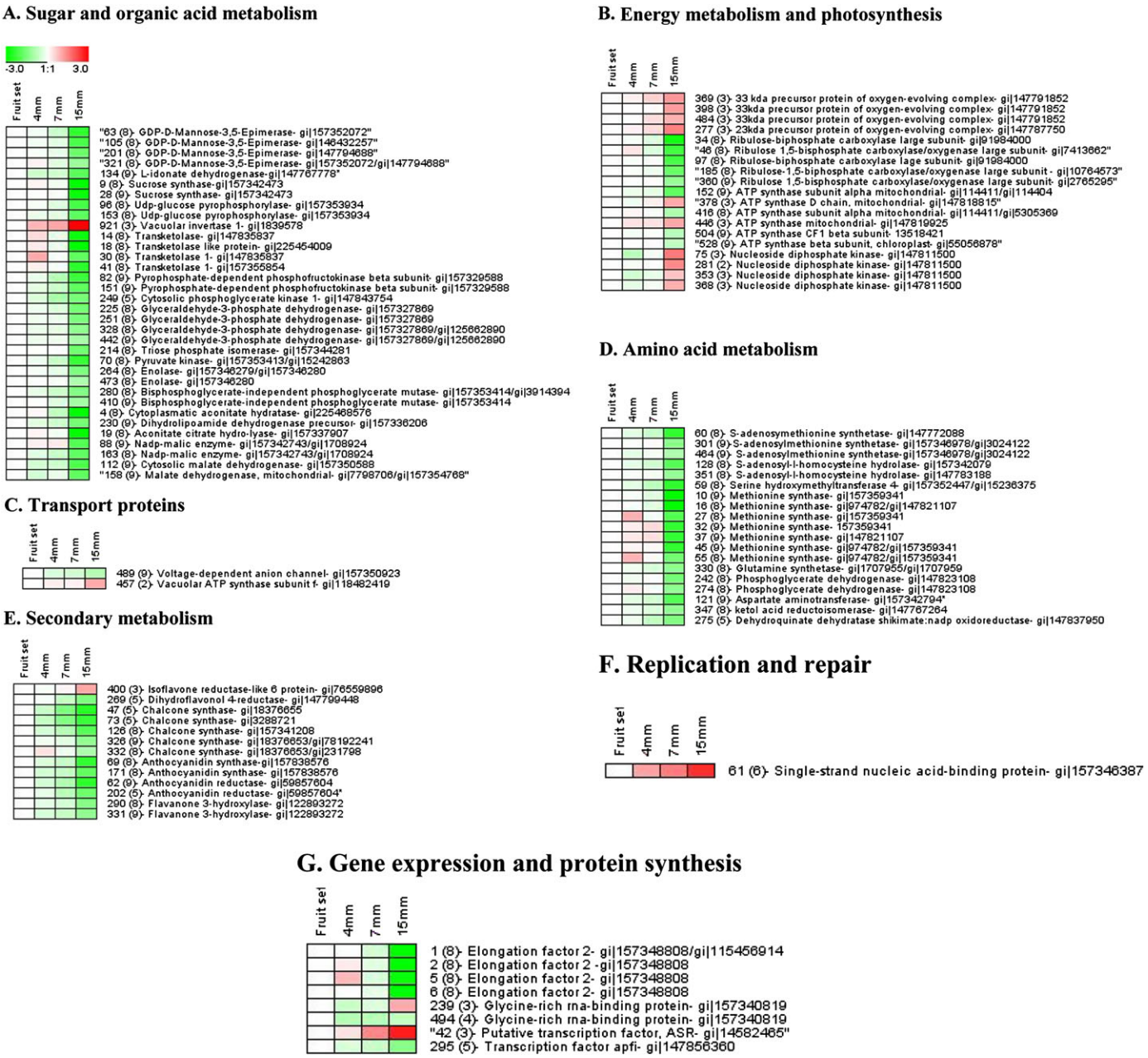

Fig. 6. Profiles of protein functional clusters during first growth period. A heat map of the relative abundance of proteins during the first growth period in relation to the FS stage was made using Genesis v1.0 (Sturn *et al.* 2002) with with $\log_2$ normalized volume for each spot. For each protein are given the spot number, number of cluster in brackets, the gene index accession number, and the sequence description assigned with Blast2GO. Proteins marked with an asterisk are those that pertain to a multiple protein spot and whose EmPAI index from MASCOT indicates a major contribution to the abundance of that spot. Proteins were grouped according to their known or putative role in metabolic pathways or cellular processes.

contrasts with that of vacuolar invertase (INV) (Spot 921g), which is almost opposite with a dramatic increase of 14-fold in the lag phase. This switch between SuSy and INV strongly correlates with the fate of sucrose being converted into malate during green development and into glucose and fructose from véraison to full ripening (Ruffner and Hawker, 1977). Taken together the profiles of sucrose-metabolizing and glycolytic enzymes suggest that the major control point for the fate of sucrose is the splitting reaction catalysed by either SuSy or INV. Between véraison (V-100) and full ripening (140 g/l) the spot containing INV did not undergo significant changes (1.2-fold, P=0.33), thus supporting the continuous accumulation of glucose and fructose in roughly equal amounts due to the action of the INV enzyme (Boss and Davies, 2001). Agasse *et al.* (2009) reported updated known mechanisms in sugar transport and sensing in grape. In their review, they correlate the existence of a functional mechanism related between INV and SuSy based in studies carried out in tomato, although there was no clear evidence provided, to support such

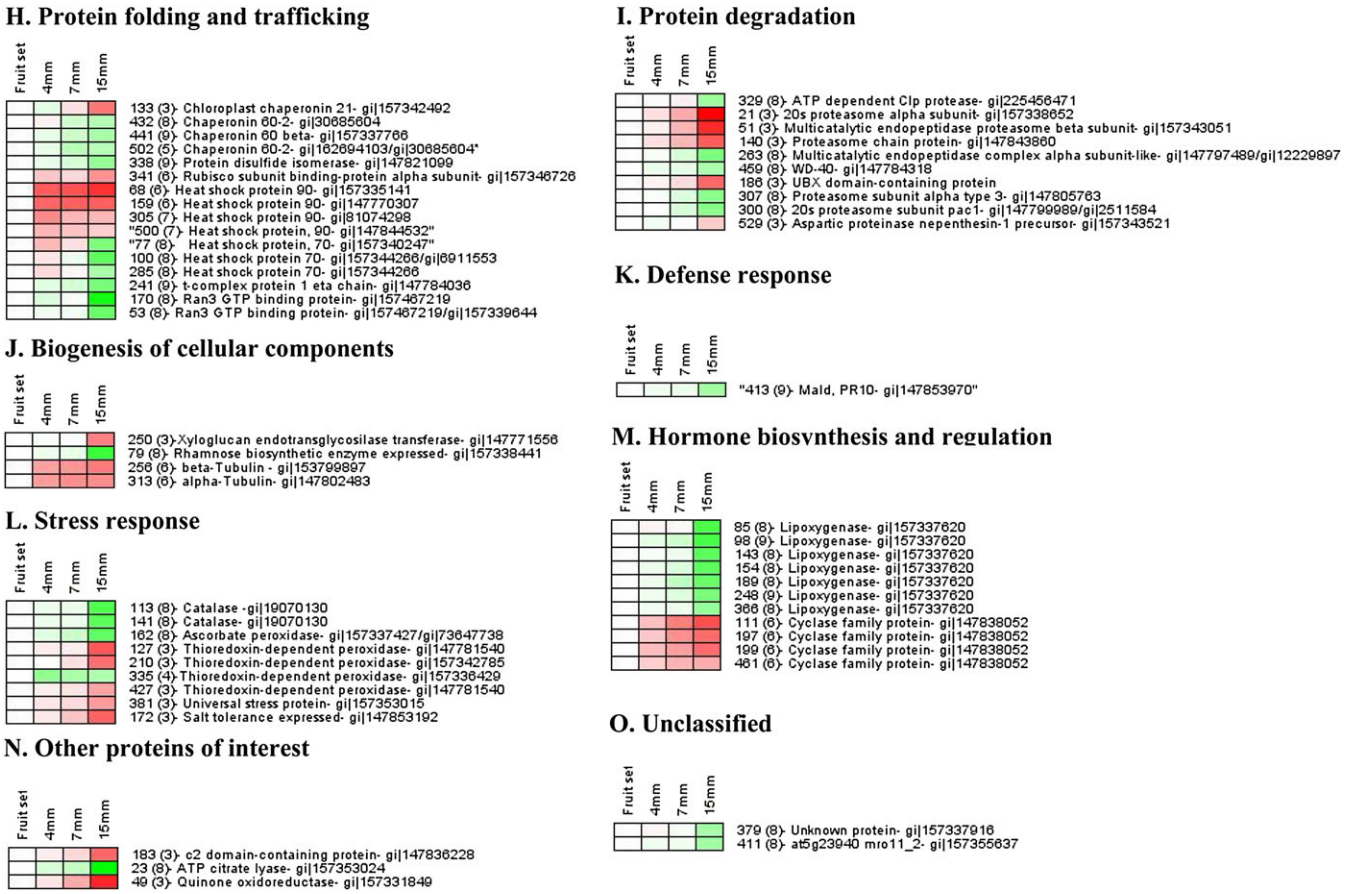

Fig. 6. Continued

a hypothesis in grape. In tomato, SuSy (not INV) is involved in sugar unloading and metabolism at the beginning of fruit development (Dali *et al.*, 1992; D'Aoust *et al.*, 1999; N'tchobo *et al.*, 1999). Later in maturation, SuSy activity is strongly reduced but sucrose unloading rates are maintained and might be driven by both sugar uptake and INV activity (D'Aoust *et al.* 1999; Nguyen-Quoc and Foyer 2001) while in grapes INV activity was found to be important in driving the import of sugars during ripening (Takayanagi and Yokotsuka, 1997). The quantitative proteomic results presented here reveal experimental evidence of this coordinate function between INV and SuSy, with a switch taking place at the pre-véraison stage (7–15 mm) and thus, support the hypothesis sustained based on previous physiological studies performed in grape and tomato.

In the flesh of ripening berries only two glycolytic/gluconeogenic enzymes, GAPDH and enolase, were found to be up-regulated in relation to V-100 indicating a reactivation of the pathway or part of it during ripening. The recent analysis of transcriptomic profiles of this pathway and earlier radiolabelling studies have led to the conclusion that gluconeogenesis could be occurring during ripening via conversion of malate to PEP by the action of cytosolic malate dehydrogenase (cMDH) and PEPCK (Beriashvili and Beriashvili, 1996; Sweetman *et al.*, 2009). Da Silva *et al.* (2005) found two transcripts, an enolase and a fructose-bisphosphatase aldolase, up-regulated during initial phase of berry growth and then after onset of véraison. This suggests that the glycolytic pathway is providing carbon skeletons as PEP to the phenylpropanoid pathway when flavonoid biosynthesis is most active (Downey *et al.*, 2003, 2004).

Malate metabolism in fruits is dependent on fruit physiology, enzyme isoforms, tissue and subcellular compartmentalization of enzymes, and availability of substrates (for review Sweetman *et al.*, 2009). In grapes, malate shows an accumulation pattern with a maximum in a pre-véraison stage before ripening is triggered (Terrier and Romieu, 2001). Cytosolic (cMDH) (Spot 112g) and mitochondrial (mMDH) (Spot 158g) isoforms of MDH and two spots containing cytosolic NADP-dependent malic enzyme (NADP-ME) (Spots 88g, 163g) showed a high level during early development with a sharp decrease in abundance at the end of the first growth period. Further, two spots containing mMDH (Spots 6r, 118r) increased in abundance after véraison and during ripening. The protein profiles described here correlate well with gene expression and enzyme activity data in grape berries. On the one hand, mMDH expression is high in early development (Or *et al.*, 2000) and on the other hand, total NAD-dependent MDH activity shows a minimum level at véraison while in early development and throughout ripening it is high (Taureilles-Saurel *et al.*, 1995). Currently, cMDH is believed to be responsible for most of the malate synthesis until véraison,

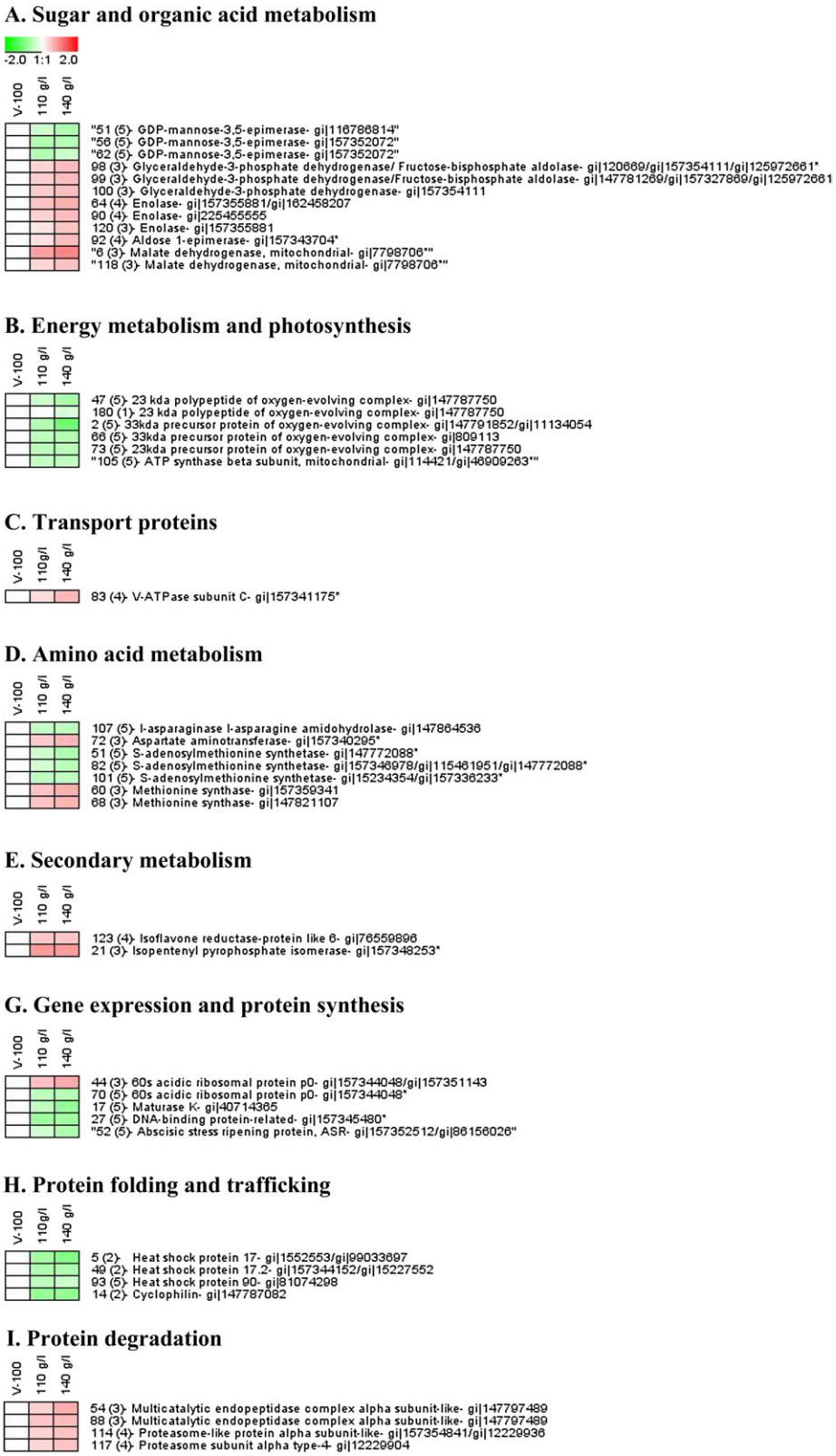

Fig. 7. Profiles of protein functional clusters during ripening. A heat map of the relative abundance of proteins during the ripening period in relation to the véraison (V-100) stage was made using Genesis v1.0 (Sturn *et al.* 2002) with $\log_2$ normalized volume for each spot. For each protein are given spot number, number of cluster in brackets, the gene index accession number, and the sequence description assigned with Blast2GO. Proteins marked with an asterisk are those that pertain to a multiple protein spot and whose EmPAI index from MASCOT indicates a major contribution to the abundance of that spot. Proteins were grouped according to their known or putative role in metabolic pathways or cellular processes.

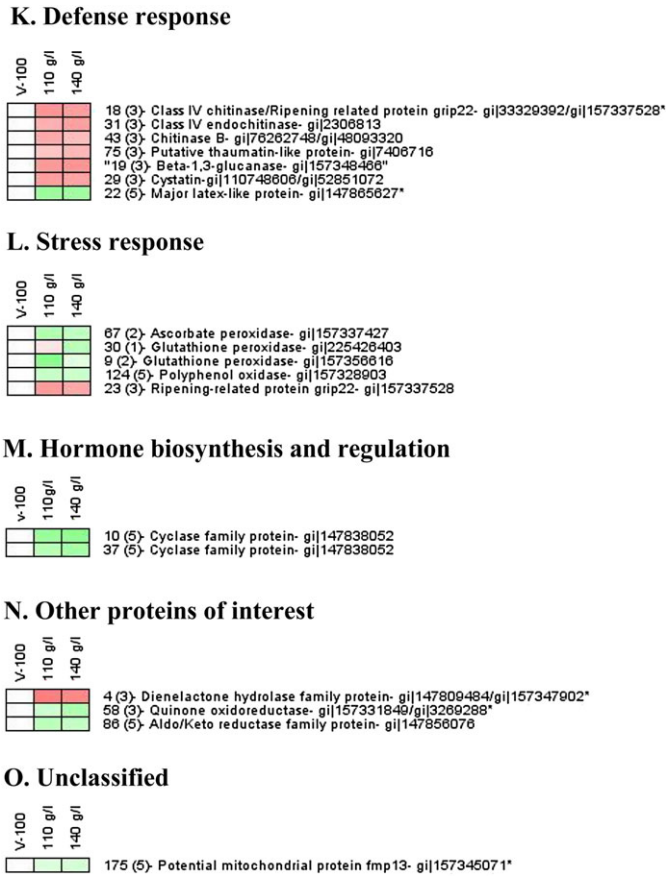

Fig. 7. Continued

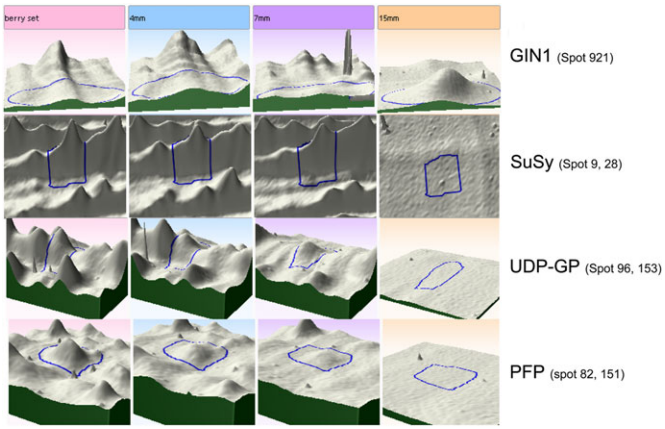

Fig. 8. Detailed 3D images from DIGE gels of FS, 4 mm, 7 mm, and 15 mm stages showing protein abundance for key enzymes in C-metabolism. Vacuolar invertase, GIN1 (gil1839578); sucrose synthase, SuSy (gil157342473); pyrophosphate-dependent phosphofructokinase β-subunit, PFP (gil157329588); UDP-glucose pyrophosphorylase, UDP-GP (gil157353934).

while the degradation of malate is mainly attributed to mMDH activity (Sweetman *et al.*, 2009). Although such roles match very well the profiles found here, the supposed malate degradation by mMDH pre-véraison has been suggested to be rather linked to respiration (Sweetman, 2009) on the basis of respiration rate profiles during grape berry development (Ollat and Gaudillère, 2000). The presence of PK (see above) and a component of the pyruvate dehydrogenase complex with the same pre-véraison abundance profile as the other enzymes suggests that part of the glycolytic products are being used for respiration but also that malate might be synthesized in cytosol via pyruvate and NADP-ME. Figure 9 shows a comprehensive schema of the relationships of carbohydrate and malate metabolism in the grape berry which includes the profiles of abundance of the identified enzymes differentially expressed through development and ripening. This schema would support a model for imported sugar fate through berry development. During early development most of the input is processed through glycolysis via PFP to PEP/pyruvate at which point part is stored as malate, in agreement with malate profiles (Coombe, 1987; Deluc *et al.*, 2007; Fenoll *et al.*, 2009) and another part is used for respiration, in agreement with CO_2 evolution profiles (Ollat and Gaudillère, 2000). Since glycolysis is active during this period, the NAD(P)H/NAD(P)$^+$ in cytosol must be kept high and thus the environment appropriate for malate synthesis. At the end of green development the switch between SuSy and INV means that most imported sugar will be stored, malate is no longer produced, and respiration is only supported by stored malate, which will be used for that function during ripening.

Two more enzymes related to organic acid metabolism, aconitase and isocitrate dehydrogenase, have been identified and belong to the same protein expression clusters in this study. Confident quantitative data could only be obtained for aconitase (Spots 4g, 19g), which presents a strong decrease in abundance of –12.5-fold at the end of the first growth period. It is the cytosolic isoenzyme that may be involved in ammonia assimilation together with isocitrate dehydrogenase (Hodges *et al.*, 2003).

Four spots (Spots 63g, 105g, 201g, 321g) with a sharp decrease in abundance in the pre-véraison stage have been identified as GDP-mannose-3', 5'-epimerase (GME). This enzyme catalyses the synthesis of GDP-L-galactose and GDP-L-gulose from GDP-mannose and may be involved in several pathways. GDP-L-galactose serves as a biosynthetic precursor of L-galactosyl, which is contained in cell wall polysaccharides, glycolipids, and glycoproteins in higher plants (Seifert, 2004; Reuhs *et al.*, 2004). GDP-L-galactose is also a precursor for the synthesis of L-ascorbic acid (AsA) in plants via the Smirnoff–Wheeler pathway; however, grape berries do not accumulate large quantities of AsA. The catabolism of AsA during early grape berry fruit development leads to the production of oxalic acid (OA) and tartaric acid (TA) in which L-idonate dehydrogenase (L-IdnDH) is the key enzyme and the only one known (Saito and Kasai, 1969; DeBolt *et al.*, 2006). Melino and co-workers (2009) demonstrated transformation of precursors GDP-mannose and GDP-galactose through the Smirnoff–Wheeler pathway to synthesize *in situ* AsA and subsequently TA/OA, thus GME can supply precursors to this pathway. L-IdnDH (Spot 134g) displays a gradual decrease from FS that becomes more pronounced as the berry grows.

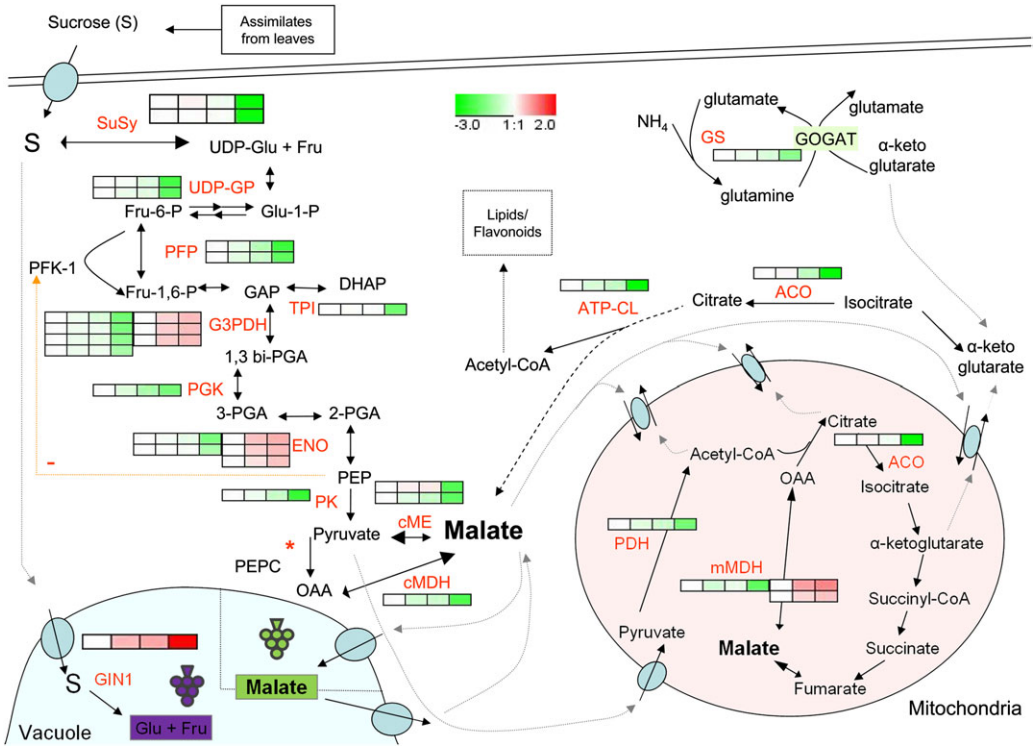

Fig. 9. Potential metabolic pathways involved in malate metabolism in grape fruits during development. Protein levels of regulated enzymes are shown in coloured squares indicating the change of expression (log_2 ratio) for each developmental stage in relation to FS stage for the first developmental phase, and V-100 stage for the ripening phase. In sequence order (left to right), stages are displayed from FS, 4 mm, 7 mm, 15 mm, V-100, 110 g/l, and 140 g/l. Different isoforms or post-translational forms of proteins are shown in different rows thus identified in different spots. Enzymes names for each catalytic step are indicated either in red, if differentially expressed and identified, or in black, if not found regulated or not identified. Black solid and dashed arrows indicate enzymatic reactions and metabolite movement, respectively. PFP, pyrophosphate-dependent phosphofructokinase; TPI, triose phosphate isomerase; G3PDH, glyceraldehide-3-phosphate dehydrogenase; PGK, phosphoglycerate kinase; ENO, enolase; cMDH, cytosolic malate dehydrogenase; cME, cytosolic malic enzyme; PDH, dihydrolipoamide dehydrogenase precursor subunit of pyruvate dehydrogenase; mMDH, malate dehydrogenase mitochondrial; cACO, cytosolic aconitase; mACO, mitochondrial aconitase; GIN1, vacuolar acid invertase; ATP-CL, ATP-citrate lyase. *PEPC was a regulated protein in seasonal but not in developmental experiments.

Thus, profiles of regulated enzymes GME and L-IdnDH are consistent with its transcript levels (Melino *et al.*, 2009) and TA accumulation in the vacuole during early cell expansion and growth phase to reach a maximum at pre-véraison stage (Moskowitz and Hrazdina, 1981; Iland and Coombe, 1988). After véraison two spots containing GME continued decreasing in abundance (Spots 51r, 56r, 62r) but as TA is no longer accumulated in these stages, the enzyme would presumably participate in another pathway.

Energy metabolism and photosynthesis (Figs 6B, 7B).: During development transcripts encoding proteins with photosynthetis-related activity are strongly expressed at flowering and early stages of berry development and then decline steadily in abundance throughout its development. Several proteins involved in photosynthesis and carbon fixation were detected, including five spots containing ribulose-1,5-bisphosphate carboxylase/oxygenase (RuBisCO) large subunit, with a more or less constant abundance from FS and a sharp decrease at the end of the first growth period towards the 15 mm pre-véraison stage. This is consistent with previous studies at several levels such as physiological, transcriptional, and enzyme activities, which indicate a rapid decrease of the capability of grapes to perform photosynthesis before véraison (Pandey and Farmahan, 1977; Famiani *et al.*, 2000; Terrier *et al.*, 2001; Waters *et al.*, 2005).

The 23 and 33 kDa subunits from the oxygen evolving complex have been identified in both pre- and post-véraison berry development, and are surprisingly up-regulated in the pre-véraison period and then down-regulated in the post-véraison period. When $NADP^+$ in the chloroplasts is in short supply (ie. NADPH is not being used), the reduced coenzyme is not being used, the hypothesis that O_2 becomes an alternative electron acceptor that leads to the production of H_2O_2 is widely accepted (Grace *et al.*, 1995). The abrupt decay of carbon fixation capacity that occurs in grape berry in the lag phase might be such a circumstance, thus, while the whole photosynthetic machinery is closing down, the oxygen evolving complex components increase to direct unused electrons towards O_2, thereby modulating H_2O_2 formation (Yang *et al.*, 2003). In line with these findings, some thioredoxin-dependent peroxidases are enhanced simultaneously (see Stress response below).

Several ATP synthase subunits were identified from both mitochondria and chloroplast. Subunit D (Spot 378g) and the 24 kDa subunit (Spot 446g) of mitochondrial ATP synthase accumulated from FS to 15 mm with a higher increase in the last stage. Conversely, the α-subunits (Spots 152g, 416g) decreased in agreement with the trend reported by others for that subunit (Giribaldi *et al.*, 2007). After véraison, β-subunits decreased (Spot 105r). In contrast, chloroplastic ATP synthase decreased at the stage of 15 mm [β-subunit (Spots 504g, 528g)] and was not found after véraison in agreement with other reports (Giribaldi *et al.*, 2007). Such profiles are consistent with respiratory and photosynthetic activities during berry development, well described for grape (Pandey and Farmahan, 1977; Ollat and Gaudillère, 2000; Famiani *et al.*, 2000; Terrier *et al.*, 2001; Waters *et al.*, 2005).

Four spots identified as a nucleoside diphosphate kinase (NDPK) (75g, 281g, 368g, 353g) had increased their expression at the end of the first growth period. All these spots were identified as the same isoform and three of them were represented in the gel as a train of spots with the same Mw and different pI, which would be due to post-translational modifications. NDPK has long been recognized as a phosphoprotein (Gilles *et al.*, 1991) and evidence of the autophosphorylation of NDPK-1, which could constitute a regulatory mechanism, has been provided (Dorion *et al.*, 2006*a*). This enzyme is widely distributed and is believed to play a role in the general homeostasis of cellular nucleoside triphosphate pools. The isoforms identified here were of NDPK Type I that lack an identifiable targeting sequence and are therefore probably localized in the cytosol (Dorion *et al.*, 2006*b*). NDPK-I has been shown to be the main isoform in plants, accounting for >70% of the total NDPK activity. Dorion *et al.* (2006*b*) found high levels of NDPK-I protein and activity in meristematic tissues in potato. They suggested that this isoform fulfils a role in early growth, in particular in primary cell wall synthesis, linked to its role sustaining the synthesis of precursors of cell walls like UDP-sugars and UDP-glucuronic acid. The overexpression of cytosolic NDPK in pericarp of grape berries and differential accumulation rates for its post-translational forms could have a relevant function in berry growth which could be related to the role suggested by Dorion *et al.* (2006*b*).

Transport proteins (Figs 6C, 7C).: V-ATPase is a tonoplast proton pump that together with the activity of vacuolar H^+-translocating inorganic pyrophosphatase (V-PPase) generates a proton gradient in the vacuole used to allow secondary transport into the vacuole. Malic acid and hexoses are the main accumulated compounds in the vacuoles of grape berry cells in the green and ripening stages, respectively, presumably through active transport at the tonoplast. V-ATPase is a large protein complex from which a number of subunits are still largely uncharacterized at the molecular level (Terrier *et al.*, 2001). Subunit F of V-ATPase (Spot 457g) has been identified and found to be most abundant in the pre-véraison stage in pericarp of grape berries. Subunit F has a relatively low expression level among all V-ATPase ESTs available in TIGR for tomato (Coker *et al.*, 2003) and is thought to be part of the central shaft of the protein (Domgall *et al.*, 2002).

The subunit F was found to increase 1.9-fold at the end of the first growth period, in contrast to a decrease of subunit B reported by Giribaldi *et al.* (2007) during development. However, the activity and abundance of vacuolar V-ATPase increase throughout grape berry ripening (Terrier *et al.*, 2001), which is consistent with the protein accumulation reported here. These later authors proposed a major role for V-ATPase in the vacuolar acidification that occurs during the green development of grape berries. During ripening, the V-ATPase subunit C (Spot 83r) is gradually accumulated. The structural features suggest that subunit C functions as a flexible stator that holds together the catalytic and membrane sectors of the enzyme (Drory *et al.*, 2004) and there is evidence of the disassembly of both sectors as a mechanism of V-ATPase regulation (Diepholz *et al.*, 2008). Therefore the accumulation during ripening suggests an enhancement of V-ATPase functionality. The proton pumping activity of V-ATPase in relation to V-PPase increases in grape berry during ripening, being the most accepted hypothesis to compensate for the increase in tonoplast leakiness (Terrier *et al.*, 2001).

An outer membrane mitochondrial porin also termed voltage-dependent anion channel (Spot 489g) was down-regulated during the first growth period. Voltage-dependent anion channel allows for exchange of some anionic metabolites in *Arabidopsis* (Colombini, 2004) and its role as a major component of the tRNA import machinery in plant mitochondria has been reported (Salinas *et al.*, 2006).

Amino acid metabolism (Figs 6D, 7D).: Gln and Asn are two central amino acids in plant nitrogen metabolism. Asn is used for nitrogen storage and transport from source to sink tissues, and is the major nitrogenous compound detected in the phloem of some plants (Lima and Sodek, 2003). Three major enzymes related to Gln and Asn metabolism were identified. During green berry development two spots containing four isoforms of cytosolic glutamine synthase (GS) (Spots 330g) and a spot containing Asp aminotransferase (AspAT) (Spot 121g) as the major protein were found to be gradually down-regulated. During berry ripening an asparaginase (Spot 107r) was down-regulated with a larger decrease from V-100 to 110 g/l, while another AspAT (Spot 72r) isoform was seen to accumulate. While Gln is a general ammonia carrier, Asn utilization by plants plays an important role in the nitrogen metabolism of developing plant tissues (Sieciechowicz *et al.*, 1988). In accordance with the transcriptional profile of one Unigene encoding L-asparaginase, with an expression peak at véraison and a decrease during ripening, Asn would be a provider of ammonia for the *de novo* synthesis of proteins during the first growth period and véraison as suggested (Deluc *et al.*, 2007). In addition, significant transcript abundance of GS was reported. Free NH_4^+ can represent up to 80% of total nitrogen in the grape berry before véraison

but decreases to 5–10% at full ripening, while free amino acids may represent up to 50% of total nitrogen in musts (Conde *et al.*, 2007). Thus the profiles of GS and AspAT before véraison and asparaginase after véraison for transcripts (Deluc *et al.*, 2007) and protein, are consistent with the levels of free NH_4^+ and the observed decrease of Gln and Glu before véraison in grape berries (Stines *et al.*, 2000). Ammonia would be released and transferred from the imported Asn by asparaginase and AspAT reactions, respectively, and further utilized by GS, presumably to feed the metabolic pathways. The decrease in asparaginase and increase in AspAT after V-100 indicates that nitrogen import in the grape berry ceases and there is a reactivation of amino group exchange. As ripe berry musts contain only seven amino acids in large quantities (Conde *et al.*, 2007) AspAT may contribute to that nitrogen distribution.

Several enzymes involved in the tetrahydrofolate- and *S*-adenosyl methionine (SAM)-dependent methylation system were identified, namely methionine synthase (Spots 10g, 16g, 27g, 32g, 37g, 45g, 55g), SAM synthase (Spots 60g, 301g, 464g), *S*-adenosyl-L-homocysteine hydrolase (Spots 128g, 351g), and serine hydroxymethyl transferase (Spot 59g). The former three appeared as isoforms encoded by different genes. Their profiles during green development are quite similar with a level more or less constant from FS to 7 mm (except for one isoform of methionine synthase found in two spots, which had a slight but significant peak at 4 mm) and a sharp decrease from 7 to 15 mm. Such profiles suggest that there is high methylation activity during green development that drops when the grape berry enters the lag phase. In addition, a phosphoglycerate dehydrogenase (Spots 242g, 274g) present in two spots had a profile similar to the above enzymes. This enzyme catalyses the first and rate-limiting step in the phosphorylated pathway of serine biosynthesis, thus controlling the supply of serine to serine hydroxymethyl transferase. Two processes that demand methyl groups: DNA synthesis; and lignin and polyphenolics synthesis take place extensively during this growth period. In contrast methionine synthase (Spots 60r, 68r) is up-regulated at onset of ripening, while SAM synthase (Spots 51r, 82r, 101r) is down-regulated. It would lead to a net production of methionine and to a decrease in SAM-dependent methylating activity. As an increase in protein synthesis occurs in véraison (Ghisi *et al.*, 1984; Tattersall *et al.*, 1997), a higher demand for amino acids including methionine must be satisfied.

Two additional proteins involved in synthesis of aromatic and branched-chain amino acids, respectively, dehydroquinate dehydratase shikimate:NADP oxidoreductase (Spot 275g) and ketol-acid reductoisomerase (Spot 347g) were also gradually down-regulated during green development. Dehydroquinate dehydratase shikimate:NADP oxidoreductase catalyses two steps of the shikimate pathway to produce Trp, Tyr, and principally Phe as precursor of phenylpropanoids and polyphenols that accumulate during green development.

Taken together, enzymes of several amino acid biosynthetic pathways (and presumably all) are found at high levels until the berry enters the lag phase and the corresponding amino acids are synthesized. When the berry enters ripening only the metabolism of certain amino acids is active.

Secondary metabolism (Figs 6E, 7E).: Flavonoids are a major type of polyphenol that determine largely organoleptic properties of grape berries and derived products. The flavonoid biosynthetic pathway starts with the condensation of 4-coumaroyl-CoA with three molecules of malonyl-CoA to produce the flavonoid ring system in two steps catalysed by chalcone synthase and chalcone isomerase (Moustafa and Wong, 1967; Kreuzaler and Hahlbrock, 1972; Sparvoli *et al.*, 1994). The subsequent hydroxylation, reduction, glycosylation, and condensation reactions lead to different end-products like anthocyanins, flavonols, and condensed tannins. Of these, flavonols accumulate mainly in mesocarp and are found in the free run juice (Makris *et al.*, 2006). Five enzymes that act consecutively in the pathway, chalcone synthase, flavanone-3-hydroxylase, anthocyanidin reductase, anthocyanidin synthase, and dihydroflavonol 4-reductase, were present and identified here, as isoforms from different isogenes or post-translational modifications. All of them have a similar pattern of down-regulation through green stages or a sharp decrease at the end of the first growth period. This pattern correlates very well with transcript abundance in the pre-véraison stage in the whole berry (Deluc *et al.*, 2007). Studies on grape berry skins during development show that there are two phases for flavonoid pathway gene expression: most of the genes are expressed at early stages, then repressed during the lag phase of development and are finally induced at véraison, which coincides with accumulation of anthocyanins in the skin (Boss *et al.*, 1996). In contrast in mesocarp we have not found any enzyme of the pathway among those spots significantly changing, which may be expected since anthocyanins are specific to the skin, and tannins are specific to the skin and seed. As described above, an enzyme of the Phe biosynthetic pathway was gradually down-regulated.

An isoflavone reductase-like protein 6 (IFRL6) was identified in green and ripe stages. From 7 to 15 mm there was a 2-fold increase in abundance and during ripening IFRL6 continued to accumulate, with a 1.4-fold change from V-100 to 140 g/l (Fig. 10B). IFRL6 presents high homology with a phenylcoumaran benzylic ether reductase AAC49608 (*Forsythia×intermedia*) (Bogs *et al.*, 2005), which is involved in the biosynthesis of important phenylpropanoid-derived plant defence compounds including lignans (Turley, 2008). Giribaldi and co-workers (2007) reported that IFRL6 decreases from véraison to the end of ripening, in disagreement with our results obtained in mesocarp of ripe berries. The proteomic study performed by Grimplet *et al.* (2009) shows that IFRL6 is more abundantly expressed in the pulp, which is in accordance with its mRNA profile (Grimplet *et al.*, 2007). Furthermore, Sarry *et al.* (2004) found that IFRL6 is an abundant spot in the pulp of ripe berries. As shown in Fig. 10A, the expression profile for the IFRL6 gene correlates with IFRL6 protein abundance confirming up-regulation during ripening.

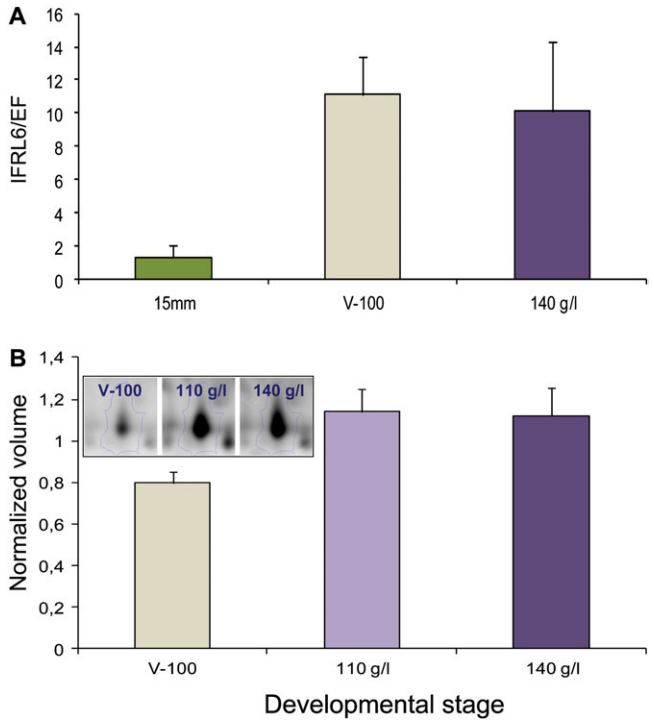

Fig. 10. Changes in the expression of IFRL6 during ripening. (A) Relative expression of *IFRL6* gene in mesocarp during ripening. IFRL6 transcribed mRNA was analysed by real time qRT-PCR. Levels of transcripts were calculated using the standard curve method with the grapevine *EFα1* gene as an internal control. Values are given as mean±standard deviation of six replicates. (B) Changes in the relative spot volume (Spot 123r) through three different stages from véraison until full ripening of cultivar Muscat Hamburg grape berry mesocarp. Values represented the mean-±standard deviation from normalized spot volume of four independent biological replicates. Inset: image of spot 123r in the 2-DE gel during ripening.

Considering the above, the results suggest that a family of phenolics in mesocarp, the flavonols, are synthesized mainly before véraison, and another family, the lignans, is synthesized after véraison.

Replication and repair (Fig 6F).: During green development a protein gradually up-regulated that participates in the DNA replication process has been identified. This protein contains a KH domain that binds both single-stranded DNA and RNA and, thus, may act in replication and transcription processes, which are very active at the beginning of véraison (Lücker *et al.*, 2009). In plants, KH-domain-containing proteins are involved in the regulation of developmental processes such as flowering time (Mockler *et al.* 2004) and fruit development (Choi *et al.*, 2004).

Gene expression and protein synthesis (Figs 6G, 7G).: In relation to gene expression two transcription factors were regulated in green berries. One of them (gi|14582465) undergoes a strong increase at the end of green development (42g) followed by a progressive decrease during ripening (52r). It has been shown to be involved in sugar and abscisic acid (ABA) signalling and binds to the promoter of the grape berry hexose transporter (Cakir *et al.*, 2003). The other one (gi|147856360) decreases during green development and is homologous to APFI from *Arabidopsis*, which was described to be involved in the expression of nuclear-encoded mitochondrial complex I genes (Barel and Ginzberg, 2008). The trend of these two transcription factors is consistent with the expression of hexose transporters in grape berries during development (Deluc *et al.*, 2007; Fillion *et al.*, 1999) and decreasing rates of respiration towards onset of ripening (Ollat and Gaudillère, 2000), respectively. Maturase K, active in splicing of several introns, and a single-strand binding protein, which interacts with RNA polymerase, decreased during ripening suggesting a gradual arrest of transcriptional activity. In green berries, four spots that contained elongation factor 2 dropped in abundance from 7 to 15 mm. Also, glycine-rich RNA-binding protein appeared as two spots that decreased from FS to 4 mm, although one of these then increased in the next stages. Glycine-rich RNA-binding protein is a type of glycine-rich protein that is regulated by a number of internal and external signals like wounding and ABA in maize and carrot, low temperature in *Arabidopsis*, and other internal inducers like circadian clock and developmental signal (Naqvi *et al.*, 1998). During ripening the 60S acidic ribosomal protein P0 was found in two spots with opposite trends in abundance (Spots 44r, 70r). Post-translational modifications such as phosphorylation are known to regulate activity of this protein, which is involved in the binding of translation factors.There may be a conversion between phosphorylated forms of this protein during grape ripening.

Identified proteins involved in protein synthesis show a decrease at the end of the first growth period, supporting high rates of protein synthesis during the first stages of development of berries when fruit is forming. It seems that protein synthesis is slowed down before véraison, which coincides with the beginning of a lag phase in the fruit. These results are consistent with previous studies that suggest that RNA and protein synthesis are more active in green tissues (Terrier *et al.*, 2001; Waters *et al.*, 2005; Giribaldi *et al.*, 2007).

Protein folding and trafficking (Figs 6H, 7H).: Several heat shock proteins were identified in both experiments with different expression patterns. In green berries chloroplast chaperonin 21 (Spot 133g) (component of the GroES complex), RuBisCO large subunit-binding protein α-subunit (341g), and heat shock protein (HSP) 90 accumulated during development; while chaperonin 60 (432g, 441g, 502g), HSP70 and TCP-1 η chain showed a decrease during that period. These changes were particularly evident from 7 to 15 mm, except the accumulation of heat shock protein 90 that occurred mainly from FS to 4 mm. During ripening, several proteins such as Hsp90 (93r) and four isoforms of small chaperones, HSP 17 kDa, were identified in two spots (5r and 49r), which showed a decrease in expression during ripening in relation to véraison.

These functional classes of proteins are involved in protein folding and act as molecular chaperones, in stabilization of unfolded polypeptides, and in recognition and cleavage of targeting signals for precursor polypeptide translocation across organelle membranes. The profiles during green development and subsequent ripening are consistent with intensive protein synthesis and trafficking during formation of berries followed by a gradual decrease during ripening. The general trend observed of HSPs increasing towards véraison and then declining during ripening is supported by previous studies (da Silva *et al.*, 2005; Giribaldi *et al.*, 2007; Negri *et al.*, 2008), which show an expression peak of HSPs at véraison. A decrease in HSPs after inception of ripening is compatible with a less intense rate of protein synthesis (see results above). The peak of HSPs at verasion has been related to the large changes in metabolism at this stage of development that demand new proteins (da Silva *et al.*, 2005).

Two isoforms of GTP-binding nuclear protein Ran-3 were found to be strongly repressed before véraison (Spots 170g and 53g). Ran is a GTP-binding protein that is essential for the translocation of RNA and proteins through the nuclear pore complex. The Ran protein is also involved in the control of DNA synthesis and cell cycle progression (Sazer and Dasso, 2000). The abundance profile correlates well with the period of cell division and enlargement during green development.

Protein degradation (Figs 6I, 7I).: Protein degradation through the main cell machinery as the proteasome and ubiquitin tagging system plays a key role in important cellular processes, removing misfolded or damaged proteins and controlling the level of certain regulatory proteins. A number of proteasome components have been identified both in green and ripening stages. The abundance behaviour of these proteins during green development is at first sight confusing since some of them show an increase while others decrease. Such divergent changes in different subunits of proteasome reflect the complex regulatory mechanism for proteolytic machinery such as the 20S proteasome (Zong *et al.*, 2008). Although the processes in which the proteasome participates are very far from being catalogued, particularly in plants (Smalle and Vierstra, 2004) this might be interpreted as a proteasome rearrangement at that stage. Unlike pre-véraison regulation, fruit undergoing ripening tended to display a commom increase in abundance of proteins belonging to the proteasome, suggesting a progressive protein degradation activity. A ubiquitin regulatory X (UBX)-domain-containing protein spot (186g) was found to accumulate 3.4-fold in the late green stage. The UBX-domain-containing proteins constitute a family of cofactors of the AAA ATPase Cdc48/p97. UBX proteins are involved in substrate recruitment to Cdc48/p97 and in the temporal and spatial regulation of its activity (Schuberth and Buchberger, 2008) and its profile correlates with that of the proteosome components. Other proteases have been identified such as aspartic proteinase nepenthesin-1 precursor (Spot 529g), a vacuolar protease found to accumulate during the first growth period.

The profile of these proteins must respond to the needs of fruit cells in relation to their developmental programme. Thus, the increase in protein degrading activity during ripening could be related to the removal of systems whose function is no longer needed such as the photosynthetic machinery in mature grapes. Proteasome activity implies the release of amino acids to the cellular free amino acid pool and could contribute to balancing reduced amino acid biosynthesis after véraison. In fact, total amino acid content of berries rises significantly during maturation in parallel with increasing total N (van Heeswijck *et al.*, 2001).

Biogenesis of cellular components (Fig. 6J).: Berry development presents two main growing periods separated by a lag phase characterizing slower growth. During the first growth period, there is cell division and cell expansion that ceases as the berry enters a lag phase. Then the grape berry enters véraison and until the full ripening stage softening occurs and berry growth is entirely due to cell expansion (Coombe, 1992). Cell division and growth must be accompanied by changes at the cell wall level such as biogenesis and remodelling (Cosgrove, 2000), that involve processes of biosynthesis and vesicular transport of cell wall components. A clathrin interactor protein homologous to epsin is one of the adaptor proteins required for clathrin-coated vesicle-mediated exo-/endocytosis (Owen *et al.*, 2004). This protein is contained in a spot (Spot 17g) that dramatically increases in abundance (5.82-fold) in pericarp of green berries from FS to 4 mm and continues accumulating up to 9-fold in relation to FS during green development (see Table 2, Cluster 6). Clathrin-coated vesicles are involved, among other functions, in the biogenesis of the cell wall through the secretory pathway carrying non-cellulosic components. The profile of the adaptor protein correlates very well with this role during green development.

In relation to cell wall biogenesis two enzymes have been identified. A rhamnose biosynthetic enzyme (Spot 79g) is present throughout the stages of green development and decreases abruptly by –4.8-fold in the last green stage analysed. The rhamnose biosynthetic enzyme contributes to the synthesis of the pectic fraction of the primary cell wall (Usadel *et al.*, 2004) and its profile is consistent with the arrest in cell division and expansion that take place during green development. In contrast, a xyloglucan endotransglycosylase (XET) has an opposite profile. Ishimaru and Kobayashi (2002) suggested that an *XET* gene plays a critical role in berry softening at véraison in the Kyoho grape by markedly increased expression at this point of development. The expansion of cells at véraison and during ripening requires a loosening of the primary cell wall, made of cellulose cross-linked by hemicelluloses in a matrix of pectin polysaccharides. XET is involved in cell wall remodelling, which acts on the hemicellulosic fraction (Sakurai and Nevins, 1997). In green stages, XET has a basal level that increases up to 2.7-fold at the end of this phase before véraison. Schlosser and co-workers (2008) found a down-regulation of the *XET* gene from 15 to 28 d post-anthesis and up-regulation again during stage II or

lag phase in mesocarp and exocarp tissues of grapes. Other studies also show that XET expression increases in grapes during ripening in pulp and skin (Nunan *et al.*, 2001; Deytieux *et al.*, 2007) but this protein was not seen to change during ripening here.

The changes undergone by fruit cells throughout development (Harris *et al.*, 1968; Coombe, 1992) must be supported by changes in cytoskeleton structure. Not surprisingly, two β- and α-tubulin proteins increased in abundance during the early stages of development until beginning of lag phase, which correlates with cell size enlargement. During ripening tubulins were not present among the regulated proteins.

Defence response (Figs 6K, 7K).: Pathogenesis-related (PR) proteins are considered as plant defence proteins and act in preventing or limiting pathogen multiplication or spread (Van Loon and Van Strien, 1999). During green development, only one of this class of proteins, highly homologous to Mal d 1, was seen to decrease in abundance from 7 to 15 mm. Mal d 1, the major apple allergen, has high sequence similarity with the Bet v 1 birch allergen (Gao *et al.*, 2005). The Bet v 1 superfamily includes the intracellular PR class 10 (PR-10) families (Radauer and Breiteneder, 2007), which are structurally related to ribonucleases and it is hypothesized that these proteins provide protection against viruses (Van Loon and Van Strien, 1999). During ripening a homologue to major latex protein (MLP) decreased from V-100 to 110 g/l stages. The function of MLPs are unknown, although have been associated with fruit and flower development and in pathogen defence responses based in their modest sequence similarity with members of the Bet v 1 superfamily (Osmark *et al.*, 1998). The protein identified in our study (gi|147865627) has 100% homology with the protein encoded by cDNA clone (AJ237994) Grip61 isolated by Davies and Robinson (2000), which is induced in berry after véraison and then declines in expression during ripening. MLPs are differentially expressed through plant development. For example, MLP28 from peach is highly expressed during early fruit growth (Ruperti *et al.*, 2002); it seems to have similar functions to PR-10 proteins (Lytle *et al.*, 2009).

All others PR proteins identified were found to accumulate only in the berry ripening phase and include three class IV chitinase isoforms (PR-4), a putative thaumatin-like protein (PR-5), β-1,3-glucanase (PR-2), and grape ripening-related proteins (Grips). PR proteins accumulate in grape berries as a normal part of the ripening process, with véraison as a trigger for PR expression (Tattersall *et al.*, 2001). Endochitinases are abundant proteins in mesocarp grape juices (Vincenzi and Curioni, 2005). They belong to the PR-4 group and have antifungal activity, which is thought to play a role in berry protection. These results agree with observations that constitutive expression of a class IV endochitinase gene and of chitinase activity increased during grape berry ripening (Robinson *et al.*, 1997). Thaumatin is one of the most abundant berry proteins induced at the onset of fruit ripening, as it is systematically expressed in many ripe fruits. It is also potentially involved in resistance to pathogen or defence in grapes (Waters *et al.*, 1996; Tattersall *et al.*, 1997).

During ripening, a β-1,3-glucanase (Glu) has been quantified (Spot 19r) with a 1.7-fold change from véraison through ripening. An endo-1,3-β-glucanase transcript has been found in mesocarp up-regulated from onset of véraison (Schlosser *et al.*, 2008). It is generally believed that endoglucanases fulfil different biological functions; their role has been classically associated with PR defence (Deytieux *et al.*, 2007). However, it has also been suggested that endo-1,3-β-glucanase plays a role in fruit ripening and softening (Cosgrove, 2000). Recent study has demonstrated differential accumulation of β-1,3-glucanase in skin/pulp, with a large abundance in berry skin and a probable role in berry ripening (Wang *et al.*, 2009).

Cystatin (Spot 29r) is a protein inhibitor of cysteine proteases, which has been found to increase during ripening. Cystatin proteins known as phytocystatins have been isolated from several plants having antifungal activity and are considered as defence proteins belonging to the PR-6 family (Ferreira *et al.*, 2007).

Two GDSL-motif lipase hydrolase family protein isoforms were identified in pulp of ripe grapes as no previous proteomic studies have reported (Spots 98r, 83r, see Table 3). A lipase-like SGNH containing the GDSL-like motif has been found in grapevine cell culture extracellular medium, increasing in response to elicitation with cyclodextrin (Martinez-Esteso *et al.*, 2009). The response observed in grapevine cells was interpreted by authors as similar to that produced against a pathogen attack.

The results obtained provide further evidence of the relationship between grape berry ripening and accumulation of PR proteins. Early studies indicate that ABA could be involved in the triggering of ripening since the application of auxin-like compounds to grapes prior to véraison delays both the increase in ABA and the onset of ripening (Coombe and Hale, 1973). The expression of genes characteristic of the ripening phase, including invertase and chitinase, were also delayed by treatment with auxin-like compounds (Davies *et al.*, 1997). Accumulation of some PR proteins seems to be induced also in response to factors occurring during ripening, such as the osmotic stress due to the high level of free hexoses, besides signalling molecules such as salicylic acid, ABA, indole-3-acetic acid (Tattersall *et al.*, 2001). It has also been shown that grapevine chitinase and β-1,3-glucanase have antifungal activity *in vitro* assays (Giannakis *et al.*, 1998; Salzman *et al.*, 1998). Thus the accumulation of PR-proteins with antifungal activity during ripening is clearly trigered by endogenous factors, but since many other developmentally regulated genes are also triggered, the question about the role of PR-proteins in the berry is still open to investigation (Robinson *et al.* 1997; Robinson and Davies, 2000).

Stress response (Figs 6L, 7L).: Several proteins related to oxidative, salt, and general stress were differentially expressed throughout grape berry development. Among enzymes involved in oxidative stress, ascorbate-,

glutathione-, and thioredoxin-dependent peroxidases, catalase, superoxide dismutase, and polyphenol oxidase were detected. In a single-stain 2-DE-based proteomic study all of these were more highly expressed in green tissues than in ripe (Giribaldi *et al.*, 2007). During green development catalase (Spots 113g, 141g) and ascorbate peroxidase (Spot 162g) stayed at high levels up to 7 mm but strongly down-regulated from 7 to 15 mm. In parallel, two isoforms of chloroplastic thioredoxin-dependent peroxidase (or peroxiredoxin) found in three spots (Spots 127g, 210g, 427g) were strongly up-regulated from 7 to 15 mm. A third isoform (Spot 335g), which was strongly down-regulated from FS to 4 mm, is a mitochondrial form having different Mw/pI (21811.36 Da/8.74 pI compared with 17250.22 Da/5.15 pI). Whereas the first set of enzymes are general detoxifiers of reactive oxygen species (ROS), peroxiredoxins have a more specific role of detoxifing ROS in chloroplasts (Goyer *et al.*, 2002) and, as discussed above, could be related to the removal of H_2O_2 produced when O_2 acts as a final electron acceptor. During ripening ascorbate peroxidase continues to decrease after véraison and two isoforms of glutathione peroxidase show higher levels at V-100 and 110 g/l stages than at the end of ripening. In tomato (Jiménez *et al.*, 2002) and strawberry (Aharoni and O'Connell, 2002; Bianco *et al.*, 2009), it has been reported that oxidative stress may play a developmental role in the ripening process. Pilati *et al.* (2007) reported that an oxidative burst, characterized by rapid accumulation of H_2O_2 starting from véraison, occurs in grape berries and that this event modulates the expression of the oxidative stress gene set, which showed little change during the late green development stages. However, also at transcriptional level, the typical oxidative stress markers seemed absent or negatively regulated at ripening (Terrier *et al.*, 2005). As noticed above, proteins of the oxygen-evolving complex potentially involved in H_2O_2 production accumulate significantly at the late green stages and thus might contribute to an increase in H_2O_2 at véraison as reported by Pilati *et al.* (2007). For grape, the occurrence of proteins involved in oxidative stress during grape development has been controversial, although the abundance pattern of the ROS scavenging enzymes described here suggests a specific developmental programme that involves specialized enzymes and isoforms, which is in line with the results reported for tomato and strawberry. As previously shown for peroxiredoxins, catalase and ascorbate peroxidase (Jiménez *et al.*, 2002), the regulation of the ROS detoxifying enzymes must be very complex, isoenzyme specific, and occurring at different levels (transcriptional, post-transcriptional, subcellular compartmentation, etc.).

A protein (Spot 381g), homologous to a universal stress protein (USP) has been identified in green berries with increasing expression towards the end of the first growing phase. Bacterial USP is up-regulated when the cell is exposed to stress agents, enhancing the rate of survival during prolonged exposure to stressing conditions (Nystrom and Neidhardt, 1992, 1993, 1994). USP homologues appear to be ubiquitous in plants, are absent in animal species, and are involved in plant stress response as is generally hypothesized (Maqbool *et al.*, 2009). The USP gene in *Gossypium arboreum* is up-regulated by growth hormones such as GA and ABA and abiotic stresses (Zahur *et al.*, 2009). The profile of USP protein in grape berry is consistent with the ABA accumulation (Coombe, 1988). Another stress-related protein (Spot 172g) homologous with a salt tolerance expressed protein has an expression profile similar to USP, but its precise function is unknown.

Polyphenol oxidases (PPOs) catalyse enzymic browning in plants, which act by oxidizing a range of phenolic substrates to produce reactive quinones. Although the roles of this enzyme are not fully clarified, it may be involved in resistance to plant pathogens and in plant senescence (Dry and Robinson, 1994). A PPO (Spot 124r) was identified whose expression decreased gradually from véraison through ripening, which is in agreement with previous reports from grape berry skin (Negri *et al.*, 2008). The calculated Mw for Spot 124r does not match the expected Mw for either the pre-protein (67 kDa), the mature protein (59 kDa), or the processed protein (36 kDa) (Dry and Robinson, 1994; Sarry *et al.*, 2004; Sellés-Marchart, 2008), which contains the active site. On the basis of matched peptides in the PPO sequence, Spot 124r should correspond to an acidic 16 kDa C-terminal domain possibly involved in the binding to thylakoidal membranes that the protein loses it when it is proteolytically activated (Sellés-Marchart, 2007). Negri *et al.* (2008) found PPO in spots whose Mw matched the active mature form (60 kDa) and C-terminal peptide (18 kDa). They suggested that the presence of this peptide may indicate that the small terminal portion of PPO is maintained in skin cells after cleavage from the catalytic unit. The fact that such C-terminal fragment is also kept in mesocarp of ripe berries and not rapidly removed suggests that it may have some role after cleavage from the mature protein during ripening.

Spot 23r contained Grip22, which is known to be abundant after véraison in ripening berries and involved in stress response (Davies and Robinson, 2000), and is expressed in both mesocarp and skin (Grimplet *et al.*, 2009). Terrier *et al.* (2005) found that transcripts encoding Grips proteins, among them Grip22, are markedly induced during berry development. Grip22-related proteins were described as allergens in Kiwi (Tamburrini *et al.*, 2005). From véraison to 110 g/l stage Grip22 increased 1.7-fold, which is one of the largest changes at this stage.

Hormone biosynthesis and regulation (Figs 6M, 7M).: During green berry development, seven spots identified as a choloroplast lipoxygenase (LOX), displayed a strong decrease in abundance from 7 to 15 mm. LOXs convert linoleic acid into 13-hydroperoxylinoleic acid providing intermediates for different final products that include volatile alcohols and aldehydes, wounding hormone, or the plant growth regulator jasmonic acid (JA). JA itself and derivatives, collectively called jasmonates, are powerful mediators of physiological and developmental responses in plants (Wasternack and Parthier, 1997). A chloroplast LOX, key enzyme of the octadecanoid defence-signalling

pathway, was found in stroma and thylakoid membranes of chloroplasts of passion fruit (*Passiflora edulis f. flavicarpa*) leaves in response to methyl jasmonate treatment and wounding (Rangel *et al.*, 2002). Chloroplasts that contain high levels of linoleic acid are thought to be the primary site of the initial steps of JA formation (Feussner *et al.*, 1995; Bleé and Joyard, 1996; Ziegler *et al.*, 2000; Froehlich *et al.*, 2001) and could possibly fuel an activated octadecanoid pathway (Douce and Joyard, 1980). No other enzyme acting downstream in the pathway was detected here. However, besides LOX, a transcript for 12-oxophytodienoate reductase that catalyses a key step in JA synthesis was expressed in grape berries, which also decreased during early development (Deluc *et al.*, 2007). Thus LOX proteins found in green pericarp here must participate at least in JA biosynthesis. Indeed, endogenous levels of JA were high in very early development stages and decreased until 41 d after flowering in skin of seedless 'Pione' grape berries coinciding with véraison (Kondo and Fukuda, 2001). It was demonstrated that endogenous JA may stimulate cell division at the beginning of fruit development in climacteric apples and in non-climateric sweet cherries (Kondo *et al.*, 2000); thus, it may have a similar role in developing grape berries.

Several isoforms of a cyclase family protein encoded by two different genes were identified in green and ripe berries. Multi-alignment and phylogenetic analyses strongly suggest that these belong to the diterpene cyclase family and are homologous to a cyclase ent-kaurene synthase (Supplementary Fig. S2 at *JXB* online). Kaurene synthase belongs to the Tpse subfamily of terpene cyclases involved in the early steps of gibberellin (GA) biosynthesis. In rice plant Sakamoto *et al.* (2004) found that the loss of OsKS1 function, likely encoding an ent-kaurene synthase involved in GA biosynthesis, resulted in a severe GA-deficient phenotype. OsKS1 closely clusters with the grape berry cyclase found here (Supplementary Fig. S2 at *JXB* online). Very little is known about the role of GA in grape berry development (Symons *et al.*, 2006) apart from its possible role in cell enlargement. The concentration of GA is high in flowers and fruits just after anthesis and then drops to lower levels through berry development. Further, there is a peak of GA at the start of lag phase, which is higher in seed than in mesocarp (Pérez *et al.*, 2000). These proteomic results here report a diterpene cyclase (Spots 10r, 37r) which has a 4.2-fold increase in abundance during green developmental stages, followed by down-regulation from véraison. Such a profile is consistent with that of GA during berry development and ripening. Moreover, a transcriptomic study (Deluc *et al.*, 2007) reported that several transcripts for GA receptors had a trend consistent with this accumulation pattern found in the study reported here.

Other proteins of interest (Figs 6N, 7N).: A C2-domain-containing protein was up-regulated 3.4-fold at the end of the first growth period (Spot 183g). Waters *et al.* (2005) found an EST encoding for a C2-domain-containing protein with an increase >3-fold in expression level at véraison. C2 domain is involved in phospholipid binding, which may be mediated by Ca^{2+}, and may be involved in the signal transduction downstream pathway via Ca^{2+}-binding proteins as a response to endogenous signalling molecules or exogenous factors such us biotic or abiotic stress (Kim *et al.*, 2008). Little is known about C2-domain-containing proteins in plants (Wang, 2002; Kim *et al.*, 2003). The results presented here are in agreement with transcriptomic data and suggest that these proteins may also have a developmental role.

Only one regulated enzyme related to lipid metabolism was identified in this study; ATP citrate lyase (Spot 23g) was down-regulated during the first stages of development, and then increased strongly before véraison. ATP citrate lyase supplies acetyl-CoA for synthesis of fatty acids as well as for a diverse set of phytochemicals including waxes, isoprenoids, stilbenes, and flavonoids. Interestingly, the profile of this enzyme coincides with that of proteins involved in the phenylpropanoid pathway, thus grouped in the same Cluster 8.

In ripe mesocarp, a seed storage protein present in several spots (Spots 6r, 13r, 24r; Table 3) with homology to a legumin-like protein has been identified. The expression of this protein in the experiment could not be quantified, due to the co-existence of several proteins with similar Mw and pI properties in the same spots. Terrier *et al.* (2005) found a transcript with high similarity to the sequence identified (gi|157349479) encoding a legumin-type storage protein in pericarp of berries strongly induced at ripening, which seems to be a new ripening-related gene in *V. vinifera.* The precise function of these new ripening-related proteins in grape berry development remains to be elucidated.

A spot corresponding to a dienelactone hydrolase family protein (Spot 4r) was one of the most strongly up-regulated at onset of ripening in mesocarp (2-fold). Although the role of dienelactone hydrolase in higher plants remains unclear, in bacteria this enzyme from the β-ketoadipate pathway acts as a detoxifying system to transform environmental toxic dienelactone to the non-toxic maleyacetate (**Beveridge and Ollis, 1995**). Hiroyuki and Shigeru (2008) and Hiroyuki and Masaharu (2006) found that dienelactone hydrolase in rice has a disulfide bond targeted by thioredoxin. During germination thioredoxin reduces the disulfide bond to activate the enzyme.

A plasma membrane quinone oxidoreductase (Spot 49g) was found to be strongly up-regulated (5.7 fold) in the pre-véraison stage. Another isoform, benzoquinone oxidoreductase (Spot 58r) was down-regulated during ripening. A protein identified as an aldo-keto reductase (Spot 86r), which belongs to an enzyme superfamily of NAD(P)H-dependent oxidoreductases as proteins above, was seen to decline by –1.4-fold after the véraison stage. This protein identified in skin of ripe berries, was 72 times more abundant at full ripeness than at véraison (Deytieux *et al.*, 2007).

Concluding remarks

Application of the DIGE technique has allowed the detection of proteome changes during the two successive

developmental stages that undergo grape berry growth. During development we detected two key points at protein level: pre-véraison (15 mm), whereby dramatic changes in the number and degree of proteins regulated were observed, largely correlated to genomic and transcriptomic changes; and after véraison (V-100), although this stage showed relatively minor changes in comparison with the first critical point. High coverage of proteome was achieved detecting differentially expressed proteins belonging to a wide range of metabolic processes. Although cross-contamination inherent to the 2-DE technique has been observed in the spots identified, most of the quantitative data (86%) was unambiguously assigned. Results obtained provide valuable data to improve our knowledge about protein profiling of grape berries as well as key proteins involved in important metabolic pathways such as sugar and organic acid metabolism in grape flesh that could lead to control of the quality traits of grapevine in future research projects. The study described here with a proteomic approach contributes more widely to the understanding of the complexity of fruit development as a model for other non-climateric species, in the same way as the tomato has been used as a model climacteric species.

Supplementary material

Supplementary Fig. S1. Overlapped DIGE images. Selection of overlapped images through stages analysed in (A) experiment A, (B) experiment B, and (C) experiment C. Each indicates the gel number and the samples that were run, labelled with either Cy3 or Cy5.

Supplementary Fig. S2. Phylogram comparing a cyclase family protein in *V. vinifera* identified (gi|147838052) with other plant cyclases. Both phylogenetic trees were generated using amino acid sequences on a Clustalw program (http://www.ebi.ac.uk/Tools/clustalw2/index.html). Accession numbers from sequences are indicated between parallel bars. (A) Phylogenetic tree A showing that by phylogenetic similarities sequence gi|147838052 is related to diterpene cyclases. (B) Phylogenetic tree B showing more detailed relationships for gi|147838052 sequence that related it to a class of diterpene cyclases: ent-kaurene synthases. Sequence of gene OsKS1 from *Oryza sativa* shaded in green.

Supplementary File S1. Blast2GO file containing sequences of proteins identified in DIGE experiment for green stages. File is opened with Blast2GO software (http://www.blast2go.org/start_blast2go).

Supplementary File S2. Blast2GO file containing sequences of proteins identified in DIGE experiment for ripe stages. File is opened with Blast2GO software (http://www.blast2go.org/start_blast2go).

Supplementary File S3. Blast2GO file containing sequences of proteins identified in DIGE experiment for season comparison. File is opened with Blast2GO software (http://www.blast2go.org/start_blast2go).

Supplementary File S4. Peptide detailed parameters for LC-MS/MS analysed proteins. For each identified protein a list of matched peptides is given.

Supplementary File S5. Peptide detailed parameters for MALDI-MS/MS analysed proteins. For each identified protein a list of matched peptides is given.

Supplementary File S6. Table of spot measurement data output of Progenesis SameSpots v3.0 in DIGE covering the first growth period. ANOVA *P* value and fold-change are given for each spot in the experiment. Column entitled 'included' indicates which spots with 'Yes' tag are selected in the experiment for successive statistical data.

Supplementary File S7. Table of spot measurement data output of Progenesis SameSpots v3.0 in DIGE covering the ripening process. ANOVA *P* value and fold-change are given for each spot in the experiment. Column entitled 'included' indicates which spots with 'Yes' tag are selected in the experiment for successive statistical data.

Supplementary File S8. Table of spot measurement data output of Progenesis SameSpots v3.0 in DIGE for seasonal comparison. ANOVA *P* value and fold-change are given for each spot in the experiment. Column entitled 'included' indicates which spots with 'Yes' tag are selected in the experiment for successive statistical data.

Acknowledgements

MJME acknowledges a grant from the University of Alicante. The authors gratefully acknowledge the collaboration of the Instituto Murciano de Investigación y Desarrollo Agrario Alimentario (IMIDA) in the provision of grape berry material. MJME acknowledges a stay in the laboratory of Dr José Miguel Martínez Zapater in order to perform RT-PCR analysis. We thank Mayte Villela Anton for her helpful technical assistance, which is highly appreciated. University of Alicante Proteomics Facility is a member of Proteored. This work was supported by the Genoma España, GRAPEGEN grant, as a part of a Genoma España–Genome Canada collaborative research and development initiative.

Author contribution

MJME contributed to the experimental design, grape sampling, protein extraction, labelling and 2-DE, bioinformatic analysis and biological interpretation, cDNA synthesis and real-time qRT-PCR. SSM contributed to grape sampling, protein extraction, labelling and protein identification by LC-MS/MS analysis. DL contributed to the RNA isolation, cDNA synthesis, real-time qRT-PCR, and data interpretation of RT-PCR. MAP contributed to experimental design and data interpretation. RBM defined the work objectives and technical approach, contributed to the experimental design, bioinformatic analysis, and data interpretation.

References

Agasse A, Vignault C, Kappel C, Conde C, Gerós H, Delrot S. 2009. Sugar transport and sugar sensing in grape. In: Roubelakis-Angelakis KA, ed. *Grapevine molecular physioloy and biotechnology*. New York: Springer, 105–139.

Aharoni A, O'Connell AP. 2002. Gene expression analysis of strawberry achene and receptacle maturation using DNA microarrays. *Journal of Experimental Botany* **53,** 2073–2087.

Alfonso P, Dolado I, Swat A, Nunez A, Cuadrado A, Nebreda AR, Casal JI. 2006. Proteomic analysis of p38 mitogen-activated protein kinase-regulated changes in membrane fractions of RAS-transformed fibroblasts. *Proteomics* **6,** S262–S271.

Barel G, Ginzberg I. 2008. Potato skin proteome is enriched with plant defence components. *Journal of Experimental Botany* **59,** 3347–3357.

Beriashvili TV, Beriashvili LT. 1996. Metabolism of malic and tartaric acids in grape berries. *Biochemistry—Moscow* **61,** 1316–1321.

Beveridge AJ, Ollis DL. 1995. A theoretical study of substrate-induced activation of dienelactone hydrolase. *Protein Engineering* **8,** 135–142.

Bianco L, Lopez L, Scalone AG, Carli MD, Desiderio A, Benvenuto E, Perrotta G. 2009. Strawberry proteome characterization and its regulation during fruit ripening and in different genotypes. *Journal of Proteomics* **72,** 586–607.

Bleé E, Joyard J. 1996. Envelope membranes from spinach chloroplasts are a site of metabolism of fatty acid hydroperoxides. *Plant Physiology* **110,** 445–454.

Bogs J, Downey MO, Harvey JS, Ashton AR, Tanner GJ, Robinson SP. 2005. Proanthocyanidin synthesis and expression of genes encoding leucoanthocyanidin reductase in developing grape berries and grapevine leaves. *Plant Physiology* **139,** 652–663.

Boss PK, Davies C. 2001. Molecular biology of sugar and anthocyanin accumulation in grape berries. In: Roubelakis-Angelakis KA, ed. *Molecular biology and biotechnology of the grapevine*. Dordrecht: Kluwer Academic Publishers, 1–33.

Boss PK, Davies C, Robinson SP. 1996. Analysis of the expression of anthocyanin pathway genes in developing *Vitis vinifera* L. cv. Shiraz grape berries and the implications for pathway regulation. *Plant Physiology* **111,** 1059–1066.

Cagney G, Emili A. 2002. De novo peptide sequencing and quantitative profiling of complex protein mixtures using mass-coded abundance tagging. *Nature Biotechnology* **20,** 163–170.

Cakir B, Agasse A, Gaillard C, Sumonneau A, Delrot S, Atanasova R. 2003. A grape ASR protein involved in sugar and abscisic acid signaling. *Plant Cell* **15,** 2165–2180.

Che FY, Fricker LD. 2005. Quantitative peptidomics of mouse pituitary: comparison of different stable isotopic tags. *Journal of Mass Spectrometry* **40,** 238–249.

Choi JW, Kim GB, Huh YC, Kwon MR, Mok IG, Kim JW, Lee TS, Kim S, Im KH. 2004. Cloning of genes differentially expressed during the initial stage of fruit development in melon (*Cucumis melo* cv. *reticulatus*). *Molecules and Cells* **17,** 237–241.

Coker JS, Jones D, Davies E. 2003. Identification, conservation, and relative expression of V-ATPase cDNAs in tomato plants. *Plant Molecular Biology Reporter* **21,** 145–158.

Colombini M. 2004. VDAC: the channel at the interface between mitochondria and the cytosol. *Molecular and Cellular Biochemistry* **256/257,** 107–115.

Conde C, da Silva P, Fontes N, Dias ACP, Tavares RM, Sousa MJ, Agasse A, Delrot S, Gerós H. . Biochemical changes throughout grape berry development and fruit and wine quality. *Food* **1,** 1–22.

Coombe BG. 1987. Distribution of solutes within the developing grape berry in relation to its morphology. *American Journal of Enology and Viticulture* **38,** 120–127.

Coombe BG. 1988. Australian Temperate Fruits Review Conference. Fruit setting, development and ripening. *ISHS Acta Horticulturae.* **240,** 209–216.

Coombe BG. 1992. Research on development and ripening of the grape berry. *American Journal of Enology and Viticulture* **43,** 101–110.

Coombe BG, Hale CR. 1973. Hormone content of ripening grape berries and the effects of growth substance treatments. *Plant Physiology* **51,** 629–634.

Cosgrove DJ. 2000. Expansive growth of plant cell walls. *Plant Physiology and Biochemistry* **38,** 109–124.

Dali N, Michaud D, Yelle S. 1992. Evidence for the involvement of sucrose phosphate synthase in the pathway of sugar accumulation in sucrose-accumulating tomato fruits. *Plant Physiology* **99,** 434–438.

D'Aoust MA, Yelle S, Nguyen-Quoc B. 1999. Antisense inhibition of tomato fruit sucrose synthase decreases fruit setting and the sucrose unloading capacity of young fruit. *Plant Cell* **11,** 2407–2418.

da Silva FGIandolino A, Al-Kayal F, *et al*. 2005. Characterization of the grape transcriptome. Analysis of expressed sequence tags from multiple *Vitis* species and development of a compendium of gene expression during berry development. *Plant Physiology* **239,** 574–597.

Davies C, Boss PK, Robinson SP. 1997. Treatment of grape berries, a nonclimateric fruit, with a synthetic auxin retards ripening and alters the expression of developmentally regulated genes. *Plant Physiology* **115,** 1155–1161.

Davies C, Robinson SP. 1996. Sugar accumulation in grape berries. Cloning of two putative vacuolar invertase cDNAs and their expression in grapevine tissues. *Plant Physiology* **111,** 275–283.

Davies C, Robinson SP. 2000. Differential screening indicates a dramatic change in mRNA profiles during grape berry ripening. Cloning and characterization of cDNAs encoding putative cell wall and stress response proteins. *Plant Physiology* **122,** 803–812.

Davies C, Wolf T, Robinson SP. 1999. Three putative sucrose transporters are differentially expressed in grapevine tissues. *Plant Science* **147,** 93–100.

DeBolt S, Cook DR, Ford CM. 2006. L-Tartaric acid synthesis from vitamin C in higher plants. *Proceedings of the National Academy of Sciences, USA* **103,** 5608–5613.

Deluc LG, Grimplet J, Wheatley MD, Tillet RL, Quilici D, Osborne C, Schlauch KA, Schooley DA, Cushman JC, Cramer GR. 2007. Transcriptomic and metabolite analyses of Cabernet Sauvignon grape berry development. *BMC Genomics* **8,** 429.

Deng Z, Zhang X, Tang W, *et al*. 2007. A proteomic study of brassinosteroid response in. *Arabidopsis. Molecular and Cell Proteomics* **6,** 2058–2071.

Deytieux C, Geny L, Lapaillerie D, Claverol S, Bonneu M, Donèche B. 2007. Proteome analysis of grape skins during ripening. *Journal of Experimental Botany* **58,** 1851–1862.

Diaz-Riquelme J, Lijavetzky D, Martínez-Zapater JM, Carmona MJ. 2009. Genome-wide analysis of MIKC^{C}-type MADS box genes in grapevine. *Plant Physiology* **149,** 354–369.

Diepholz M, Borsch M, Bottcher B. 2008. Structural organization of the V-ATPase and its implications for regulatory assembly and disassembly. *Biochemical Society Transactions* **36,** 1027–1031.

Domgall I, Venzke D, Liittge U, Ratajczak R, Bottcher B. 2002. Three-dimensional map of a plant V-ATPase based on electron microscopy. *Journal of Biological Chemistry* **277,** 13115–13121.

Dorion S, Dumas F, Rivoal J. 2006 *a*. Autophosphorylation of *Solanum chacoense* cytosolic nucleoside diphosphate kinase on Ser117. *Journal of Experimental Botany* **57,** 4079–4088.

Dorion S, Matton DP, Rivoal J. 2006 *b*. Characterization of a cytosolic nucleoside diphosphate kinase associated with cell division and growth in potato. *Planta* **224,** 108–124.

Douce R, Joyard J. 1980. Plant galactolipids. In: Stumpf PK, ed. *The biochemistry of plant lipids: structure and function*, Vol 4. New York: Academic Press, 175–214.

Downey MO, Harvey JS, Robinson SP. 2003. Analysis of tannins in seeds and skins of Shiraz grapes throughout berry development. *Australian Journal of Grape and Wine Research* **9,** 15–27.

Downey MO, Harvey JS, Robinson SP. 2004. The effect of bunch shading on berry development and flavonoid accumulation in Shiraz grapes. *Australian Journal of Grape and Wine Research* **10,** 55–73.

Drory O, Frolow F, Nelson N. 2004. Crystal structure of yeast V-ATPase subunit C reveals its stator function. *EMBO Reports* **5,** 1148–1152.

Dry IB, Robinson SP. 1994. Molecular cloning and characterization of grape berry polyphenol oxidase. *Plant Molecular Biology* **26,** 495–502.

Famiani F, Walker RP, Técsi L, Chen Z-H, Proietti P, Leegood RC. 2000. An immunohistochemical study of the compartmentation of metabolism during the development of grape (*Vitis vinifera* L.) berries. *Journal of Experimental Botany* **51,** 675–683.

FAO: Food and Agriculture Organization of the United Nations. 2007. http://faostat.fao.org/site/567/DesktopDefault.aspx?PageID=567#ancor (16 December 2010, date last accessed).

Fenoll J, Manso A, Hellin P, Ruiz L, Flores P. 2009. Changes in the aromatic composition of the *Vitis vinifera* grape Muscat Hamburg during ripening. *Food Chemistry* **114,** 420–428.

Fernandez L, Torregrosa L, Terrier N, Sreekantan L, Grimplet J, Davies C, Thomas MR, Romieu C, Ageorges A. 2007. Identification of genes associated with flesh morphogenesis during grapevine fruit development. *Plant Molecular Biology* **63,** 307–323.

Ferreira RB, Monteiro S, Freitas R, Santos CN, Chen Z, Batista LM, Duarte J, Borges A, Teixeira AR. 2007. The role of plant defence proteins in fungal pathogenesis. *Molecular Plant Pathology* **8,** 677–700.

Feussner I, Hause B, Vörös K, Parthier B, Wasternack C. 1995. Jasmonate-induced lipoxygenase forms are localized in chloroplast of barley leaves (*Hordeum vulgare* cv. Salome). *Plant Journal* **7,** 949–957.

Fillion L, Ageorges A, Picaud S, Coutos-Thévenot P, Lemoine R, Romieu C, Delrot S. 1999. Cloning and expression of a hexose transporter gene expressed during the ripening of grape berry. *Plant Physiology* **120,** 1083–1093.

Froehlich JE, Ioth A, Howe GA. 2001. Tomato allene oxide synthase and fatty acid hydroperoxidase lyase, two cytochrome P450s involved in oxylipin metabolism, are targeted to different membranes of chloroplast envelope. *Plant Physiology* **125,** 306–317.

Gao ZS, van de Weg WE, Schaart JE, *et al*. 2005. Genomic cloning and linkage mapping of the Mal d 1 (PR–10) gene family in apple (*Malus domestica*). *Theoretical and Applied Genetics* **111,** 171–183.

Ghisi R, Jannini B, Passera C. 1984. Changes in the activities of enzymes involved in nitrogen and sulphur assimilation during leaf and berry development of. *Vitis vinifera. Vitis* **23,** 257–267.

Giannakis C, Bucheli CS, Skene KGM, Robinson SP, Steele Scote N. 1998. Chitinase and β-1,3-glucanase in grapevine leaves: a possible defence against powdery mildew infection. *Australian Journal of Grape and Wine Research* **4,** 14–22.

Gilles AM, Presecan E, Vonica A, Lascu I. 1991. Nucleoside diphosphate kinase from human erythrocytes. Structural characterization of the two polypeptide chains responsible for heterogeneity of the hexameric enzyme. *Journal of Biological Chemistry* **266,** 8784–8789.

Giribaldi M, Perugini I, Sauvage FX, Shubert A. 2007. Analysis of protein changes during grape berry ripening by 2-DE and MALDI-TOF. *Proteomics* **7,** 3154–3170.

González MC, Sánchez R, Cejudo FJ. 2003. Abiotic stresses affecting water balance induce phosphoenolpyruvate carboxylase expression in roots of wheat seedlings. *Planta* **216,** 985–992.

Görg A, Drews O, Weiss W. 2006. Isoelectric focusing in immobilized pH gradient strips using the IPGphor unit: sample cup loading. CSH Protocols *doi:10.1101/pdb.prot4231* .

Götz S, García-Gómez JM, Terol J, Williams TM, Nueda MJ, Robles M, Talón M, Dopazo J, Conesa A. 2008. High-throughput functional annotation and data mining with the Blast2GO suite. *Nucleic Acids Research* **36,** 3420–3435.

Goyer A, Haslekas C, Miginiac-Maslow M, Klein U, Marechal PL, Jacquot J-P, Decottignies P. 2002. Isolation and characterization of a thioredoxin-dependent peroxidase from. *Chlamydomonas reinhardtii. European Journal of Biochemistry* **269,** 272–282.

Grace S, Pace R, Wydrzynski T. 1995. Formation and decay of monodehydroascorbate radicals in illuminated thylakoids as determined by EPR spectroscopy. *Biochimica et Biophysica Acta* **1229,** 155–165.

Grimplet J, Deluc LG, Tillett RL, Wheatley MD, Schlauch KA, Cramer GR, Cushman JC. 2007. Tissue-specific mRNA expression profiling in grape berry tissues. *BMC Genomics* **8,** 187.

Grimplet J, Wheatley MD, Jouira HB, Deluc LG, Cramer GR, Cushman JC. 2009. Proteomic and selected metabolite analysis of grape berry tissues under well-watered and water-deficit stress conditions. *Proteomics* **9,** 2503–2528.

Gygi SP, Corthals GL, Zhang Y, Rochon Y, Aebersold R. 2000. Evaluation of two-dimensional gel electrophoresis-based proteome analysis technology. *Proceedings of the National Academy of Sciences, USA* **97,** 9390–9395.

Gygi SP, Rist B, Gerber SA, Turecek F, Gelb MH, Aebersold R. 1999. Quantitative analysis of complex protein mixtures using isotope-coded affinity tags. *Nature Biotechnology* **17,** 994–999.

Hale CR. 1962. Synthesis of organic acids in the fruit of the grape. *Nature* **195,** 917–918.

Harris JM, Kriedmann PE, Possingham JV. 1968. Anatomical aspects of grape berry development. *Vitis* **7,** 106–119.

Hawker JS. 1969. Changes in the activities of malic enzyme, malate dehydrogenase, phosphopyruvate carboxylase and pyruvate decarboxylase during the development of a non-climacteric fruit (the grape). *Phytochemistry* **8,** 19–23.

Hiroyuki Y, Masaharu K. 2006. Disulfide proteome yields a detailed understanding of redox regulations: a model study of thioredoxin-linked reactions in seed germination. *Proteomics* **6,** 294–300.

Hiroyuki Y, Shigeru K. 2008. Introduction of the disulfide proteome: application of a technique for the analysis of plant storage proteins as well as allergens. *Journal of Proteome Research* **7,** 3071–3079.

Hodges M, Flesch V, Gálvez S, Bismuth E. 2003. Higher plant $NADP^+$-dependent isocitrate dehydrogenases, ammonium assimilation and NADPH production. *Plant Physiology and Biochemistry* **41,** 577–585.

Iland PG, Coombe BG. 1988. Malate, tartrate, potassium, and sodium in flesh and skin of Shiraz grapes during ripening: concentration and compartimentation. *American Journal of Enology and Viticulture* **39,** 71–76.

Ishihama Y, Oda Y, Tabata T, Sato T, Nagasu T, Rappsilber J, Mann M. 2005. Exponentally modified protein abundance index (emPAI) for estimation of absolute protein amount in proteomics by the number of sequenced peptides per protein. *Molecular and Cell Proteomics* **4,** 1265–1272.

Ishimaru M, Kobayashi S. 2002. Expression of a xyloglucan endo-transglycosylase gene is closely related to grape berry softening. *Plant Science* **162,** 621–628.

Jaillon O, Aury JM, Noel B, *et al*. The French-Italian Public Consortium for Grapevine Genome Characterization. 2007. The grapevine genome sequence suggests ancestral hexaploidization in major angiosperm phyla. *Nature* **449,** 463–467.

Jellouli N, Ben Jouira H, Skouri H, Ghorbel A, Gourgouri A, Mliki. 2008. A proteomic analysis of Tunisian grapevine cultivar Razegui under salt stress. *Journal of Plant Physiology* **165,** 471–481.

Jiménez A, Creissen G, Kular B, Firmin J, Robinson S, Verhoeyer M, Mullineaux P. 2002. Changes in oxidative processes and components of the antioxidant system during tomato fruit ripening. *Planta* **214,** 751–758.

Kanellis AK, Roubelakis-Angelakis KA. 1993. Grape. In: Seymour G, Taylor J, Tucker G, eds. *Biochemistry of fruit ripening*. London: Chapman and Hall, 189–234.

Kim CY, Koo YD, Jin JB, *et al*. 2003. Rice C2-domain proteins are induced and translocated to the plasma membrane in response to a fungal elicitor. *Biochemistry* **42,** 11625–11633.

Kim YC, Kim SY, Choi D, Ryu CM, Park JM. 2008. Molecular characterization of a pepper C2 domain-containing SRC2 protein implicated in resistance against host and non-host pathogens and abiotic stresses. *Planta* **227,** 1169–1179.

Kolkman A, Dirksen EH, Slijper M, Heck AJ. 2005. Double standards in quantitative proteomics: direct comparative assessment of difference in gel electrophoresis and metabolic stable isotope labeling. *Molecular and Cell Proteomics* **4,** 255–266.

Kondo S, Fukuda K. 2001. Changes of jasmonates in grape berries and their possible roles in fruit development. *Scientia Horticulturae—Amsterdam* **91,** 275–288.

Kondo S, Tomiyama A, Seto H. 2000. Changes of endogenous jasmonic acid and methyl jasmonate in apples and sweet cherries during fruit development. *Journal of the American Society for Horticultural Science* **125,** 282–287.

Kreuzaler F, Hahlbrock K. 1972. Enzymatic synthesis of aromatic compounds in higuer plants: formation of naringerin (5,7,4,'-trihydroxyflavone) from p-coumaroyl coenzyme A and malonyl coenzyme A. *FEBS Letters* **28,** 69–72.

Lima JD, Sodek L. 2003. N-stress alters aspartate and asparagine levels of xylem sap in soybean. *Plant Science* **165,** 649–656.

Lücker J, Laszczak M, Smith D, Lund ST. 2009. Generation of a predicted protein database from EST data and application to iTRAQ analyses in grape (*Vitis vinifera* cv. Cabernet Sauvignon) berries at ripening initiation. *BMC Genomics* **10,** 1–17.

Lund ST, Bohlmann J. 2006. The molecular basis for wine grape quality—a volatile subject. *Science* **311,** 804–805.

Lytle BL, Song J, de la Cruz NB, Peterson FC, Johnson KA, Bingman CA, Phillips GN, Volkman BF. 2009. Structures of two *Arabidopsis thaliana* major latex proteins represent novel helix-grip folds. *Proteins* **2,** 237–243.

Makris DP, Kallithraka S, Kefalas P. 2006. Flavonols in grapes, grape products and wines: burden, profile and influential parameters. *Journal of Food Composition and Analysis* **19,** 396–404.

Maqbool A, Zahur M, Husnain T, Riazuddin S. 2009. GUSP1 and GUSP2, two drought-responsive genes in *Gossypium arboreum* have homology to universal stress proteins. *Plant Molecular Biology Reporter* **27,** 109–114.

Marino NC, Tamames EL, Jares CMG. 1995. Contribution to the study of the aromatic potential of three Muscat *Vitis vinifera* varieties: identification of new compounds. *Food Science and Technology International* **1,** 105–116.

Martinez-Esteso MJ, Selles-Marchart S, Vera-Urbina JC, Pedreño MA, Bru-Martinez R. 2009. Changes of defense proteins in the extracellular proteome of grapevine (*Vitis vinifera* cv. Gamay) cell cultures in response to elicitors. *Journal of Proteomics* **73,** 331–341.

Méchin V, Balliatu T, Chateau-Joubert S, Davanture M, Negroni L, Thevenot C, Zivy M, Damerval C, Langela O. 2004. A two-dimensional proteome map of maize endosperm. *Phytochemistry* **65,** 1609–1618.

Melino VJ, Soole KL, Ford CM. 2009. Ascorbate metabolism and the developmental demand for tartaric and oxalic acids in ripening grape berries. *BMC Plant Biology* **9,** 145.

Mockler TC, Yu Shalitin D, *et al*. 2004. Regulation of flowering time in *Arabidopsis* by K homology domain proteins. *Proceedings of the National Academy of Sciences, USA* **111,** 12759–12764.

Moskowitz AH, Hrazdina G. 1981. Vacuolar contents of fruit subepidermal cells from Vitis species. *Plant Physiology* **68,** 686–692.

Moustafa E, Wong E. 1967. Purification and properties of chalcone-flavanone isomerase from soya bean seed. *Phytochemistry* **6,** 625–632.

Naqvi SMS, Park KS, Yi SY, Lee HW, Bok SH, Choi D. 1998. A glycine rich RNA binding protein gene is differentially expressed during acute hypersensitive response following Tobacco Mosaic Virus infection in tobacco. *Plant Molecular Biology* **37,** 571–576.

Negri AS, Prinsi B, Rossoni M, Failla O, Scienza A, Cocucci M, Espen L. 2008. Proteome changes in the skin of the grape cultivar Barbera among different stages of ripening. *BMC Genomics* **9,** 378.

Neuhoff V, Arold N, Taube D, Ehrhardt W. 1988. Improved staining of proteins in polyacrylamide gels including isoelectric focusing gels with clear background at nanogram sensitivity using Coomassie Brilliant Blue G-250 and R-250. *Electrophoresis* **9,** 255–262.

Nguyen-Quoc B, Foyer CH. 2001. A role of 'futile cycles' involving invertase and sucrose synthase in sucrose metabolism of tomato fruit. *Journal of Experimental Botany* **52,** 881–889.

N'tchobo H, Dali N, Nguyen-Quoc B, Foyer CH, Yelle S. 1999. Starch synthesis in tomato remains constant throughout fruit development and is dependent on sucrose supply and sucrose synthase activity. *Journal of Experimental Botany* **50,** 1457–1463.

Nunan KJ, Davies C, Robinson SP, Fincher GB. 2001. Expression patterns of cell wall-modifying enzymes during grape berry development. *Planta* **214,** 257–264.

Nystrom T, Neidhardt FC. 1992. Cloning, mapping and nucleotide sequencing of a gene encoding a universal stress protein in *Escherichia coli. Molecular Microbiology* **6,** 3187–3198.

Nystrom T, Neidhardt FC. 1993. Isolation and properties of a mutant of *Escherichia coli* with an insertional inactivation of the *uspA* gene, which encodes a universal stress protein. *Journal of Bacteriology* **175,** 3949–3956.

Nystrom T, Neidhardt FC. 1994. Expression and role of the universal stress protein, UspA, of *Escherichia coli* during growth arrest. *Molecular Microbiology* **11,** 537–544.

Ollat N, Gaudillère JP. 2000. Carbon balance in developing grapevine berries. In: Bravdo BA. *Proceedings of the V international symposium on grapevine physiology* **526,** 345–350.

Ong S, Blagoev B, Kratchmarova I, Kristensen DB, Steen H, Pandey A, Mann M. 2002. Stable isotope labeling by amino acids in cell culture, SILAC, as a simple and accurate approach to expression proteomics. *Molecular and Cell Proteomics* **1,** 376–386.

Or E, Baybik J, Sadka A, Saks Y. 2000. Isolation of mitochondrial malate dehydrogenase and phosphoenolpyruvate carboxylase cDNA clones from grape berries and analysis of their expression pattern throughout berry development. *Journal of Plant Physiology* **157,** 527–534.

Osmark P, Boyle B, Brisson N. 1998. Sequential and structural homology between intracellular pathogenesis-related proteins and a group of latex proteins. *Plant Molecular Biology* **38,** 1243–1246.

Owen DJ, Collins BM, Evans PR. 2004. Adaptors for clathrin coats: structure and function. *Annual Review of Cell and Developmental Biology* **20,** 153–191.

Pandey RM, Farmahan HL. 1977. Changes in the rate of photosynthesis and respiration in leaves and berries of *Vitis vinifera* grapevines at various stages of berry development. *Vitis* **16,** 106–111.

Pérez FJ, Viani C, Retamales J. 2000. Bioactive gibberellins in seeded and seedless grapes: identification and changes in content during berry development. *American Journal of Enology and Viticulture* **51,** 315–318.

Pilati S, Perazzolli M, Malossini A, Cestaro A, Dematte L, Fontana P, Dal Ri A, Viola R, Velasco R, Moser C. 2007. Genome-wide transcriptional analysis of grapevine berry ripening reveals a set of genes similarly modulated during three seasons and the occurrence of an oxidative burst at véraison. *BMC Genomics* **8,** 428.

Radauer C, Breiteneder H. 2007. Evolutionary biology of plant food allergens. *Journal of Allergy and Clinical Immunology* **120,** 518–525.

Rangel M, Machado OLT, da Cunha M, Jacinto T. 2002. Accumulation of chloroplast-targeted lipoxygenase in passion fruit leaves in response to methyl jasmonate. *Phytochemistry* **60,** 619–625.

Rao KCS, Carruth RT, Miyagi M. 2005. Proteolytic O18 labeling by peptidyl-lys metalloendopeptidase for comparative proteomics. *Journal of Proteome Research* **4,** 507–514.

Rappsilber J, Ryder U, Lamond AI, Mann M. 2002. Large-scale proteomic analysis of the human spliceosome. *Genome Research* **12,** 1231–1245.

Reid KE, Olsson N, Schlosser J, Peng F, Lund ST. 2006. An optimized grapevine RNA isolation procedure and statistical determination of reference genes for real-time RT-PCR during berry development. *BMC Plant Biology* **6,** 27.

Reuhs BL, Glenn J, Stephens SB, Kim JS, Christie DB, Glushka JG, Zablackis E, Albersheim P, Darvill AG, O'Neill MA. 2004. l-Galactose replaces l-fucose in the pectic polysaccharide rhamnogalacturonan II synthesized by the l-fucose-deficient mur1 *Arabidopsis* mutant. *Planta* **219,** 147–57.

Ribéreau-Gayon P, Boidron JN, Terrier A. 1975. Aroma of Muscat grape varieties. *Journal of Agricultural and Food Chemistry* **23,** 1042–1047.

Robinson SP, Davies C. 2000. Molecular biology of grape berry ripening. *Australian Journal of Grape and Wine Research* **6,** 175–188.

Robinson SP, Jacobs AK, Dry IB. 1997. A class IV chitinase is highly expressed in grape berries during ripening. *Plant Physiology* **114,** 771–778.

Ross PL, Huang YN, Marchese JN, *et al*. 2004. Multiplexed protein quantitation in *Saccharomyces cerevisiae* using amine-reactive isobaric tagging reagents. *Molecular and Cellular Proteomics* **3,** 1154–1169.

Ruffner HP. 1982. Metabolism of tartaric acid and malic acids in *Vitis*: a review—part A. *Vitis* **21,** 247–259.

Ruffner HP, Hawker JS. 1977. Control of glycolysis in ripening berries of. *Vitis vinifera. Phytochemistry* **16,** 1171–1175.

Ruffner HP, Kliewer WM. 1975. Phosphoenolpyruvate carboxykinase activity in grape berries. *Plant Physiology* **56,** 67–71.

Ruperti B, Bonghi C, Ziliotto F, Pagni S, Rasori A, Varotto S, Tunutti P, Giovannoni J, Ramina A. 2002. Characterization of a major latex protein (MLP) gene down-regulated by ethylene during peach fruit let abscission. *Plant Science* **163,** 265–272.

Saito K, Kasai Z. 1969. Tartaric acid synthesis from L-ascorbic acid-1-14C in grape berries. *Phytochemistry* **8,** 2177–2182.

Sakamoto T, Miura K, Itoh H, *et al*. 2004. An overview of gibberellin metabolism enzyme genes and their related mutants in rice. *Plant Physiology* **134,** 1642–1653.

Sakurai N, Nevins DJ. 1997. Relationship between fruit softening and wall polysaccharides in avocado (*Persea americana* Mill) mesocarp tissues. *Plant and Cell Physiology* **38,** 603–610.

Salinas T, Duchene A-M, Delage L, Nilsson S, Glaser E, Zaepfel M, Marechal-Drouard L. 2006. The voltage-dependent anion channel, a major component of the tRNA import machinery in plant mitochondria. *Proceedings of the National Academy of Sciences, USA* **103,** 18362–18367.

Salzman RA, Tikhonova I, Bordelon BP, Hasegawa PM, Bressan RA. 1998. Coordinate accumulation of antifungal proteins and hexoses constitutes a developmentally controlled defense during fruit ripening in grape. *Plant Physiology* **117,** 465–472.

Saravanan RS, Rose JKC. 2004. A critical evaluation of sample extraction techniques for enhanced proteomic analysis of recalcitrant plant tissues. *Proteomics* **4,** 2522–2532.

Sarry JE, Sommerer N, Sauvage FX, Bergoin A, Rossignol M, Albagnac G, Romieu C. 2004. Grape berry biochemistry revisited upon proteomic analysis of the mesocarp. *Proteomics* **4,** 201–215.

Sazer S, Dasso M. 2000. The ran decathlon: multiple roles of Ran. *Journal of Cell Science* **113,** 1111–1118.

Schlosser J, Olsson N, Weis M, Reid K, Peng F, Lund S, Bowen P. 2008. Cellular expansion and gene expression in the developing grape (*Vitis vinifera* L.). *Protoplasma* **232,** 255–265.

Schuberth C, Buchberger A. 2008. UBX domain proteins: major regulators of the AAA ATPase Cdc48/p97. *Cellular and Molecular Life Science* **65,** 2360–2371.

Seifert GJ. 2004. Nucleotide sugar interconversions and cell wall biosynthesis: how to bring the inside to the outside. *Current Opinion in Plant Biology* **7,** 277–284.

Sellés-Marchart S, Casado-Vela J, Bru-Martínez R. 2007. Effect of detergents, trypsin and unsaturated fatty acids on latent loquat fruit polyphenol oxidase: basis for the enzyme's activity regulation. *Archives of Biochemistry and Biophysics* **464,** 295–305.

Sellés-Marchart S, Ignacio L, Casado-Vela J, Martínez-Esteso MJ, Bru-Martínez R. 2008. Proteomics of multigenic families from species underrepresented in databases: the case of loquat (*Eriobotrya japonica* Lindl.) polyphenol oxidases. *Journal of Proteome Research* **7,** 4095–4106.

Shevchenko A, Jensen ON, Podtelejnikov AV, Sagliocco F, Wilm M, Vorm O, Mortensen P, Shevchenko A, Boucherie H, Mann M. 1996. Linking genome and proteome by mass spectrometry: large-scale identification of yeast proteins from two dimensional gels. *Proceedings of the National Academy of Sciences, USA* **93,** 14440–14445.

Sieciechowicz KA, Joy KW, Ireland RJ. 1988. The metabolism of asparagine in plants. *Phytochemistry* **27,** 663–671.

Smalle J, Vierstra RD. 2004. The ubiquitin 26S proteasome proteolytic pathway. *Annual Review of Plant Biology* **55,** 555–590.

Sparvoli F, Martin C, Scienza A, Gavazzi G, Tonelli C. 1994. Cloning and molecular analysis of structural genes involved in flavonoid and stilbene biosynthesis in grape (*V. vinifera* L.). *Plant Molecular Biology* **24,** 743–755.

Stines AP, Grubb J, Gockowiak H, Henschke PA, Høj PB, van Heeswijck R. 2000. Proline and arginine accumulation in developing berries of *V. vinifera* in Australian vineyards: influence of vine cultivar, berry maturity and tissue type. *Australian Journal of Grape and Wine Research* **6,** 150–158.

Sturn A, Quackenbush J, Trajanoski Z. 2002. Genesis: cluster analysis of microarray data. *Bioinformatics* **18,** 207–208.

Swanson CA, Elshishiny EDH. 1958. Translocation of sugars in the Concord grape. *Plant Physiology* **33,** 33–37.

Sweetman C, Deluc LG, Cramer GR, Ford CM, Soole KL. 2009. Regulation of malate metabolism in grape berry and other developing fruits. *Phytochemistry* **70,** 1329–1344.

Symons GM, Davies C, Shavrukov Y, Dry IB, Reid JB, Thomas MR. 2006. Grapes on steroids. Brassinosteroids are involved in grape berry ripening. *Plant Physiology* **140,** 150–158.

Takayanagi T, Yokotsuka K. 1997. Relationship between sucrose accumulation and sucrose-metabolizing enzymes in developing grapes. *American Journal of Enology and Viticulture* **48,** 403–407.

Tamburrini M, Cerasuolo I, Carratore V, Stanziola AA, Zofra S, Romano L, Camardella L, Ciardiello MA. 2005. Kiwellin, a novel protein from kiwi fruit. Purification, biochemical characterization and identification as an allergen. *Journal of Protein Chemistry* **24,** 423–429.

Tattersall D, Pocock K, Hayasaka Y, Adams K, van Heeswijck R, Waters E, Hoj P. 2001. Pathogenesis related proteins – their accumulation in grapes during berry growth and their involvement in white wine heat instability. Current knowledge and future perspectives in relation to winemaking practices. In: Roubelakis-Angelakis KA, ed. *Molecular biology and biotechnology of the grapevine*. New York: Kluwer Academic Publishers, 183–201.

Tattersall DB, van Heeswijck R, Høj PB. 1997. Identification and characterization of a fruit-specific, thaumatin-like protein that accumulates at very high levels in conjunction with the onset of sugar accumulation and berry softening in grapes. *Plant Physiology* **114,** 759–769.

Taureilles-Saurel C, Romieu CG, Robin JP, Flanzy C. 1995. Grape (*Vitis vinifera* L.) malate dehydrogenase. II. Characterization of the major mitochondrial and cytosolic isoforms and their role in ripening. *American Journal of Enology and Viticulture* **46,** 29–36.

Terrier N, Francois-Xavier S, Ageorges A, Romieu C. 2001. Changes in acidity and in proton transport at the tonoplast of grape berries during development. *Planta* **213,** 20–28.

Terrier N, Romieu C. 2001. Grape berry acidity. In: Roubelakis-Angelakis KA, ed. *Molecular biology and biotechnology of the grapevine.*. New York: Kluwer Academic Publishers, 35–57.

Terrier N, Glissant GJ, Barrieu F, *et al*. 2005. Isogene specific oligo arrays reveal multifaceted changes in gene expression during grape berry (*Vitis vinifera* L.) development. *Planta* **222,** 832–847.

Tonge R, Shaw J, Middleton B, Rowlinson R, Rayner S, Young J, Pognan F, Hawkins E, Currie I, Davison M. 2001. Validation and development of fluorescence two-dimensional

differential gel electrophoresis proteomics technology. *Proteomics* **1,** 377–396.

Turley RB. 2008. Expression of a phenylcoumaran benzylic ether reductase-like protein in the ovules of *Gossypium hirsutum. Biologia Plantarum* **52,** 759–762.

Unlu M, Morgan ME, Minden JS. 1997. Difference gel electrophoresis: a single gel method for detecting changes in protein extracts. *Electrophoresis* **18,** 2071–2077.

Usadel B, Kuschinsky AM, Rosso MG, Eckermann N, Pauly M. 2004. RHM2 is involved in mucilage pectin synthesis and is required for the development of the seed coat in. *Arabidopsis. Plant Physiology* **134,** 286–295.

van Heeswijck R, Stines AP, Grubb J, Møller IS, Høj PB. 2001. Molecular biology and biochemistry of proline accumulation in developing grape berries. In: Roubelakis-Angelakis KA, ed. *Molecular biology and biotechnology of the grapevine*. New York: Kluwer Academic Publishers, 87–108.

van Loon LC, van Strien EA. 1999. The families of pathogenesis related proteins, their activities, and comparative analysis of PR-1 type proteins. *Physiological and Molecular Plant Pathology* **55,** 85–97.

Velasco R, Zharkikh A, Troggio M, *et al*. 2007. A high quality draft consensus sequence of the genome of a heterozygous grapevine variety. *PLoS ONE* **2,** e1326.

Vincent D, Ergul A, Bohlman MC, *et al*. 2007. Proteomic analysis reveals differences between *Vitis vinifera* L. cv. Chardonnay and cv. Cabernet Sauvignon and their responses to water deficit and salinity. *Journal of Experimental Botany* **58,** 1873–1892.

Vincent D, Wheatley MD, Cramer GR. 2006. Optimization of protein extraction of mature grape berry clusters. *Electrophoresis* **27,** 1853–1865.

Vincenzi S, Curioni A. 2005. Anomalous electrophoretic behavior of a chitinase isoform from grape berries and wine in glycol chitin containing sodium dodecyl sulfate-polyacrylamide gel electrophoresis gels. *Electrophoresis* **26,** 60–63.

Wang W, Scali M, Vignani R, Spadafora A, Sensi E, Mazzuca S, Cresti M. 2003. Protein extraction for two-dimensional electrophoresis from olive leaf, a plant tissue containing high levels of interfering compounds. *Electrophoresis* **24,** 2369–2375.

Wang X. 2002. Phospholipase D in hormonal and stress signaling. *Current Opinion in Plant Biology* **5,** 408–414.

Wang Z, Martin J, Abubucker S, Yin Y, Gasser RB, Mitreva M. 2009. Systematic analysis of insertions and deletions specific to nematode proteins and their proposed functional and evolutionary relevance. *BMC Evolutionary Biology* **9,** 23.

Wasternack C, Parthier B. 1997. Jasmonate-signalled plant gene expression. *Trends in Plant Science* **2,** 302–307.

Waters DLE, Holton TA, Ablett EM, Lee LS, Henry RJ. 2005. cDNA microarray analysis of the developing grape (*Vitis vinifera* cv. Shiraz) berry skin. *Functional and Integrative Genomics* **5,** 40–58.

Waters DLE, Holton TA, Ablett EM, Slade LL, Henry RJ. 2006. The ripening wine grape berry skin transcriptome. *Plant Science* **171,** 132–138.

Waters EJ, Shirley NJ, Williams PJ. 1996. Nuisance proteins of wine are grape pathogenesis-related proteins. *Journal of Agricultural and Food Chemistry* **44,** 3–5.

Wilson B, Strauss C, Williams P. 1986. The distribution of free and glycosidically bound monoterpenes among skin, juice and pulp fractions of some white grape varieties. *American Journal of Enology and Viticulture* **37,** 107–111.

Wu WW, Wang G, Baek SJ, Shen R- F. 2006. Comparative study of three proteomic quantitative methods, DIGE, cICAT, and iTRAQ, Using 2D Gel- or LC−MALDI TOF/TOF. *Journal of Proteome Research* **5,** 651–658.

Yang EJ, Oh YA, Lee ES, Park AR, Cho SK, Yoo YJ, Park OK. 2003. Oxygen-evolving enhancer protein 2 is phosphorylated by glycine-rich protein 3/wall-associated kinase 1 in *Arabidopsis. Biochemical and Biophysical Research Communications* **305,** 862–868.

Yang Y, Thannhauser TW, Li L, Zhang S. 2007. Development of an integrated approach for evaluation of 2-D gel image analysis: impact of multiple proteins in single spots on comparative proteomics in conventional 2-D gel/MALDI workflow. *Electrophoresis* **28,** 2080–2094.

Zahur M, Maqbool A, Irfan M, Younas M, Barozai K, Rashid B, Riazuddin S, Husnain T. 2009. Isolation and functional analysis of cotton universal stress protein promoter in response to phytohormones and abiotic stresses. *Journal of Molecular Biology* **43,** 578–585.

Zhang J, Ma H, Feng J, Zeng L, Wang Z, Chen S. 2008. Grape berry plasma membrane proteome analysis and its differential expression during ripening. *Journal of Experimental Botany* **59,** 2979–2990.

Ziegler J, Stenzel I, Hause B, Maucher H, Hamberg M, Grimm R, Ganal M, Wasternack C. 2000. Molecular cloning of allene oxide cyclase. *Journal of Biological Chemistry* **275,** 19132–19138.

Zong C, Young GW, Wang Y, Lu H, Deng N, Drews O, Ping P. 2008. Two-dimensional electrophoresis-based characterization of post-translational modifications of mammalian 20S proteasome complexes. *Proteomics* **8,** 5025–5037.